



Design and Implementation of Anti-collision  
Algorithms for Dense RFID Systems

Der Technischen Fakultät der Universität Erlangen-Nürnberg

zur Erlangung des Grades

DOKTOR-INGENIEUR

vorgelegt von

Hazem Abdelall Ahmed Elsaid Ibrahim

Supervisor

Prof. Dr.-Ing. Albert Heuberger

December 30, 2016

## Acknowledgment



## **Abstract**



# Contents

<b>1</b>	<b>Introduction</b>	<b>1</b>
1.1	Motivation . . . . .	1
1.2	Thesis Contribution . . . . .	3
1.3	Document Outline . . . . .	5
<b>2</b>	<b>System Description</b>	<b>7</b>
2.1	Historical Development of RFID . . . . .	7
2.2	system components . . . . .	8
2.3	Frequency Bands . . . . .	12
2.4	RFID Standards . . . . .	13
2.5	Collision Problems . . . . .	14
<b>3</b>	<b>RFID Anti-collision Protocols</b>	<b>17</b>
3.1	PHY-Layer Anti-collision Protocols . . . . .	17
3.2	MAC-Layer Anti-collision Protocols . . . . .	18
3.3	Cross Layer Anti-Collision Protocol . . . . .	27
<b>4</b>	<b>Estimation of the Tag Population</b>	<b>29</b>
4.1	State-of-the-Art Estimation Protocols . . . . .	30
4.2	Novel Collision Recovery Aware Tag Estimation . . . . .	36
<b>5</b>	<b>Frame Length Optimization</b>	<b>47</b>
5.1	Time Aware System . . . . .	48
5.2	Time and Collision Recovery Aware System . . . . .	59
5.3	Multiple Collision Recovery Aware System . . . . .	66
5.4	Time And Multiple Collision Recovery System . . . . .	74
5.5	Summary Results . . . . .	80

<b>6 Compatible Improvements of UHF Standard</b>	<b>85</b>
6.1 EPCglobal C1 G2 Reading Process . . . . .	86
6.2 Proposed System Description . . . . .	87
6.3 Performance Analysis . . . . .	92
6.4 Measurement And Simulation Results . . . . .	95
<b>7 Conclusion And Future Work</b>	<b>99</b>
7.1 Conclusion . . . . .	99
7.2 Future Work . . . . .	99
<b>Bibliography</b>	<b>103</b>

# List of Tables

2.1	Frequency Bands for RFID Systems . . . . .	11
2.2	RFID standards classification . . . . .	12
5.1	Available slots duration constants $C_t$ of the EPCglobal C1 G2 standards . . . . .	54
6.1	Set of 8 orthogonal sequences [1] . . . . .	89
6.2	Proposed switch command . . . . .	89
6.3	Example for unique pilot collision scenarios for up to eight colliding tags per slot [2] . . . . .	92
6.4	System Parameters of EPCglobal class 1 gen 2 standards [3] . .	94



# List of Figures

1.1	Dense RFID network with single RFID reader . . . . .	2
2.1	RFID System components . . . . .	8
2.2	Multiple readers to a single tag collision . . . . .	13
2.3	Multiple readers interference . . . . .	14
2.4	Multiple tags to a single reader collision . . . . .	15
3.1	Common existing PHY-Layer anti-collision protocols . . . . .	19
3.2	Common existing MAC-Layer anti-collision protocols . . . . .	20
3.3	Binary tree anti-collision algorithm example . . . . .	21
3.4	Query tree anti-collision algorithm example . . . . .	22
3.5	Example for pure ALOHA protocol . . . . .	23
3.6	Example for slotted ALOHA . . . . .	24
3.7	Example for Frame Slotted ALOHA . . . . .	25
3.8	Slots of Dynamic Frame Slotted ALOHA . . . . .	25
3.9	Flow chart of Dynamic Framed Slotted ALOHA (DFSA) . . . . .	26
4.1	Heuristics Q-Slot Family, variable frame length procedure EPC-global C1 G2 [3] . . . . .	30
4.2	Relative estimation error $\epsilon$ vs normalized number of tags $n/L$ for the common state-of the-art estimation algorithms . . . . .	34
4.3	Mean identification time versus the number of tags in the reading area for the common state-of the-art estimation algorithms . . . . .	35
4.4	Physical layer collision recovery capability . . . . .	37
4.5	Capture probability versus the signal to noise ratio . . . . .	42
4.6	Relative estimation error $\epsilon$ vs normalized number of tags $n/L$ . . . . .	43

4.7	Relative estimation error vs. collision recovery probability $\alpha$ , where $L = n$	44
4.8	Average identification delay	45
5.1	Equal and unequal views of slots in Frame Slotted ALOHA with frame length $L = 6$ .	48
5.2	Slots durations measurements, $f_s = 8$ MHz, tag Backscatter Link Frequency $BLF = 160$ kbps	49
5.3	Slot durations during tag inventory rounds for the ISO 18000-6C standard	53
5.4	Optimum frame length $L_{TA}$ as a function of the slot duration constant $C_t$ ( $n = 100$ tags). The conventional case with identical slot durations corresponds to $C_t = 1$ .	56
5.5	Maximum reading efficiency	57
5.6	Percentages of saving time using the proposed TAFSA for an ideally known number of tags (1000 iterations for each step)	58
5.7	Percentages of saving time using the proposed TAFSA compared to the conventional frame length $L = n$ for different anti-collision algorithms using $C_t = 0.2$	59
5.8	Average collision recovery probability versus the signal to noise ratio	63
5.9	Optimum frame length $L_{TCA}$ as a function of the slot duration constant $C_t$ ( $n = 100$ tags) for the capture probabilities $\alpha = 0.25, 0.5, 0.75$ .	64
5.10	Percentages of saving time using the proposed TCRA compared to the conventional frame length $L = n$ for perfect number of tags estimation using $C_t = 0.2$ and different values of $\alpha$	66
5.11	Percentages of saving time using the proposed TCRA compared to the conventional frame length $L = n$ for different anti-collision algorithms using $C_t = 0.2$ and $\alpha = 0.1$	67
5.12	Distribution of collision probability for a collided slot in FSA, under condition of $\frac{n}{2} \leq L \leq 2n$	68
5.13	Collision recovery coefficients versus SNR using the strongest tag reply receiver. (example)	71

5.14 Frame length comparison between the proposed formula and the numerical solution versus the SNR using the strongest tag reply receiver. . . . .	72
5.15 Percentages of saving time using the proposed MCR compared to the conventional frame length $L = n$ for perfect number of tags estimation using $C_t = 0.2$ and different $SNR$ values . . . . .	73
5.16 Percentages of saving time using the proposed MCRA compared to the conventional frame length $L = n$ using different anti-collision algorithms with $C_t = 0.2$ and $SNR = 4$ dB . . . . .	74
5.17 Frame length comparison between the proposed formula and the numerical solution versus the SNR using the strongest tag reply receiver. . . . .	77
5.18 Percentages of saving time using the proposed TMCRA compared to the conventional frame length $L = n$ for perfect number of tags estimation using $C_t = 0.2$ . . . . .	79
5.19 Percentages of saving time using the proposed TMCRA compared to the conventional frame length $L = n$ using different anti-collision algorithms with $C_t = 0.2$ and $SNR = 8$ dB . . . . .	80
5.20 Comparison between the average reading time of the proposed systems, conventional FSA and the theoretical limit . . . . .	82
6.1 Conventional tag response . . . . .	86
6.2 Two tags collided slot according to EPCglobal class 1 gen 2 standards . . . . .	87
6.3 Tag response of the proposed tags including the new pilot sequences . . . . .	88
6.4 Modified part of tags state diagram . . . . .	90
6.5 Example of the proposed pseudo parallel successful slot with parallel Query command and RN16 followed by successive Acknowledgment commands and EPCs . . . . .	91
6.6 Communication link measurement . . . . .	94
6.7 Reading efficiency for the conventional FSA and different acknowledgment scenarios using 8-orthogonal pilots . . . . .	95

6.8 Comparison between the average reading time for different systems . . . . .	96
---	----

# **Chapter 1**

## **Introduction**

(RFID) is a technology that uses communication through radio waves to transfer data between a reader and electronic tags attached to the object either to be identified or tracked. RFID technology gives more benefits than other identification technologies such as no line-of-sight connection, fully automotive identification process, robustness, identification speed, bidirectional communication, reliability in different environment conditions, bunch detection and secured communication. Thus, RFID became particularly optimum solution for several applications where other identification technologies such as barcodes are unsuitable e.g. inventory tracking, supply chain management, automated manufacturing, etc. Due to the clear importance of the RFID system in different real applications, RFID systems have received large attention from both research groups and industry. Recently, a lot of work has been published on the area of RFID systems either in hardware and software design or in protocols and applications, etc.

The rest of this chapter presents the motivations behind our research. Afterward, the thesis contributions will be highlighted, and finally the outline of the thesis document will be presented.

### **1.1 Motivation**

Over the recent years, the number of applications that use Radio-Frequency Identification Systems (RFID) has increased, and their number will further grow in the near future. One main application is the area of logistics, where

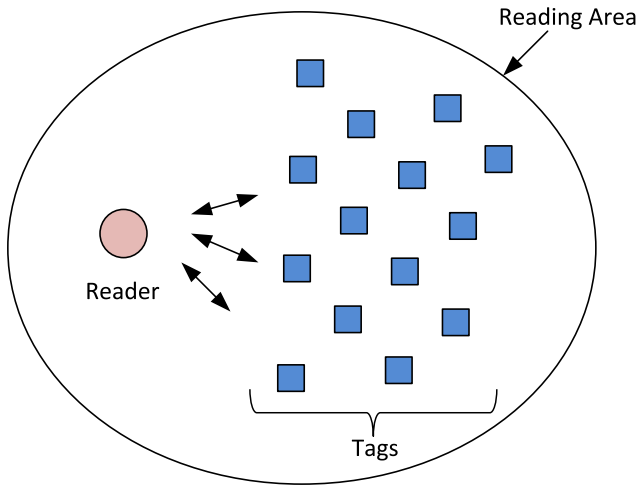


Figure 1.1: Dense RFID network with single RFID reader

e.g. hundreds of tags (transponders) may be closely placed on pallets. Thus, in our system we have single RFID reader responsible to identify bunch of tags in the reading area as shown in figure 1.1. This naturally requires fast RFID readers (interrogators), in order to not slow down the delivery process of the actual goods. Commonly used RFID standards in the area of logistics (e.g. ISO 18000-6C [3]) base on TDMA (time division multiple access), which leads to a certain probability of tag-collisions on the communications channel. As the tags are of low price and simple design, they neither can sense the channel nor communicate with the others. Hence, the readers are responsible for coordinating the network, and for the avoidance of collisions using anti-collision algorithms.

According to the previously published RFID work, (FSA) [4] is the most widely used MAC (Medium Access Control) anti-collision protocol for RFID systems due to its simplicity and robustness. In FSA, the communication timing between the reader and the tags is divided into TDMA frames, each frame includes a specific number of slots. The frame length is function of the exist number of tags in the reading area. During the reading process, each active tag randomly assigns itself to one of the available slots in a frame. Therefore, each slot can take one of the three different states: 1) Successful Slot: Only one tag chooses this slot, is fully identified, and then deactivated by the reader. 2) Collided Slot: Multiple tags reply, resulting in a collision. The collided tags

normally remain in their active state and retry their transmission in the next frame. 3) Empty Slot: No tag responds and the slot remains unused. Therefore, the reading efficiency is limited by the effect of three parameters:

1. The number of empty slots in FSA.
2. The number of collided slots in FSA.
3. The robustness of the number of tags estimation algorithm, as in real applications, the number of tags in the reading area is unknown.

Recent research groups have focused to use the PHY (Physical) Layer properties to convert part of the collided slots into successful slots. This phenomena is called Collision Recovery. This decrease the losses which come from the collision. Moreover, modern RFID readers have the ability to identify the type of the slot (successful, collided, or empty). Then, the readers are able to terminate the slot earlier when they recognizes that there is no tag reply, which eliminate the effect of the empty slots.

According to the previous discussion, the number of tags estimation algorithm and the optimum FSA frame length are strongly depend on the PHY-layer properties of the used system.

## 1.2 Thesis Contribution

Our research aims to improve the performance of existing RFID systems, mainly by minimizing the total identification delay. We focus on optimizing FSA frame length and the number of tags estimation algorithm taking into consideration the PHY-layer parameters. Moreover, we give feedback decision for the PHY-Layer to start resolving the collision or not. We call it cross layer optimization. The main contributions of this thesis could be summarized in the following points:

1. A novel tag estimation method taking into consideration the collision recovery capability of the system. The main advantage of the proposed method is that it gives a novel closed form solution for the tag population estimator that considers the collision recovery probability of the used

system. Simulation results indicate that the proposed solution is more accurate compared to the literature. Timing comparisons presented in the simulation results show the reduced identification delay of the proposed estimation method compared to other proposals.

2. A closed form solution for the optimum frame length for FSA by optimizing the Time-Aware Framed Slotted ALOHA reading efficiency, which considers the differences in the slot durations. Simulations indicate that the proposed solution gives the most accurate results with respect to the exact solution. Moreover a gain of approx. 10% in terms of reading time wrt. the classical algorithm using parameters of the ISO 18000-6C UHF-RFID standard.
3. A closed form solution for optimum frame length for FSA by optimizing the Time and constant collision recovery coefficients Aware reading efficiency. The proposed solution gives a novel closed form equation for the frame length considering the different slot durations and the collision recovery capability with equal coefficients. Moreover, we present a new method to calculate the capture probability per frame. Simulations indicate that the proposed solution gives accurate results for all relevant parameter configurations without any need for Multi-dimensional look-up tables.
4. A novel closed form solution for the optimal FSA frame length which considers the differences in the collision recovery probabilities. The values of the collision recovery coefficients are extracted from the physical layer parameters. Timing comparisons are presented in simulation results to show the mean reduction in reading time using the proposed frame length compared to the other proposals.
5. A novel closed form solution for the optimal Frame Slotted ALOHA (FSA) frame length. The novel solution considers the multiple collision recovery probability coefficients, and the different slot durations. Timing comparisons are presented in the simulation results to show the reading time reduction using the proposed frame length compared to other the state-of-the-art algorithms.

6. Finally, we propose a compatible improvements of UHF standard. In this system, we have some compatible modifications in the UHF RFID tags/Readers, to be able to acknowledge more than single tag per slot.

### 1.3 Document Outline

The remainder of this document is organized as follows. Chapter 2 presents the historical background and literature survey of RFID systems. Chapter 3 presents the collision problem in the RFID systems and the existing anti-collision algorithms. Moreover we will define the concept of proposed cross-layer anti-collision algorithm. Chapter 4 presents the most commonly used number of tags estimation algorithms in the RFID system. Afterwards, the proposed collision recovery aware Maximum likelihood estimation algorithm. In this part, we will propose a closed-form solution for the estimated number of tags in the reading area taking into consideration the collision recovery capability of the used system. Chapter 5 shows different case studies for FSA frame optimization. Each case depends on the PHY-layer parameters. In each case a closed-form solution for the optimum FSA frame length is analytically derived function of the estimated number of tags and the PHY-layer parameters. Chapter 6 presents a compatible improvements of UHF standard. In this system, we have some compatible modifications in the UHF RFID tags/Readers, to be able to acknowledge more than single tag per slot. Finally, Chapter 7 concludes this document by highlighting the main issues addressed in this thesis and outlining some of the future research directions.



# **Chapter 2**

# **System Description**

This chapter provides an overview of the historical development of the RFID. Afterwards, we will describe the basic principles and the major technical aspects related to the RFID technology and its standardization. Finally, we will present the collision problem, which is major RFID problem in dense networks

This chapter is organized as follow: section 1 gives an overview about the historical development of the RFID. Section 2 presents the main components of the system. In section 3, we shows the operating frequency bands in the RFID. Afterwards, we will describe the classification of the RFID standards in section 4. Finally, the RFID collision problem will be presented in section 5.

## **2.1 Historical Development of RFID**

In 1935, the first idea of RFID system was invented by Scottish physicist called Robert Alexander. In 1950, the British government developed the first prototype of the RFID system, which known as Identify Friend (IFF) system. This system was designed for aeronautical applications. Between 1950s and 1960s, There was a big development in the RFID systems for different applications, such as application of the Microwave homodyne [5] and radio transmission system with modulatable passive responder [6]. In the 1970s, RFID was intensively applied to logistics, transportation, vehicle tracking, livestock tracking and in industrial automation. The first US patent in this field was published on 1973 for the invention of an active RFID tag with rewritable memory [7]. In the recent days, the low power ultra high frequency UHF-RFID system research

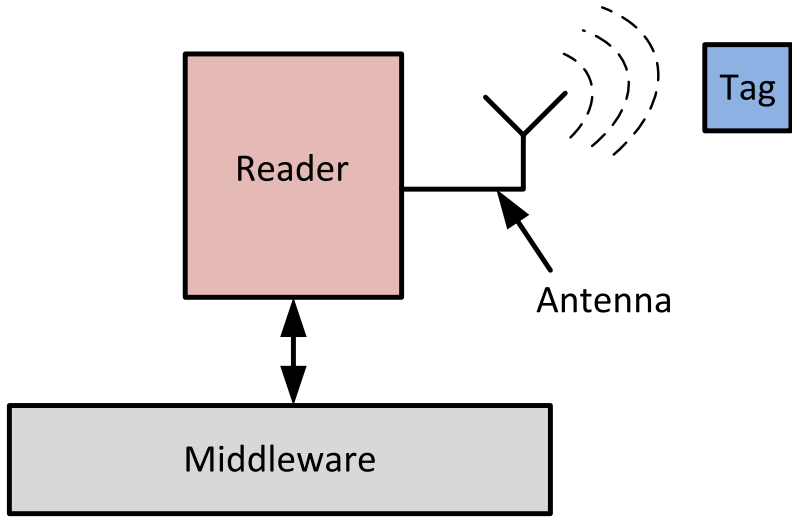


Figure 2.1: RFID System components

has gained a lot of importance. In 2008, the US Department of Defense, have said they plan to use electronic product code (EPC) technology to track goods in their supply chain. In Europe, RFID was intended to improve industrial applications and to enable short-range systems for animal control. In Japan, RFID was used for contact less payments in transportation systems.

## 2.2 system components

As shown in figure 2.1, conventional RFID systems consist of three main components:

- RFID tags or transponders which are attached to the object which is requested to be identified or tracked.
- RFID reader and antennas which control data transmission and the whole identification process.
- Processing device commonly called Middle-ware. It is always software processing device. All the external processing depending on the application is done on this device using the EPC code which is identified by the reader from the tag.

In the following sections, we will describe each of these components in more depth.

### 2.2.1 Tags

Tag is the device, which is attached to the object and stores information it and might be incorporate sensors. This information includes their unique EPC (Electronic Product Code), which is a standardized identification code. When tags are within the reading range, they receive a command from the reader asking them about their EPC. They reply with their identification data to the reader, which processes the information according to the current application. Generally, RFID tags is categorized into the following categories:

#### 2.2.1.1 Passive tags

Passive tags are the most commonly used tags in the tracking and supply chain market. they are extremely simple and inexpensive devices (less than 0.1 Euro). Passive tags do not contain any power source so they derive all of the required energy for their operation from the signals emitted by the reader. This energy activates the circuit of the tags. Then, they produce a reply signal that includes their information. The maximum communication range up to few meters.

#### 2.2.1.2 Active tags

Active tags are the second commonly used type of tags. they have a fully autonomous power source. The cost of these devices is much higher than passive ones (starting from 10 Euro) because they incorporate circuits with a micro-processor and a memory to read, write, rewrite or erase data from an external device. However, there are some advantage of active tags compared to the passive tags:

- Active tags support long reading distance, more than 100 meters.
- Immunity to the interference especially in the hard environment e.g. environments with high amounts of metals, such as shipping containers.

- Because they have power supply, they are easier to be connected with sensors to monitor the environment depending on the application e.g. food or drug shipments.

### **2.2.1.3 Semi-passive tags**

In this kind of tags, batteries are used on board to power the controller or the chip and may contain additional devices such as sensors. The signals which are generated by the reader are only used to activate tags in coverage. Then, the tag's reply is generated using the energy from the internal batteries. Semi-passive tags can communicate over longer distance than the normal passive tags. Moreover, the circuitry activation of the semi-passive tags is faster than in passive tags.

## **2.2.2 Readers**

The RFID reader is the most important element in a RFID system. It is responsible to access tag information. The reader decode the received date from the tags then send this information to the middle-ware. We can classify readers according to the type of tags as follow:

- Readers which deal with active tags. In active RFID systems, since active tags are able to initiate the communication between them, any active tag can act as a reader, when active tags act as a reader, they must be connected to a computer or a network (via a wired or wireless link) to send the received data from its network.
- Readers dealing with passive tags. They have to meet the following key requirement: their transmission power must be enough to feed the surrounding passive tags. The tags obtain energy from the transmitted signal using back-scattering technique. Back-scattering technique is the reflection of the reader's carrier wave and modulating the signal which includes the tag's data. Then, the reader detects the Tags response and processes the signal and reads the information sent by the tag.

Table 2.1: Frequency Bands for RFID Systems

Frequency Band	Range	Common Frequencies
Low Frequency (LF)	0.5 m	125 kHz, 134.2 kHz
High Frequency (HF)	1 – 3 m	13.56 MHz
Ultra High Frequency (UHF)	10 m	866 MHz Europe 915 MHz USA
Microwave ( $\mu$ W)	+10 m	2.45 GHz, 3.0 GHz

### 2.2.3 Antennas

Antenna designs are strongly depend on the operating frequency. In case of low range applications, such as LF (125 kHz) or HF (13.56 MHz) range, antennas are embedded in the readers. However in case of UHF applications, antennas have to be external. Moreover, polarization of the used antenna is one of the most critical issues. Antenna polarization affects directly the RFID system performance. In RFID system, there are two types of antenna polarization:

- Linearly polarized antennas: In this system, the electrical field component of the transmitted signal is propagated in a plane, and tags have to be also orientated in same direction of the transmitted signal. This technique requires also linearly polarized tags.
- Circularly Polarized antennas: In this system, the electromagnetic waves are transmitted in circularly polarized patterns. we use this type of polarization when we can not control the orientation of the tags with respect to the reader. Using circularly polarized antennas we can communicate with both (linearly and circularly) tags. However, circularly polarized antennas have a shorter read range than linearly polarized antennas.

### 2.2.4 Middle-ware

In some applications, the tag identifier is used as an input for a database to get an information related to this object e.g. shipment orders, expiring date. etc. This kind of processing is done in a set of software tools called middle-ware. EPCglobal standards [3] define some specifications for the middle-ware of RFID systems. However, RFID systems are still evolving technology. Thus, RFID

Table 2.2: RFID standards classification

Standards Classification	Description
Generation 1, Class 0	Read only passive tags Unique EPC programmed in the factory
Generation 1, Class 0+	Identical to the normal Generation 1, Class 0 tags Tags can be programmed by users
Generation 1, Class 1	Similar to Generation 1, Class 0 or 0+ tags Identified by readers from different companies
Generation 2, Class 1	Faster data rates than Generation 1 tags Rewritable memories
Generation 2, Class 2	Similar to Generation 2, Class 1 tags More noise immunity
Generation 2, Class 3	Semi-passive or battery assisted tags
Generation 2, Class 4	Active tags
Generation 2, Class 5	Active tags Capability to power on other tags

middle-ware should be flexible enough so that it could be adapted to the future changes with minimal efforts.

## 2.3 Frequency Bands

The most important differentiation criteria for RFID systems are the operating frequency of the reader. Selecting the most adequate frequency is a function of the following properties:

- The technical properties of the application e.g. The RFID channel contains metals or not.
- The cost of the system.
- The behavior of the electromagnetic waves at these different frequencies.

First RFID users started with low frequency (LF) band RFID systems. After few years, the RFID systems have operated in high-frequency (HF) band. Using only these two band made a big limitation on the RFID applications. Thus, Recent years, the number of RFID systems operating in the UHF range have increased because of the dramatic decrease in its component's price. Thus, it is

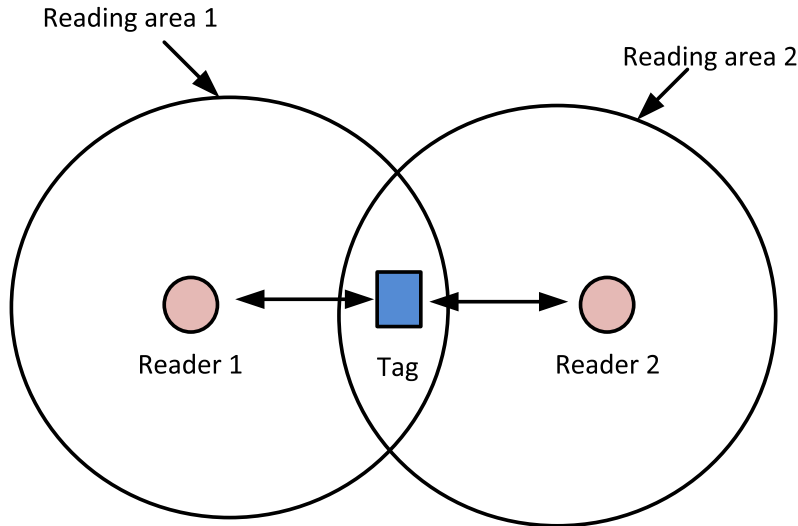


Figure 2.2: Multiple readers to a single tag collision

expected to see the RFID microwave band more available and affordable in the market. The availability of all bands with affordable costs will give the RFID users more facilities to take easier decision in which band they need to build up their applications.

Table 2.1 presents the most common frequencies for each band as well as the maximum allowed distance for each band. It is necessary to note that Table 2.1 does not present the only possible operating frequencies. It presents only the most commonly used frequencies in each band. Thus, it is possible to find systems, operating at different frequencies, within each frequency band.

## 2.4 RFID Standards

There are different standards of communication between the RFID reader and the corresponding tags. Although EPC-C1G2 standard is the most extended and adopted for passive dense RFID networks, there are also other standards. Table 2.2 shows the most common RFID standards with a short description for each one. In this work, we are interested in Generation 2, Class 1 standard, because it is the most suitable standard for dense RFID network, as the cost of the system is ideal for such applications.

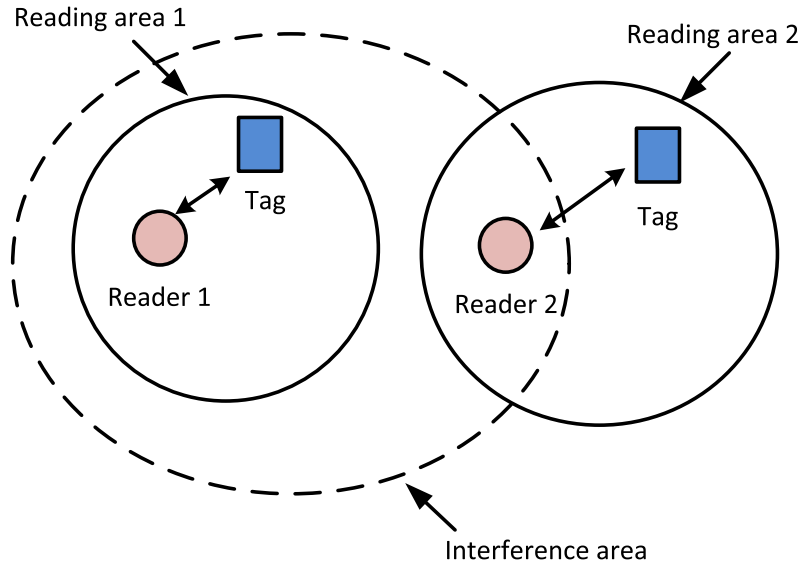


Figure 2.3: Multiple readers interference

## 2.5 Collision Problems

In RFID systems, both the readers and tags communicate at the same channel with the same frequencies. Thus, simultaneous transmission could be happened, and this leads to collision. Collisions destroy the Identification number (EPC) of the tag and may also interfere control commands of the readers. Thus, collisions problem is main source of delays in the identification process.

In RFID systems, there are two types of collisions: reader collisions and tag collisions. The following sections will describe in details both types and how each of them affects the performance of the system.

### 2.5.1 Readers Collisions

There are two main types of readers collisions or interference in RFID systems: multiple readers to tag collision and reader to reader collision.

#### 2.5.1.1 Multiple Readers to Tag Collision

multiple readers to tag collision occurs when one tag is simultaneously located in an overlapped area between two neighbors reading areas, and both readers communicate simultaneously with the shared tag as shown in figure 2.2. In this

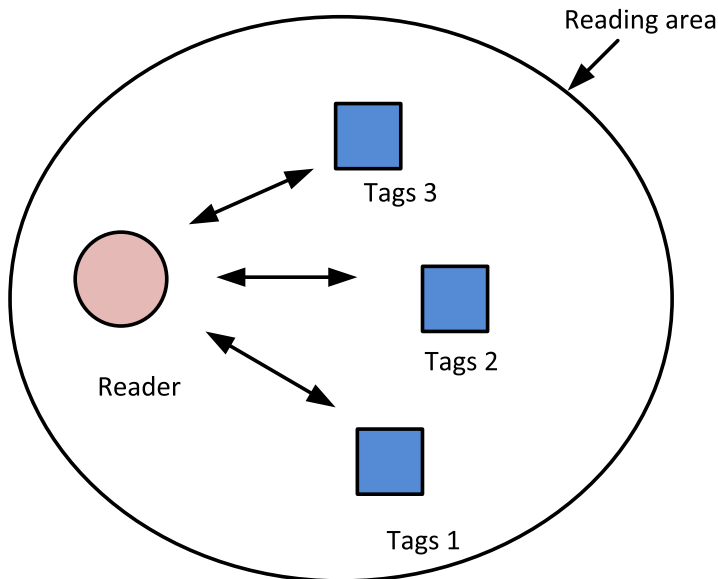


Figure 2.4: Multiple tags to a single reader collision

situation, the tag will not be able to determine such communication, because of the interference between the two readers commands. Therefore, the tag will not respond to any of the readers. Finally, this slot would be an empty slot and leads to losses in the total identification time.

### 2.5.1.2 Reader to Reader Collision

Reader to reader collision or interference occurs when the signal generated by a reader acts as a jamming signal for a neighbor reader as shown in figure 2.3. This signal might prevent the second reader from communicating with its tags in its reading area. Such interference can occur even if there is no overlapping area between the reading areas. This interference affects the total identification time of the interfered system.

### 2.5.2 Tags Collisions

This type of collision is the most common type of collision happened in the dense RFID systems. In such systems, we have single RFID reader versus multiple tags as shown in figure 2.4. The main objective is to identify all tags in the reading area in the minimum possible time. Different research groups are

currently are associated with how efficiently develop an anti-collision protocol for such systems.

Anti-collision protocols can be classified into two main types: Physical layer protocols and MAC layers protocols.

In this work, we assume that the system includes only single RFID reader and dense RFID tags. The main motivation of this work is to minimize the total identification time for a dense RFID networks. Therefore, we are interested mainly to solve tags collisions problem by enhancing the existing anti-collision protocols taking into consideration the physical layer parameters. Moreover, this work is presented for the EPCglobal C1 G2 standards [3], thus the improvements are done only in the reader side. Finally we will propose in chapter 6 a slide modifications in the standard to have further improvements and compare the results together.

# Chapter 3

## RFID Anti-collision Protocols

In this chapter, we will present the most common anti-collisions algorithms for passive RFID systems, either using Physical layer or using MAC layer. We will concentrate more on the anti-collision algorithms which are compatible with the EPCglobal Generation 2 Class 1 standard, as it is the focus of this thesis.

This chapter is organized as follow: section 1 gives an overview about the physical layer anti-collision algorithms. In section 2, we presents different MAC-layer anti-collision algorithms, and we will discuss the main differences between them. Finally, section 3 will give an introduction about the main idea of the cross layer anti-collision algorithm, which we will focus on it in the remaining part of this thesis.

### 3.1 PHY-Layer Anti-collision Protocols

There are different physical layer anti-collision protocols have been developed to separate colliding signals at the Physical layer. Figure 3.1 shows the most common physical layer anti-collision protocols, which are: FDMA, SDMA, CDMA and TDMA. These algorithms will be briefly discussed in the following paragraphs:

#### 3.1.1 Frequency Division Multiple Access (FDMA)

In this protocol, the frequency band is divided into different sub-frequency bands and tags are distributed among them. However, this technique adds com-

plexity to the system. Readers should be dedicated for each channel. Moreover, tags should be able to select its desirable sub-channel. Only active tags can do such functionality.

### **3.1.2 Space Division Multiple Access (SDMA)**

This technique make use of spreading tags over the reading area. It provides a high increase in the reading efficiency. It is a sufficient technique in cases of single RFID reader versus dense RFID tags. The main drawback is the cost of implementing the RFID reader with multiple antennas.

### **3.1.3 Code Division Multiple Access (CDMA)**

This protocol uses spread-spectrum modulation techniques to transmit the data over the entire spectrum. CDMA is the ideal procedure for many applications, e.g. navigation systems. However in case of RFID systems, the cost of the tags will be dramatically increase. Thus, it is not a sufficient protocol for dense RFID networks.

### **3.1.4 Time Division Multiple Access (TDMA)**

In this protocol, a single frequency band is divided in time slots and is assigned to tags. One of the most important features of this technique is that each tag must be synchronized to the time slots and send its information at the beginning of the selected slot. This technique can be directly applied to passive RFID systems. In such systems, the simplicity of tags transfer the complexity to the readers. As the reader has to control the time synchronization. However in active RFID systems, synchronization can be either centralized or distributed on the tags.

## **3.2 MAC-Layer Anti-collision Protocols**

Unfortunately, the Physical layer anti-collision proposals are not cost effective for the market challenges of the passive RFID technologies. Therefore, collision solutions are commonly implemented at the MAC layer. In this section, we will

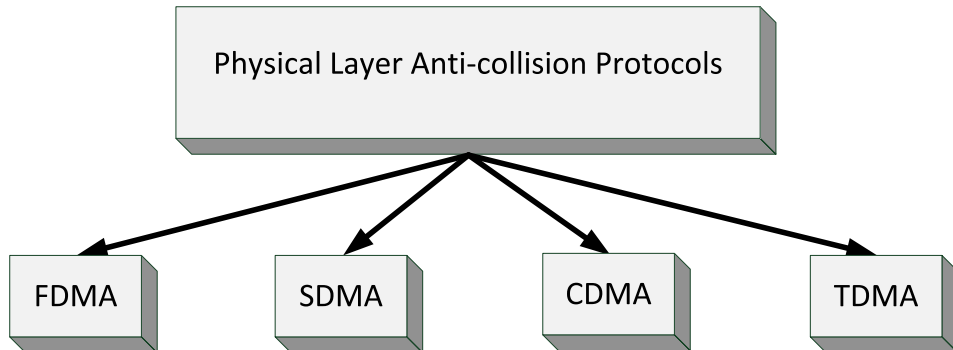


Figure 3.1: Common existing PHY-Layer anti-collision protocols

discuss the most common MAC-layer anti-collision protocols used in systems use single RFID reader wants to identify dense RFID tags.

Figure 3.2 presents the main classification of the most common MAC-layer anti-collision protocols. According to figure 3.2, MAC-layer anti-collision protocols is classified into two main categories. Deterministic protocols and probabilistic protocols. Deterministic protocols is used in the systems with known number of tags to be identified in the reading area. these types of protocols use mainly tree algorithms in their identification processes. However, the probabilistic protocols are in systems with unknown number of tags (most commonly used). Probabilistic protocols are mainly based on ALOHA algorithm.

The following sections will discuss in details the most commonly used anti-collision algorithms either deterministic or probabilistic based algorithm.

### 3.2.1 Deterministic Anti-collision Protocols

It is commonly named Tree-based anti-collision protocols. In such algorithms, the reader aims to identify a set of tags in the coverage area in successive time slots. Each time slot contains a Query packet, transmitted from the reader, and the response of tags in reading area. If there is more than one tag reply, a collision occurs and the reader tries to split the tags into two subgroups. The reader repeats the splitting procedure until receiving a single tag reply. Tree based anti-collision protocols can be classified into two groups:

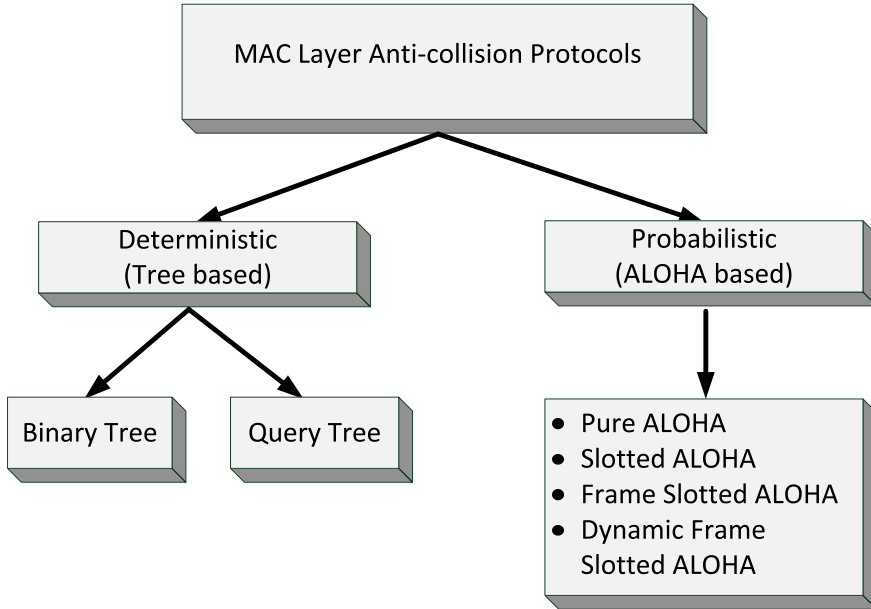


Figure 3.2: Common existing MAC-Layer anti-collision protocols

### 3.2.1.1 Binary Tree

Binary tree algorithm [8] is commonly used in tree-based anti-collision protocols. In this algorithm, if a collision occurs in a time slot, Each collided tag select randomly 0 or 1. Thus the colliding tags will be separated into two subgroups. The tags, which have selected 0 transmit their IDs to the reader first always. If a collision occurs again, the collided tags are split again by selecting 0 or 1. The tags which have selected 1 have to wait until all other tags which have select 0 are successfully identified by the reader. This procedure continues recursively until the subset is reduced to one tag, that is identified without collisions.

Figure 3.3 shows an example for the binary tree algorithm resolving the collision of 4 tags in a reading area. Thus, we have a collided time slot at the beginning. At time slot 2, each collided tag has to choose 0 or 1 randomly. In our example, tags 1 and 2 have selected 0. However, tags 3 and 4 have selected 1. According to binary tree algorithm, tags 3 and 4 have to wait until tags 1 and 2 are successfully identified. Therefore, time slot 2 is a collided slot due to the collision between tags 1 and 2. Due to collision, both tag 1 and 2 have to choose either 0 or 1. In this example, both tag 1 and 2 have selected

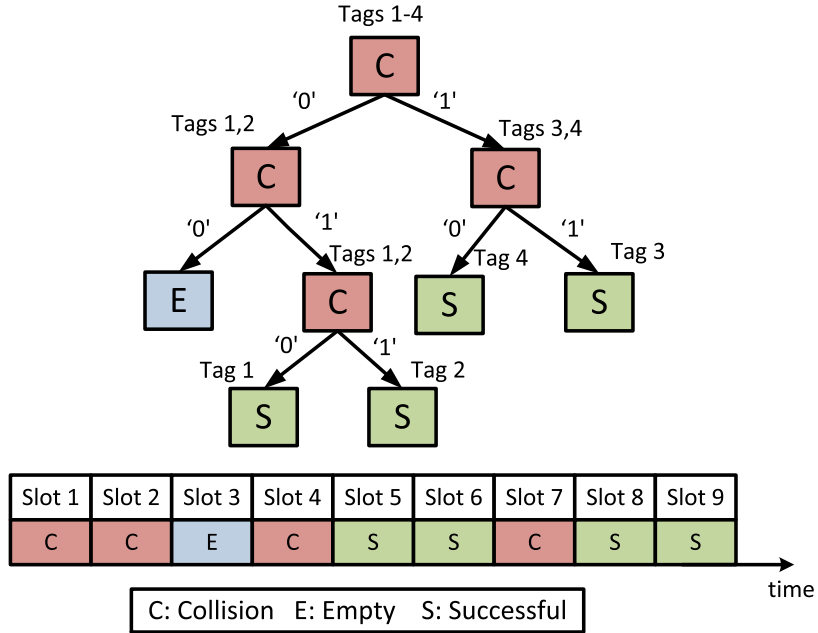


Figure 3.3: Binary tree anti-collision algorithm example

1. This resulted and empty slot in time slot 3 and collided slot in time slot 4.
2. Afterwards, tag 1 has selected 0 and tag 2 has selected 1. This random selection made them separated and resulted two successive successful slots in time slots 5 and 6. At this moment, tags 3 and 4 started their identification process. The reader repeat the previous process until identifying all the tags in the reading area.

### 3.2.1.2 Query Tree

Query tree algorithm [9] is also commonly used in tree-based anti-collision algorithm. In this algorithm, the broadcast a query signal asking the tags for a reply. If there is a collision, it starts splitting the collided tags into two groups by sending a new query signal with a single bit 0 or 1 randomly. The tags in the reading area receive this signal and match this bit with its ID. If this bit matches their ID they transmit their ID. IF a collision happened again, the reader adds another random bit 0 or 1 to its next query signal. This process is repeated until the reader receive a successful single tag reply.

Figure 3.4 presents an example for the query tree algorithm resolving the collision of 4 tags in a reading area. at time slot 1 the reader broadcast a query

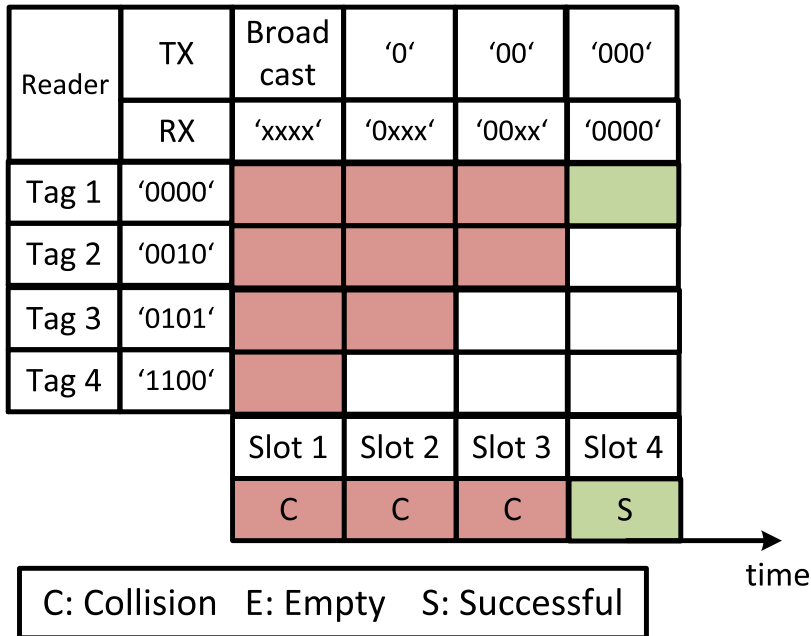


Figure 3.4: Query tree anti-collision algorithm example

signal asking them for a reply. a collision between the four tags is happened. The reader sends a '0' in a new query signal at time slot 2. However, there are three tags sharing this bit, so a collision between the three tags is happened. Thus, the reader has sent a '00' in its next query signal in time slot 3. At this time, we had a collision between two tags, which lead the reader to send '000' in time slot 4. Finally, the reader has received a single successful reply from tag 1. This process is repeated until the reader identify all the tags in the reading area.

### 3.2.2 Probabilistic Anti-collision Protocols

The main problem of using Tree-based protocols is that Tree-based protocols are not efficient in dense network (large number of tags), because of the increase in identification time. Therefore, in dense network, ALOHA anti-collision protocols are more suitable. ALOHA anti-collision protocols are the most commonly used in UHF active and passive RFID. In these protocols, the readers do not know exactly the number of tags in the reading area to be identified. ALOHA anti-collision protocols are classified into the following four groups:

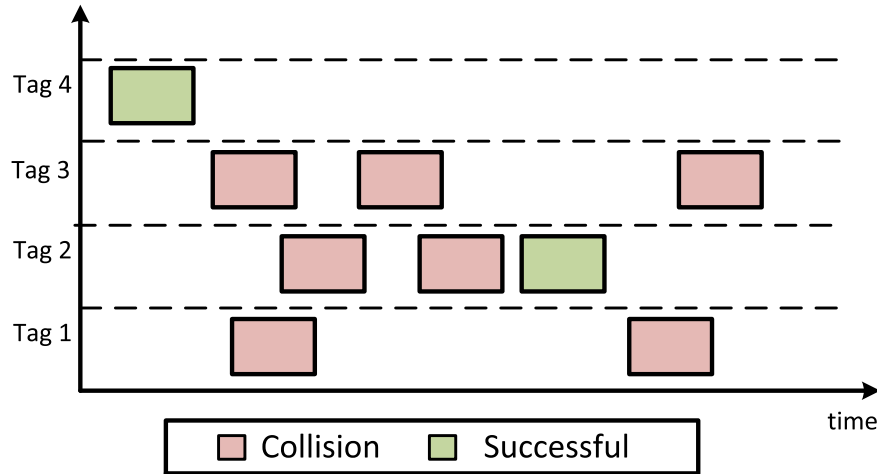


Figure 3.5: Example for pure ALOHA protocol

### 3.2.2.1 Basic ALOHA

The first one is the widely known basic ALOHA [10] anti-collision protocol. Basic ALOHA is the simplest anti-collision protocol for passive read only memory RFID tags. The protocol works as follow: The reader send a Query signal to power on tags. Then, tags send their ID randomly in time. The reader can only recognize the single tag reply, without any ability to handle the collision. Figure 3.5 shows an example of basic ALOHA for a single reader identifying four tags.

### 3.2.2.2 Slotted ALOHA

The second ALOHA anti-collision protocol is the slotted ALOHA protocol [11]. As shown in figure 3.6, slotted ALOHA is based on basic ALOHA. However, time is divided into slots. In this protocol, the reader broadcasts a query signal includes the start of each slot. Each tag chooses randomly if it will transmit at this slot or wait for another slot. The main advantage of this technique compared to basic ALOHA is: In slotted ALOHA, the tags replies are completely synchronized, which make the collided slots are due to completely overlapped tags replies. However, in basic ALOHA protocol, the partial overlapping is exist.

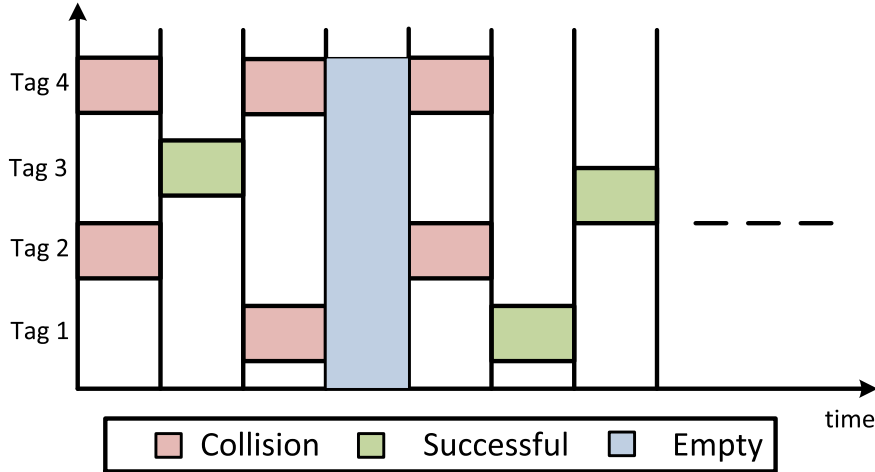


Figure 3.6: Example for slotted ALOHA

### 3.2.2.3 Framed Slotted ALOHA (FSA)

The third group is FSA (Framed Slotted ALOHA) [12]. FSA anti-collision protocol uses fixed frame length. Thus, the frame length is fixed during the complete tags identification process. At the beginning of each frame, the reader broadcasts a Query signal to all the tags. This signal includes the frame size. Each tag has to choose random number between 0 and  $L - 1$ , where  $L$  is the frame length. If a collision happened, the colliding tags has to wait for the next frame.

Figure 3.7 presents an example for the identification process for 4 tags using FSA. In this example, the frame length is selected to be 4 slots. According to figure 3.7, tag 4 transmits at the first slot alone. Thus, it is a successful slot. At the second slot, no tag has replied. So, it was an empty slot. At the third slot, tags 3, 4 have replied together, which resulted a collided slot. According to the FSA rules, tags 3, 4 are not allowed to resubmit their IDs again during the same frame. Thus at slot 4, tag 1 only is allowed to reply to have another successful slot. In the next frame, the same procedure is repeated until we have the all tags are identified.

### 3.2.2.4 Dynamic Frame Slotted ALOHA (DFSA)

The final type of ALOHA anti-collision protocols is DFSA (Dynamic Framed Slotted ALOHA) [13]. In this algorithm, the number of slots per frame is vari-

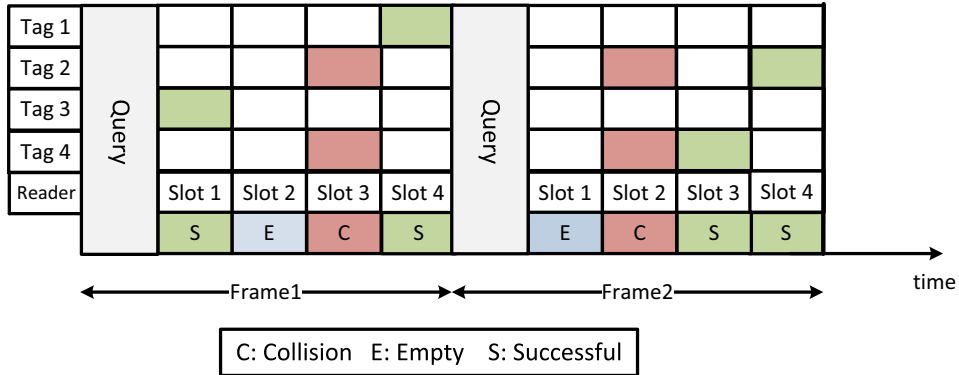


Figure 3.7: Example for Frame Slotted ALOHA

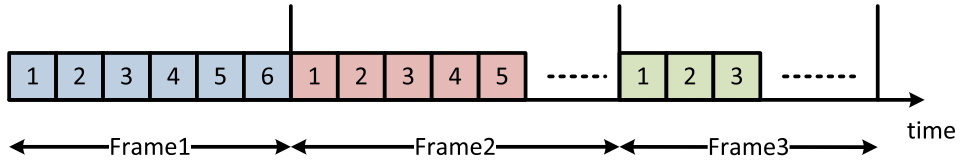


Figure 3.8: Slots of Dynamic Frame Slotted ALOHA

able as shown in figure 3.8. According to the previously published RFID work, DFSA [4] is the most widely used anti-collision protocol for RFID systems due to its simplicity and robustness. In DFSA, the reading process is divided into successive frames, each frame includes a specific number of slots. During the reading process, each active tag randomly assigns itself to one of the available slots in a frame. Therefore, each slot can take one of the three different states:

1. Successful Slot: Only one tag chooses this slot, is fully identified, and then deactivated by the reader within the following frames.
2. Collided Slot: Multiple tags reply, resulting in a collision. The collided tags normally remain in their active state and retry their transmission in the next frame.
3. Empty Slot: No tag responds and the slot remains unused.

Increasing the reading speed can directly be translated into the maximization of the number of successful slots wrt. the number of idle or collided slots. Based on the Random Access Theory [14], for a given number of  $n$  tags, the expected

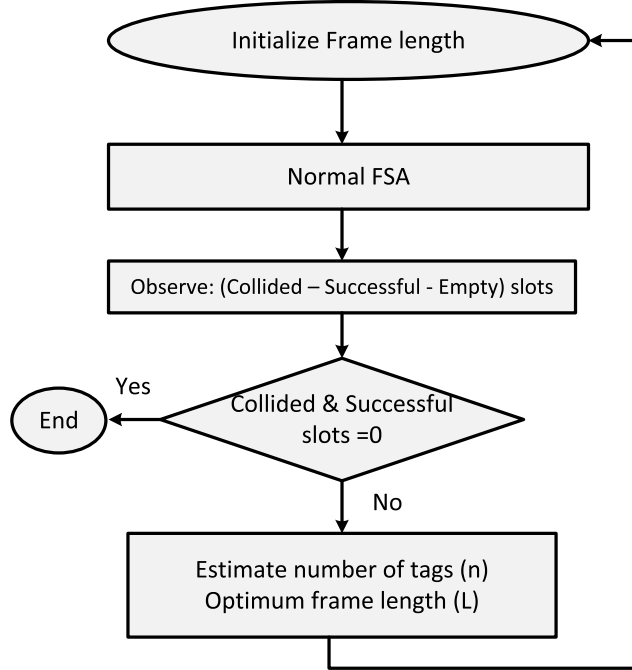


Figure 3.9: Flow chart of Dynamic Framed Slotted ALOHA (DFSA)

number of empty  $E$ , successful  $S$ , and collided  $C$  slots in each frame with a length of  $L$  slots can be expressed by the following equations:

$$E = L \left(1 - \frac{1}{L}\right)^n, S = n \left(1 - \frac{1}{L}\right)^{n-1}, C = L - E - S \quad (3.1)$$

The conventional definition of the expected reading efficiency  $\eta_{conv}$  is given by the ratio between the expected number of successful slots  $S$  in a frame and the frame length  $L$  [15]:

$$\eta_{conv} = \frac{S}{L} \quad (3.2)$$

Based on (3.1) and (3.2), this results in the conventional definition of the efficiency:

$$\eta_{conv} = \frac{n}{L} \left(1 - \frac{1}{L}\right)^{n-1} \quad (3.3)$$

The main goal for optimizing the DFSA algorithm is finding the optimal frame length  $L$ , which maximizes the reading efficiency  $\eta_{conv}$ . Based on (3.3), the reading efficiency  $\eta_{conv}$  is maximized when  $L_{opt} = n$  as shown in [15]. However,

in practical applications, the number of tags  $n$  in the interrogation region is unknown. Furthermore, the number of tags may even vary, e.g. when the tags are mounted on moving goods, and because successfully read tags get inactive in the following frames. Therefore, such applications employ DFSA [16]. First, DFSA has to estimate the number of tags in the interrogation area, and then has to calculate the optimal frame size  $L$  for the next reading frame. Therefore, the system performance mainly depends on the precision of the estimated number of tags  $\hat{n}$  then adapting the frame length of DFSA to keep on working with maximum efficiency. Figure 3.9 presents a summary for dynamic Framed Slotted ALOHA (DFSA). As shown in the chart, The reader starts with initial frame length. The reader broadcasts this frame length to the tags in the reading area. Afterwards, it performs normal FSA. At the end of the frame, the reader checks if there is any successful or collided slots. If yes, the reader estimates the remaining number of tags in the reading area, and then optimizes the next frame length and starts again normal FSA. If no, it would be the end of the reading cycle.

### 3.3 Cross Layer Anti-Collision Protocol

Recently, some research groups (e.g. [17,18]) have concentrated on the resolving the collided slots and converting them into successful slots using the spatial diversity of the received signal. They have proposed the following reading efficiency equation:

$$\eta = P(1) + \alpha \cdot \sum_{i=2}^n P(i), \quad (3.4)$$

where  $\sum_{i=2}^n P(i)$  is the probability of collision,  $\alpha$  is the average collision resolving probability coefficient. In this efficiency equation, the RFID reader can convert part of the collided slots into successful slots. The authors here have assumed unlimited and equal collision resolving probabilities coefficients. For example, the probability to resolve two collided tags is identical to the probability to resolve ten collided tags. Another research group [19] considered the limited RFID reader capability of collision resolving. They have proposed a limited reading efficiency expressed as:

$$\eta = \sum_{i=1}^M P(i), \quad (3.5)$$

where  $P(i) = \binom{n}{i} \left(\frac{1}{L}\right)^i \left(1 - \frac{1}{L}\right)^{n-i}$ , and  $M$  represents the number of collided tags that the reader is capable to recover. The authors assumed that the probability to recover one tag from  $i$  collided tags equals to 100%, independent of  $i$ .

According to the above short discussion, resolving the collisions in the RFID systems is improved using two main methods:

- Physical layer: In this method, some of the collided slots are converted to successful slot using the physical layer properties.
- MAC layer: In this method, DFSA is used to maximize the reading efficiency. The number of tags in the reading area should precisely estimated, and then the frame length should be optimized.

The main lack in the above work is that each layer is optimized independent on the other layer which gives sub-optimal solutions. Thus, in this work, we will concentrate on optimizing DFSA anti-collision protocol, either number of tags estimation or frame length optimization. In the proposed algorithm, we take into consideration the physical layer parameters which are presented on the physical collision recovery capability of the RFID reader. Afterwards, we will propose some backward modifications in the EPCglobal C1 G2 tags to increase the reading efficiency of the RFID systems.

# Chapter 4

## Estimation of the Tag Population

The conventional anti-collision algorithm in EPCglobal C1 G2 [3] is the Dynamic Framed Slotted ALOHA (DFSA) algorithm [14]. In such systems, only the answer of a single tag is considered as a successful slot, and if multiple tags respond simultaneously, a collision occurs. Then all the replied tags are discarded. The performance of DFSA-based protocols is maximized by adapting the frame length  $L$  to the number of tags  $n$ . However in practical applications, the number of tags  $n$  in the reading area is unknown. Therefore, Dynamic Framed Slotted ALOHA (DFSA) [16] is commonly used. DFSA first estimates the number of tags in the interrogation area, then calculates the optimal frame size  $L$  for the next reading cycle. Therefore, the system performance is controlled by the precision and the speed of the number of tags estimation.

In this chapter, we will present the most common estimation algorithms, which follow the EPCglobal C1 G2 standard [3]. Afterwards, a novel number of tags estimation method called: Collision Recovery Aware Tag Estimation will be presented. The proposed method takes into consideration the collision recovery probability from the physical layer.

This chapter is organized as follow: section 1 shows the conventional number of tags estimation algorithms with a brief performance analysis comparisons between them. Section 2 presents a novel collision recovery aware number of tags estimation method. In this algorithm, a closed form solution for the estimated number of tags will be presented. The proposed solution gives a

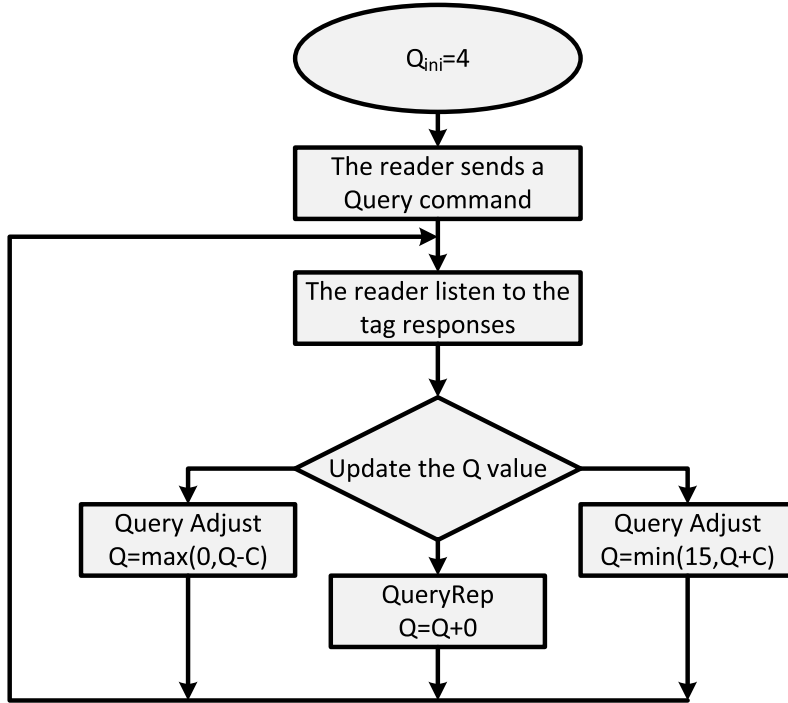


Figure 4.1: Heuristics Q-Slot Family, variable frame length procedure EPC-global C1 G2 [3]

direct relation between the estimated number of tags and the frame length, successful and collided number of slots and the physical layer collision recovery probability.

## 4.1 State-of-the-Art Estimation Protocols

In this section, we will classify the most common estimation algorithms into four groups. Heuristic Q-slot family, indirect heuristics Q-frame family, Error minimization estimation, and maximum likelihood estimation.

### 4.1.1 Heuristics Q-slot family

The EPCglobal C1 G2 standard [3] proposes an alternative frame length adaptation mechanism without any prior tag estimation. In this mechanism, the initial frame length is fixed  $Q_{ini} = 4$ , then the frame length is adjusted slot by slot according to the slot type: empty, successful, or collided. Figure 4.1 shows

the reader procedure using Heuristics Q-Family. According to figure 4.1, the performance of this scheme strongly depends on the value of the variable  $C$ , where  $C \in (0.1, 0.5)$ . Since the value of  $C$  is not clearly defined in the standard, there are different proposals optimizing the value of  $C$ .

#### 4.1.1.1 $Q^{+-}$ Algorithm

This algorithm is proposed by [20]. In this algorithm, Query command is transmitted only if the reader has to calculate a new value of  $Q$ . Otherwise, the reader transmits QueryRep command, because the Query command length is 22 bits and QueryRep command length is only 4 bits. Moreover, The variable  $C$  is replaced by two variables:  $C_e$  and  $C_c$ .

$C_e$  is used when empty slot is detected by the reader.  $C_c$  is used when collided slot is detected by the reader. The values of  $C_e$  and  $C_c$  are calculated numerically regardless the number of tags in the reading area. Therefore, this method gives better performance than the static EPC algorithm only.

#### 4.1.1.2 Optimum-C Algorithm

This algorithm is proposed by [21]. In this algorithm, the optimum value of  $C$  is calculated numerically versus the previous value of  $Q$ . This is done by simulating a passive RFID system for all range of  $Q \in [0, \dots, 15]$ . For each  $Q$ ,  $C \in [0.1, \dots, 0.5]$  with step 0.1. Finally the best combination is the combination which gives the minimum identification delay.

#### 4.1.1.3 Slot Count Selection (SCS) Algorithm

This algorithm is proposed by [22]. In this algorithm, the variable  $C$  is replaced by two variables  $C_1$  and  $C_2$  like  $Q^{+-}$  approach [20]. However,  $C_1$  and  $C_2$  in SCS algorithm are calculated slot by slot as a function of other parameters. These parameters depend mainly on the Reader to Tags (R-T) and Tags to Reader (T-R) data rates. According to [22], the system performance well be improved if the values of  $C_2$  and  $C_1$  are set to be  $C_2 \in [0.1, 1]$  and  $C_1 = 0.1$ . However, the authors neglected the effect of the modulation and the encoding scheme, as the correct value of (T-R) data rate strongly depends on the modulation and the encoding scheme. Therefore results of [22] should be revised.

### 4.1.2 Indirect heuristics Q-frame family

In this family, the proposed algorithms first estimate the number of tags in the reading area  $\hat{n}$  is calculated and then adjust the optimum frame length  $L$  that maximizes the reading efficiency. The estimation process is based on information about the previous frame.

#### 4.1.2.1 Lower Bound

This method is proposed by [16]. It assumes a very trivial assumption for the lower bound of the number of tags in the reading area  $\hat{n}$ . It assumes that each collided slot involves two collided tags. There for it is presented as:

$$\hat{n}_i = S_i + 2 \cdot C_i \quad (4.1)$$

where  $i$  presents the frame index,  $S_i$ , and  $C_i$  are successively present the number of successful and collided slots in frame  $i$ .

#### 4.1.2.2 Schoute Algorithm

Schoute [13] proposed a posterior expected factor of 2.39 to estimate the number of tags in the interrogation area. Thus it could be presented as:

$$\hat{n}_i = 2.39 \cdot C_i \quad (4.2)$$

This expected value is exact if and only if the the prior distribution of the tags is Poisson distribution with mean equal to 1.

#### 4.1.2.3 C-Ratio

In C-Ratio estimation method [23], the authors proposed a binomial distribution for the number of tags which select a slot with probability of success  $P = \frac{1}{L}$ , where  $L$  is the frame length. The definition of the collision ration is the ratio between the number of collided slots  $C_i$  and the frame length  $L_i$ , where  $i$  is the frame index. Therefore, C-Ratio could be expressed as:

$$C_{ratio} \triangleq \frac{C_i}{L_i} = 1 - \left(1 - \frac{1}{L_i}\right)^{n_i} - \left(1 + \frac{n_i}{L_i - 1}\right) \quad (4.3)$$

The optimum value of  $\hat{n}_i$  is obtained by searching for the all possible values of  $n$  that makes the right hand side of (4.3) gives the closest value of C-Ratio, under condition that  $n_i \geq 2 \cdot C_i$ . However, (4.3) is undefined when the number of collided slots is equal to the frame length ( $C_i = L_i$ ). This could occur when the frame length is short compared to the number of tags in the reading area.

In [24], the authors used the same concept of the C-Ratio. However, they assume independent binomial distribution of the tags in each slot. Thus, the modified C-Ratio could be expressed as:

$$\frac{C_i}{L_i} = \sum_{j=2}^{n_i} \binom{n_i}{j} \left(\frac{1}{L_i}\right)^j \left(1 - \frac{1}{L_i}\right)^{n_i-1} \quad (4.4)$$

This estimator suggest applying an upper bound to estimate the number of tags.

#### 4.1.3 Error Minimization Estimation

Vogt proposes in [14] an estimation algorithm based on Minimum Squared Error (MSE) estimation. It minimizes the distance between the observed empty  $E$ , successful  $S$ , collided  $C$  slots and their expected values  $E_{exp}$ ,  $S_{exp}$ ,  $C_{exp}$  for a given frame length  $L$ . It is presented as:

$$\varepsilon_{conv}(L, S, C, E) = \min_n \{|E_{exp} - E| + |S_{exp} - S| + |C_{exp} - C|\} \quad (4.5)$$

where

$$E_{exp} = L_i \left(1 + \frac{1}{L_i}\right)^n, S_{exp} = n \left(1 + \frac{1}{L_i}\right)^{n-1}, C_{exp} = L_i - E_{exp} - S_{exp} \quad (4.6)$$

However, This method requires numerical searching to find the optimum value of the number of tags  $n$ . Moreover, the author assumed that tags are identically distributed over slots, which is generally not an accurate assumption.

#### 4.1.4 Maximum Likelihood (ML) Tag Estimation

The main concept of ML tag estimation is to compute the conditional probability of an observed event assuming that this conditional probability is function

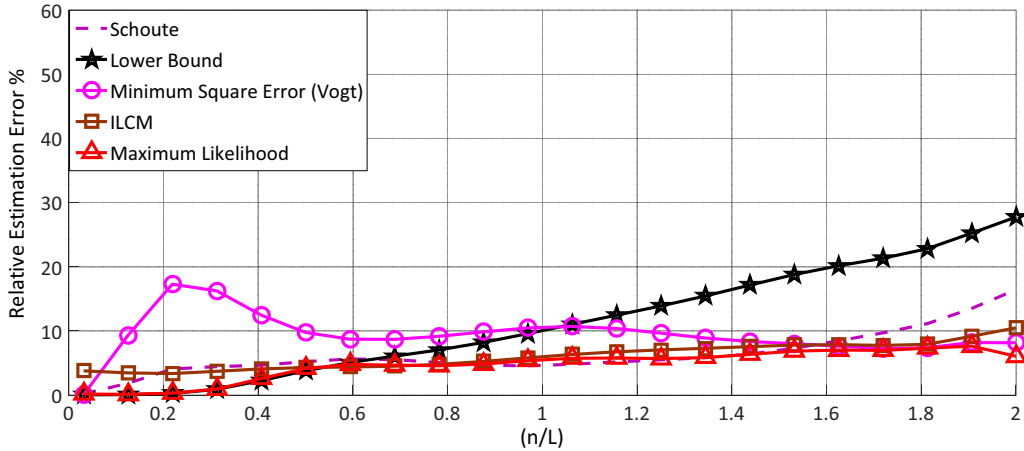


Figure 4.2: Relative estimation error  $\epsilon$  vs normalized number of tags  $n/L$  for the common state-of the-art estimation algorithms

of the number of tags  $n$ . Afterwards, we select the  $n$  which maximizes this conditional probability. The most common ML tag estimation in the state of the art is presented in [25]. The author modeled the problem by finding the optimum  $n$  that gives exact  $E$  empty slots,  $S$  successful slots,  $C$  collided slots if there are  $L$  slots. The author assumes a multinomial distribution with  $L$  repeated independent trials, where each trial has one of three possibilities:  $P_e$  empty,  $P_s$  successful, or  $P_c$  collision. where  $P_e$ ,  $P_s$ , and  $P_c$  follow binomial distribution and could be presented as:

$$P_e = \left(1 + \frac{1}{L}\right)^n, P_s = \frac{n}{L} \left(1 + \frac{1}{L}\right)^{n-1}, P_c = 1 - P_e - P_s \quad (4.7)$$

The probability that in  $L$  trials,  $E$  empty slots,  $S$  successful slots, and  $C$  collided slots occur is:

$$P(n|L, S, C, E) = \frac{L!}{E!S!C!} P_e^E P_s^S P_c^C, \quad (4.8)$$

This probability is the general term of the multinomial expansion of  $(P_e + P_s + P_c)^L$ . Therefore, for a read cycle with frame length  $L$ , we have a posteriori probability for the number of tags  $n$  when  $E$  empty slots,  $S$  successful slots, and  $C$  collided slots are observed, as shown in (4.8).

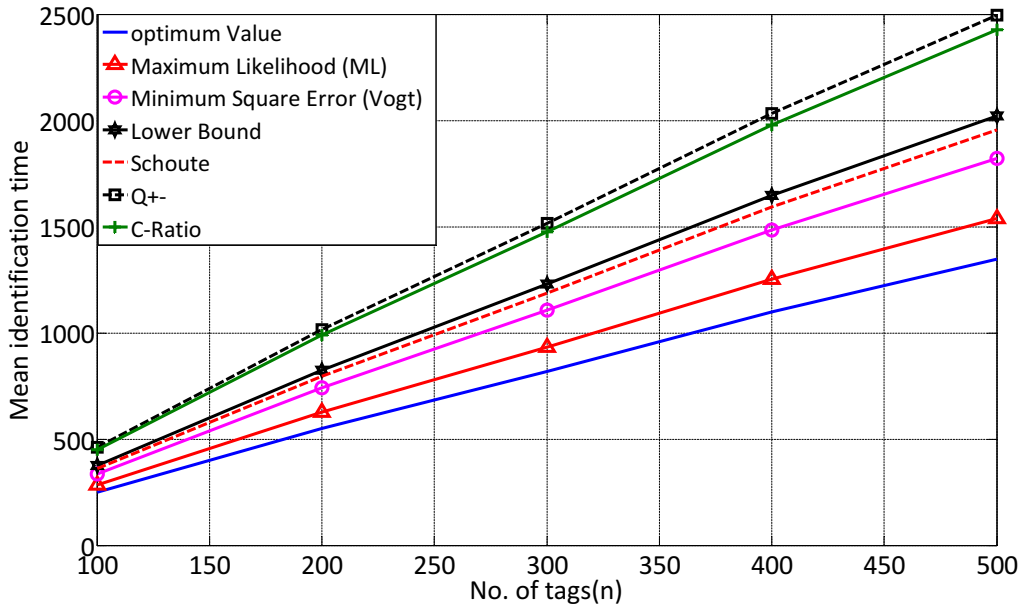


Figure 4.3: Mean identification time versus the number of tags in the reading area for the common state-of the-art estimation algorithms

#### 4.1.5 Performance Comparison for Existing Estimation Protocols

Firstly, we will define a performance metric called relative estimation error  $\epsilon$ . It presents the absolute difference between the actual number of tags and the estimated one divided by the actual number of tags in the reading area. Thus, it can be defined as

$$\epsilon = \left| \frac{\hat{n} - n}{n} \right| \times 100 \% \quad (4.9)$$

Figure 4.2 shows the relative estimation error  $\epsilon$  comparison versus the normalized number of tags  $n/L$  between the most common number of tags estimation algorithms in the passive UHF RFID systems. According to figure 4.2, Maximum Likelihood (ML) [25] estimation method is the most accurate estimation algorithm. It gives the minimum relative estimation error even in dense RFID networks, which is the main focus of the proposed work. However, the complexity of ML algorithm is much higher than the other estimation algorithm. This disadvantage make ML estimation not a practical solution for the dense RFID networks.

Figure 4.3 shows another comparison metric, which is the mean identifica-

tion time required to identify  $n$  number of tags. The comparison is between the average identification time using FSA algorithm with the most common existing number of tags estimation protocols. The optimum value presents the mean identification time using FSA with known number of tags in the reading area. According to figure 4.3, the Maximum Likelihood (ML) estimator [25] achieves the closest approach to the optimal algorithm. However, the numerical searching complexity of the ML estimator [25] might lead to numerical instability problems for simple low-end devices as described in [26]. This leads us to search for a method to compromise between the accuracy of the protocol and the stability of its implementation for dense RFID networks. Moreover, all these method do not take into consideration the collision recovery capabilities effect from the modern RFID physical layer.

## 4.2 Novel Collision Recovery Aware Tag Estimation

Modern systems have the capability to convert part of collided slots into successful slots. In such systems, the number of collided and successful slots which delivered to the MAC layer are not accurate information about the real number of tags at the reading area. Therefore we should take into consideration the collision recovery probability  $\alpha$ . [17] used the estimation approach of [14] taking into consideration the collision recovery probability. However this method leads to have Multi-dimensional searching, which time consuming and high complexity.

In this section, I propose a novel closed form solution for the estimated number of tags  $n$  taking into consideration the collision recovery probability of the system. Then I will show how to calculate the collision recovery probability from the physical layer parameters. The proposed solution gives a direct relation between the estimated number of tags  $n$  and the frame length  $L$ , successful and collided number of slots  $S, C$ , and the collision recovery probability  $\alpha$ .

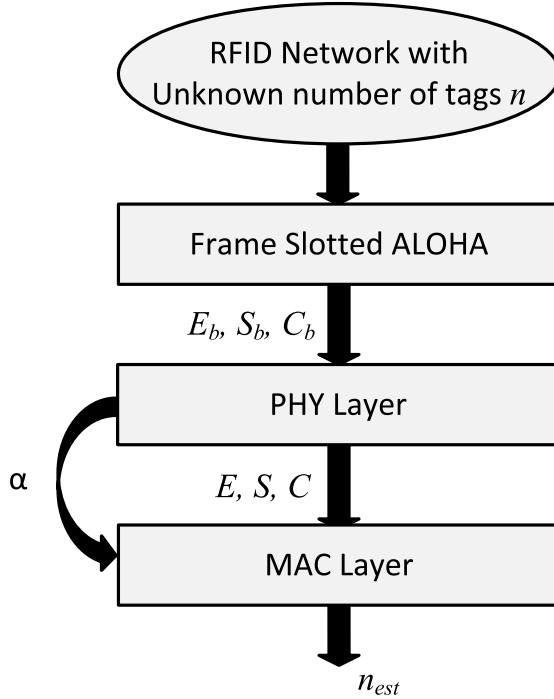


Figure 4.4: Physical layer collision recovery capability

#### 4.2.1 System Model Under Collision Recovery Probability

Now, a novel collision recovery aware number of tags estimation method will be described. The proposed method is based on the classical Maximum Likelihood (ML) estimation presented in [25]. According to the classical ML estimation method, we search for the optimum value of  $\hat{n}$  which maximizes the conditional probability of the observing vector  $v = \langle C, S, E \rangle$  given that  $n$  tags transmit at a frame length  $L$ :

$$P(n|L, S, C, E) = \frac{L!}{E!S!C!} P_e^E P_s^S P_c^C, \quad (4.10)$$

where  $C, S, E$  are successively the number of collided, successful, and empty slots per a frame length  $L$ , and  $P_e, P_s, P_c$  are respectively the probabilities of empty, successful and collided transmissions per slot. However, modern RFID readers have a collision recovery capability. Thus, the physical layer converts part of collided slots into successful slots based on the following relation:

$$E = E_b, S = S_b + \alpha \cdot C_b, C = C_b - \alpha \cdot C_b, \quad (4.11)$$

where  $C_b$ ,  $S_b$ ,  $E_b$  are successively the number of collided, successful, and empty slots before the collision recovery of the system, and  $C$ ,  $S$ ,  $E$  are respectively the number of collided, successful, and empty slots after collision recovery of the system.  $\alpha$  is the collision recovery probability. Figure 4.4 clarifies the flow diagram of the proposed system. In this system, the physical layer gives the MAC layer information about its collision recovery capability.

In the MAC layer, only the values of  $C$ ,  $S$ ,  $E$  after the collision recovery are known, and there is no information about these values before the collision recovery. Thus, the conventional estimation systems including the classical ML number of tags estimation in (4.10) use the values of  $C$ ,  $S$ ,  $E$  after collision recovery in their calculations. However, these values are not an accurate indicator for the actual number of tags in the reading area. In the proposed system, we estimate the value of the current average collision recovery probability  $\alpha$  as shown in [27]. Afterwards, we calculate the expected corresponding values of  $C_b$ ,  $S_b$ ,  $E_b$  as:

$$E_b = E, C_b = \left\lfloor \frac{C}{1 - \alpha} \right\rfloor, S_b = S - \left\lceil \frac{\alpha}{1 - \alpha} \right\rceil C \quad (4.12)$$

Under the condition:

$$L = E_b + S_b + C_b \quad (4.13)$$

Thus,  $C_{b(max)} = L - E_b$  and  $S_{b(min)} = 0$ . Therefore, the proposed collision recovery aware ML conditional probability can be formalized as:

$$P(n/L, S, C, E, \alpha) = \frac{L!}{E_b! S_b! C_b!} P_e^{E_b} P_s^{S_b} P_c^{C_b} \quad (4.14)$$

In this work, we are interested in the dense RFID network so we can use the approximation suggested in [26] for the tag probability of transmission per slot, which are considered as independent Poisson random variables with unknown mean  $\gamma = \frac{n_{est}}{L}$  to have:

$$P_e = e^{-\gamma}, P_s = \gamma \cdot e^{-\gamma}, P_c = 1 - e^{-\gamma} - \gamma \cdot e^{-\gamma} \quad (4.15)$$

After substituting by (4.15) in (4.14) and normalizing the resulting equation from the constant  $\frac{L!}{E_b!S_b!C_b!}$ , the proposed conditional probability is:

$$P(n/L, S, C, E, \alpha) = \gamma^{S_b} \cdot e^{-\gamma \cdot L} \cdot (e^{-\gamma} - 1 - \gamma)^{C_b} \quad (4.16)$$

#### 4.2.2 Derivation of The Proposed Closed Form Solution

The computation of (4.16) is done numerically to obtain the optimum value of  $\hat{n}$  which maximizes (4.16). Thus, the calculation of (4.16) may lead to numerical instability problems using low-complexity devices. Therefore, in this section, we propose a closed form solution for the collision recovery aware estimation. This is achieved by differentiating (4.16) with respect to  $\gamma$  and equate the results to zero. After differentiating, the equation can be simplified as:

$$e^{-\gamma} \left( 1 + \frac{\gamma(\gamma \cdot L - S_b)}{(\gamma \cdot L - S_b - \gamma \cdot C_b)} \right) - 1 = 0 \quad (4.17)$$

The analysis of (4.17) indicates that the relevant values for  $\gamma$  are in the region close to one [27]. Hence, we can develop a Taylor series for  $e^{-\gamma}$  around one which leads to:

$$e^{-\gamma} \simeq 1 - \gamma + \frac{1}{2}\gamma^2 - \frac{1}{6}\gamma^3. \quad (4.18)$$

After substituting (4.17) and some additional simplifications, the final equation is a fourth order polynomial:

$$\underbrace{\frac{1}{120}(L - C_b)\gamma^4}_{(a)} + \underbrace{\frac{1}{24}\left(L - C_b - \frac{S_b}{5}\right)\gamma^3}_{(b)} + \underbrace{\frac{1}{6}\left(L - C_b - \frac{S_b}{4}\right)\gamma^2}_{(c)} + \underbrace{\frac{1}{2}\left(L - C_b - \frac{S_b}{3}\right)\gamma}_{(d)} - \underbrace{\left(C_b + \frac{S_b}{2}\right)}_{(e)} = 0 \quad (4.19)$$

Equation (4.19) has four roots [28]:

$$\begin{aligned}\gamma_{1,2} &= -\frac{b}{4a} - S \pm 0.5 \sqrt{\underbrace{-4S^2 - 2P + \frac{q}{S}}_X} \\ \gamma_{3,4} &= -\frac{b}{4a} + S \pm 0.5 \sqrt{\underbrace{-4S^2 - 2P - \frac{q}{S}}_Y},\end{aligned}\tag{4.20}$$

where  $P = \frac{8ac-3b^2}{8a^2}$ ,  $q = \frac{b^3-4abc+8a^2d}{8a^3}$

$$\text{and, } S = 0.5 \sqrt{-\frac{2}{3}P + \frac{1}{3a} \left( Q + \frac{\Delta_0}{Q} \right)}, \quad Q = \sqrt[3]{\frac{\Delta_1 + \sqrt{\Delta_1^2 - 4\Delta_0^3}}{2}}.$$

$$\text{with, } \Delta_0 = c^2 - 3bd + 12ae, \quad \Delta_1 = 2c^3 - 9bcd + 27ad^2 - 72ace$$

According to equation (4.13), we can prove that the signs of the polynomial coefficients are constant and can be as follows:  $a = +$ ,  $b = +$ ,  $c = +$ ,  $d = +$ , and  $e = -$ .

Using Descartes' rules of sign [28], we can count the number of real positive solutions of a polynomial has. Assume that the polynomial in (4.19) is  $P(\gamma)$ , and let  $\nu$  be the number of variations in the sign of the coefficients  $a, b, c, d, e$ , so  $\nu = 1$ . Let  $n_p$  be the number of real positive solutions. According to Descartes' rules of sign [28]:

- $n_p \leq \nu$  which means that  $n_p = 0$  or  $1$ .
- $\nu - n_p$  must be an even integer. Therefore,  $n_p = 1$ .

According to the above Descartes' rules of sign, there is only one valid real positive solution for the equation. Now, we will identify which solution is the valid one. There are two possibilities for the solutions:

1. One positive real solution and the remaining three solutions are negative. In this case, all solutions are real and we need just to identify what is the root which has the largest values from the four solutions. According to (4.20), the value of the square roots  $\sqrt{X}$  and  $\sqrt{Y}$  are positive reals, because we do not have complex solutions. This means,  $\gamma_1 > \gamma_2$  and also  $\gamma_3 > \gamma_4$ . So, the solution will be either  $\gamma_1$  or  $\gamma_3$ . Moreover, the value of  $S$  should be also positive real,

and  $q$  has always negative real value. so  $\gamma_3 > \gamma_1$  which means in this case that our solution is  $\gamma_3$ .

2. Two complex solutions, one real positive solution, and one negative solution. In this case, we have either  $\gamma_{1,2}$  or  $\gamma_{3,4}$  real solutions.  $S$  should be positive real number, and the complex value comes only from the square roots  $\sqrt{X}$  and  $\sqrt{Y}$ . Moreover,  $q$  has always negative real value. Therefore, in (4.20) the value of  $X < Y$ . So  $\gamma_{1,2}$  must be the complex roots, and as mentioned before that  $\gamma_3 > \gamma_4$ , so  $\gamma_4$  is the negative root and  $\gamma_3$  is the positive real root.

Based on the above discussion, the proposed closed form solution for the collision recovery aware tag estimation is:

$$\hat{n} = \left( -\frac{b}{4a} + S + 0.5\sqrt{-4S^2 - 2P - \frac{q}{S}} \right) \cdot L \quad (4.21)$$

### 4.2.3 Collision Recovery Probability Calculation

The collision recovery capability is the ability of the reader to actively convert collided slots into successful slots. This ability is a function of two main parameters: First, is the characteristic of the RFID reader e.g. (receiver type, number of antennas, etc.). Second, a function of the current Signal to Noise Ratio (SNR). Therefore, it extends the capture probability, which is mainly an effect of the channel, resulting in a significantly higher probability to recover collided slots. Figure 5.8 shows three receivers proposed by [29]. The three receivers are the MMSE (Minimum Mean-Square Error) receiver, the ZF (Zero Forcing) receiver with two receiver antennas, and the ZF receiver with a single receiver antenna. The authors of [29] present Bit Error Rate (BER) curves for the different receiver types as a function of the SNR. Thus, the BER can be mapped to a Packet Error Rate (PER) by means of simulations using the same methodology presented in [27]. Afterwards, the collision recovery probability is calculated as:  $\alpha = (1 - PER)$ . Figure 4.5 presents the values of the capture probabilities versus the average signal to noise ratio per frame. In this work, we calculate the average capture probability from the corresponding average SNR at the current frame.

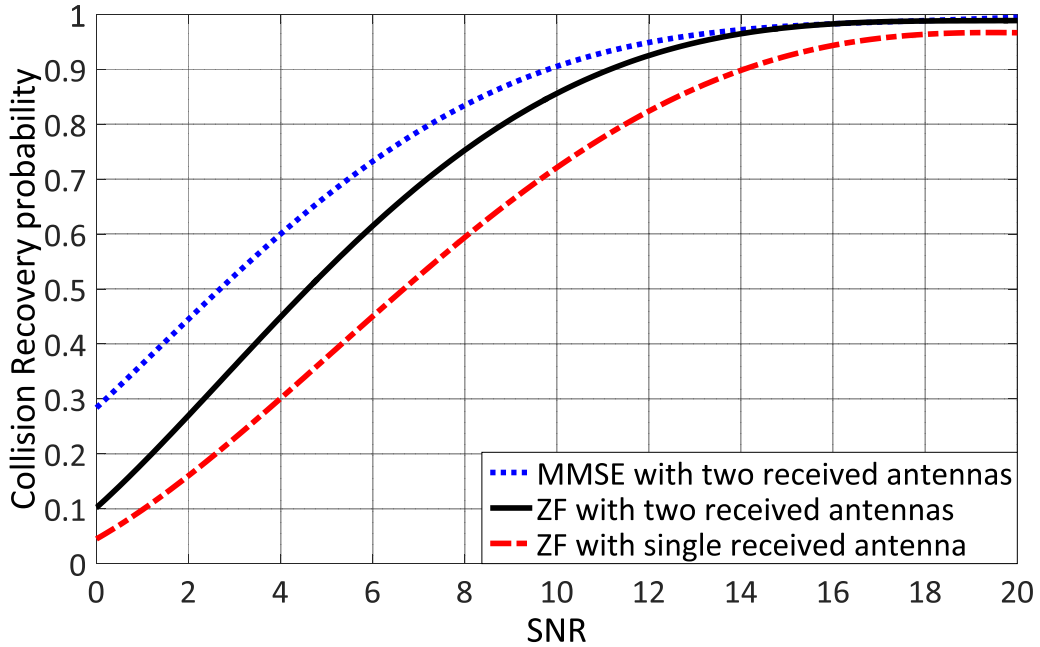
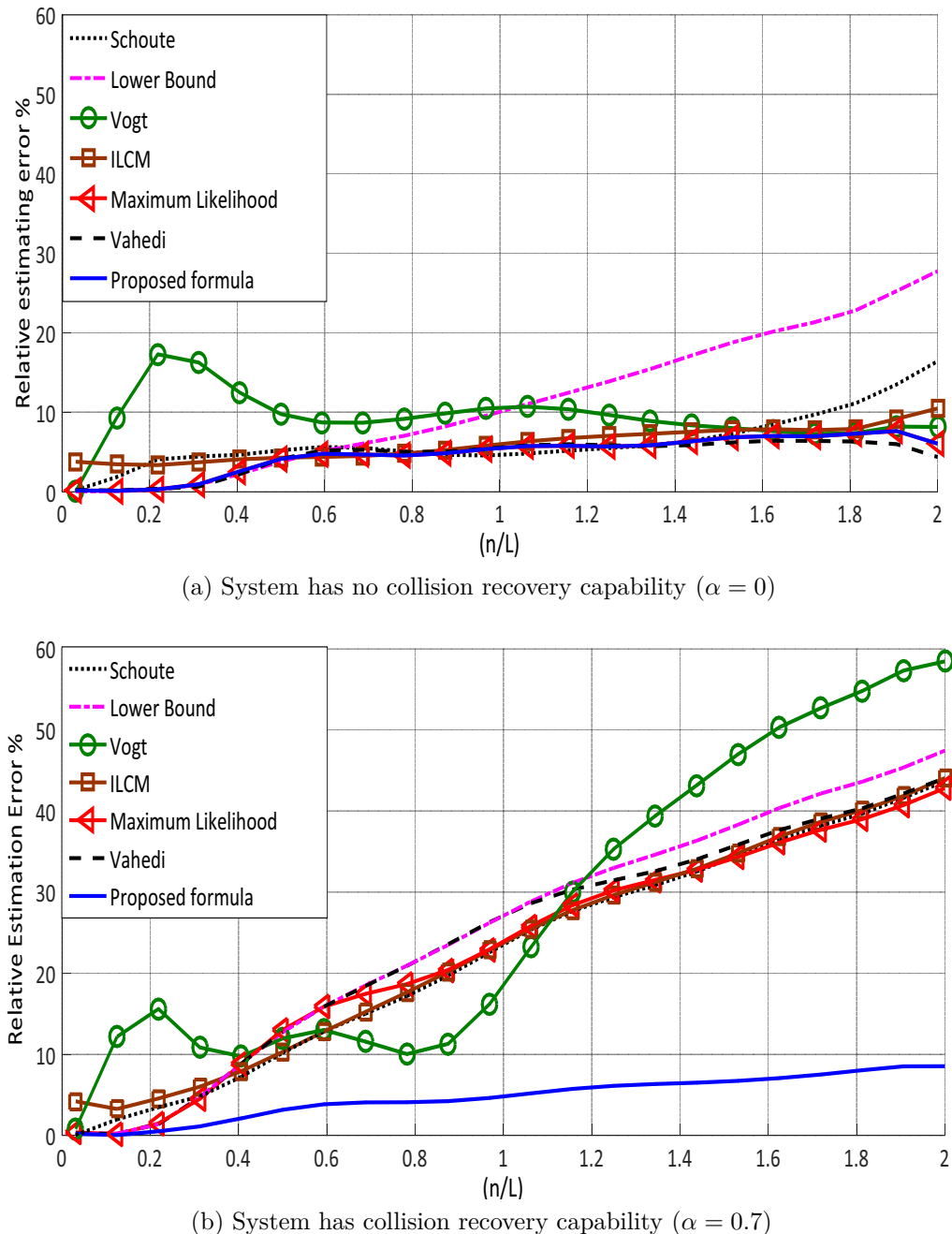


Figure 4.5: Capture probability versus the signal to noise ratio

#### 4.2.4 Performance Analysis

Figure 4.6 shows the percentage of the relative estimation error for the proposed system compared to the literature versus the normalized number of tags  $n/L$ . Figure 4.6a shows system which has no collision recovery capability ( $\alpha = 0$ ). According to figure 4.6a, the proposed system gives identical relative estimation error compared to [25]. However the proposed system gives a closed form solution but the solution of [25] is based on numerical searching, [30] which included the mutual independence of slot types has almost the same results compared to the proposed results. However, it includes a very complex searching algorithms compared to the proposed closed form solution. Figure 4.6b shows an example for modern systems, which have collision recovery capability. We used collision recovery probability  $\alpha = 0.7$ . According to figure 4.6b, The proposed curve has more accurate estimation performance compared to all the literature. Figure 4.7 shows the relative estimation error versus the collision recovery probability  $\alpha$  assuming that the number if tags in the reading area is equal to the frame length i.e.  $n = L$ . Based on figure 4.7, when the value of the collision recovery probability increases, the performance of all other proposals decreases,

Figure 4.6: Relative estimation error  $\epsilon$  vs normalized number of tags  $n/L$

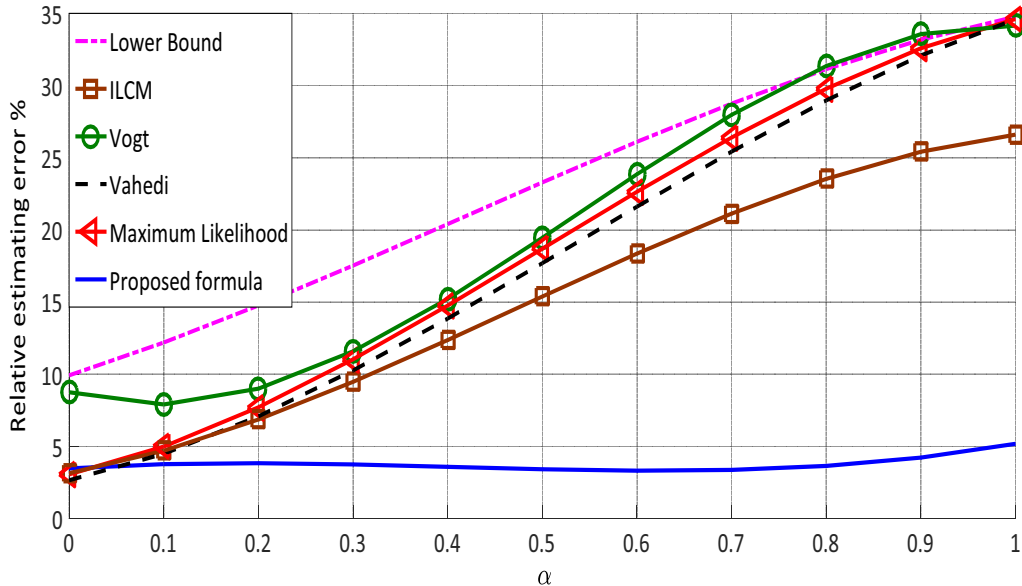


Figure 4.7: Relative estimation error vs. collision recovery probability  $\alpha$ , where  $L = n$

except the proposed method has almost constant performance independent on the value of the collision recovery probability.

Figure 4.8 shows the average identification delay for a bunch of tags. Figure 4.8a shows the identification time for systems with no collision recovery capability ( $\alpha = 0$ ). In these simulations we have assumed that the optimum frame length is the nearest quantized  $2^Q$  for  $L = n$ . According to 4.8a, the proposed system gives identical results compared to [25] and [30] better than the other literature. Figure 4.8b, shows the average identification delay for systems has a collision recovery probability  $\alpha = 0.7$ . According to figure 4.8b, the average identification delay has decreased for all the systems due to the collision recovery capability. However the proposed system saves the total identification time with almost 10 % compared to the others due to the performance of estimation only.

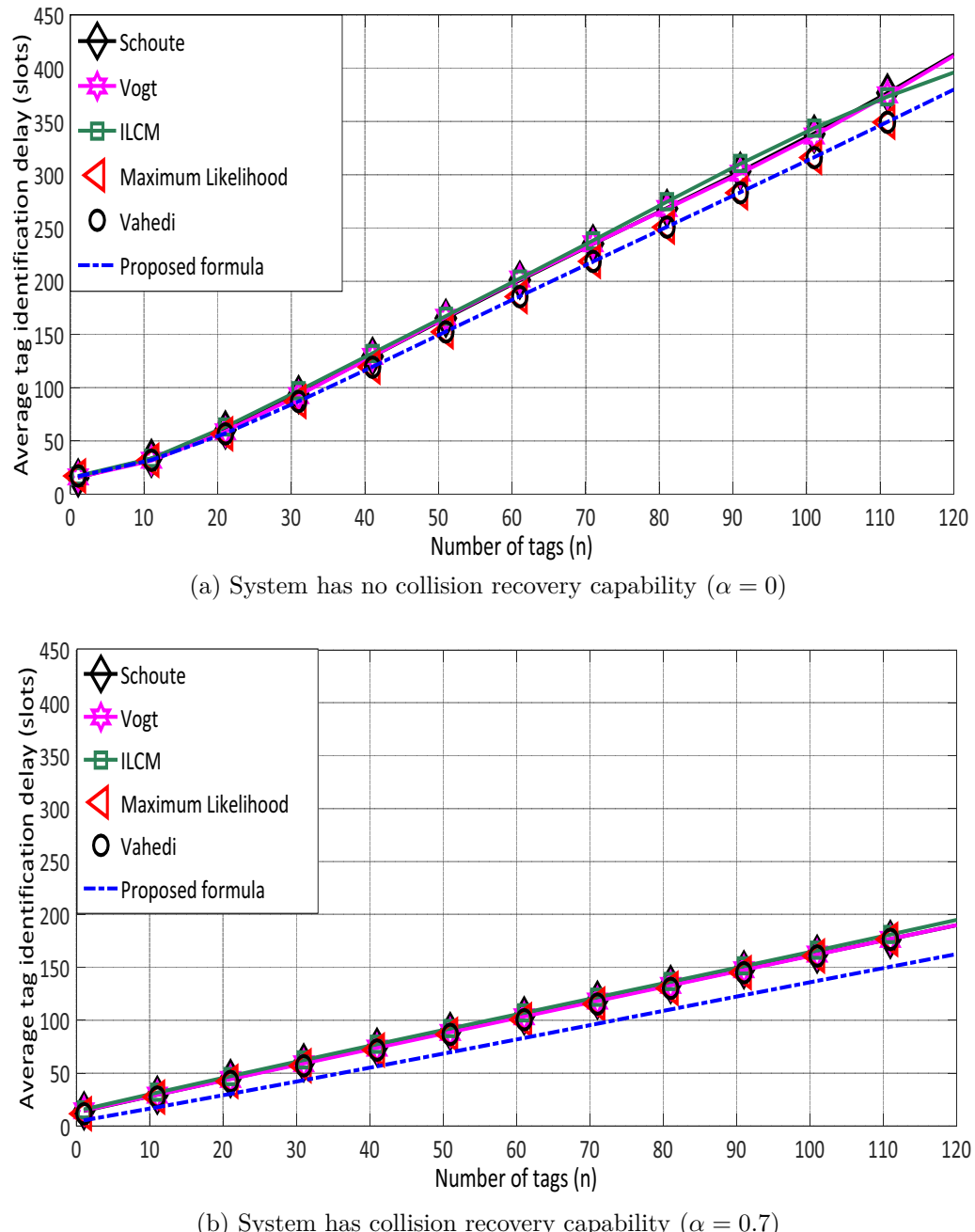


Figure 4.8: Average identification delay



# Chapter 5

## Frame Length Optimization

In FSA, there are two main factors control the reading efficiency, and hence the reading time in RFID systems. First, Number of tags estimation, this factor is discussed in the previous chapter. Second, calculating the optimal frame length for FSA, which will be discussed in details in this chapter. Previous studies have focused on the frame length calculations using the conventional Framed Slotted ALOHA (FSA) algorithms. In such systems, only the answer of a single tag is considered as a successful slot, and if multiple tags respond simultaneously, a collision occurs. Then all the replied tags are discarded. However, as mentioned before, that modern systems have the capability of recovering this collision and convert the collided slot into a successful slot. In addition, most of the previous studies assumed constant slot durations regardless the type of slot. However, the duration of the slots in RFID systems depends on whether the slot is idle, successful, or collided.

In this chapter, we will consider the collision recovery capability and the differences in slots durations effects in different scenarios depending on the RFID system.

This chapter is organized as follows: Section 1 presents the effect of the time differences in slot durations on the reading efficiency to have a new performance metric called time aware reading efficiency. Afterwards, we propose a new closed form solution for the optimum frame length which maximizes the reading efficiency. In section 2, we take the effect of the collision recovery probability in addition to the time differences in slot durations to have a new reading efficiency called Time and collision recovery aware reading efficiency. However,

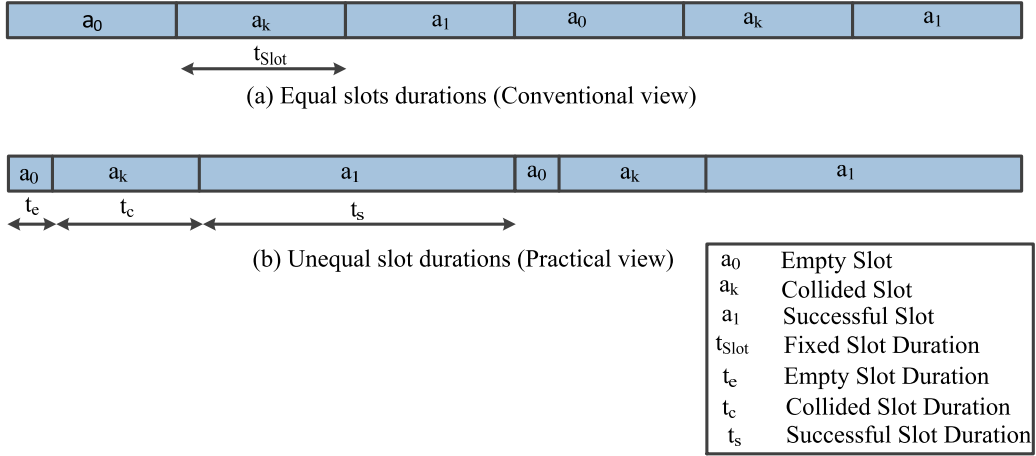


Figure 5.1: Equal and unequal views of slots in Frame Slotted ALOHA with frame length  $L = 6$ .

we have assumed that, the working system has constant collision recovery coefficient. Then, a novel closed form solution for the optimum frame length which maximize the system performance will be presented. Section 3 shows the effect of using multiple collision recovery coefficients without the effect of the time differences in slots duration on the reading efficiency to have a new reading efficiency called Multiple collision recovery coefficients reading efficiency. Then, a novel closed form solution for the optimum frame length is also derived for this system. Finally, section 4 shows a new closed form solution for the optimum frame length for a system takes into consideration the time difference in slot durations in addition to the multiple collision recovery coefficients in section.

## 5.1 Time Aware System

Modern RFID readers can quickly identify the type of a slot (i.e. idle, successful, or collided). Hence, the durations of the different slot types are not identical, which reduces the overall reading time. Figure 5.1 shows two frames, each one with a frame length of  $L = 6$  slots. The first frame in (a) presents the conventional view of the frame with equal slots durations  $t_{Slot}$  for all slot types. The second frame in (b) presents the behavior of the real RFID slots behavior. Here, the slot duration depends on the slot type.

Figure 5.2 shows an example of a real measurements for slots durations

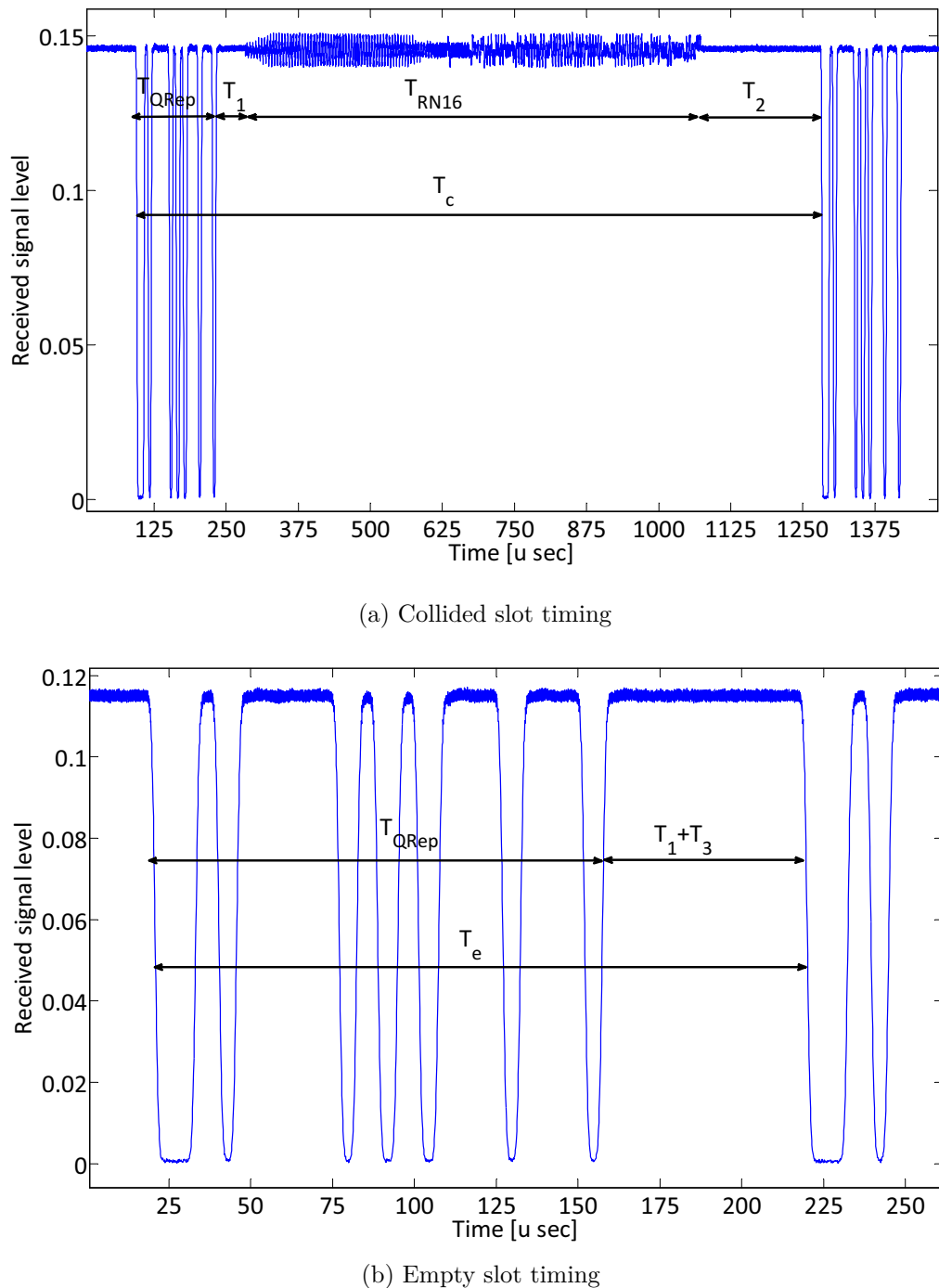


Figure 5.2: Slots durations measurements,  $f_s = 8 \text{ MHz}$ , tag Backscatter Link Frequency  $BLF = 160 \text{ kbps}$

using a Universal Software Radio Peripheral (USRP B210) [31]. In these measurements, we used sampling frequency of  $f_s = 8 \text{ MHz}$ , because the total RFID bandwidth in the European system is 4 MHz, tags Backscatter Link Frequency  $BLF = 160 \text{ kbps}$ .

In the recent years, some research groups concentrated on optimizing the frame length in the case of non-equal slot durations: [32], and [33], proposed a numerical solution for the optimal frame length. This method depends on searching for the optimal frame length which maximizes the reading efficiency. Moreover, this searching depends also on the tag to reader data rate, which makes the searching process more complicated. [34] optimized the mean number of resolved tags in unit time by taking into consideration the different slot durations. However, this approach bases on a complex multidimensional table look-up, which is relatively time consuming. [35] proposed to search for the optimum frame length that minimizes the mean time needed to resolve a bunch of tags. However, the author reached to a recursive Bellman-equation, which is complex to be applied in systems with real time restrictions.

In this section, we propose a novel closed form solution for the optimum frame length in FSA for RFID systems. The proposed solution gives a direct relation between the frame length  $L$ , and the number of tags  $n$  in the reading area. Furthermore, it includes a factor representing the different slot durations.

### 5.1.1 A Novel Closed Form Solution for Time Aware System

For calculating the proposed optimal Time-Aware frame size  $L_{TA}$ , which takes into consideration the different slot durations, we firstly have to define the Time-Aware reading efficiency  $\eta_{TA}$ . Let the Time-Aware reading efficiency be the ratio between the total successful time and the total frame time:

$$\eta_{TA} = \frac{t_s \cdot S}{t_e \cdot E + t_s \cdot S + t_c \cdot C}, \quad (5.1)$$

where  $t_s \cdot S$ ,  $t_e \cdot E$ , and  $t_c \cdot C$  are respectively the expected total successful, idle, and collided times. Furthermore,  $S$ ,  $E$ , and  $C$  are the expected numbers of successful, empty and collided slots.  $t_s$ ,  $t_e$ ,  $t_c$  are respectively the successful, idle, and collided slot durations.

The next step is to derive the new optimum frame length  $L_{TA}$  under the Time-Aware environment.  $L_{TA}$  can be optimized by finding the value of  $L$  which maximizes the Time-Aware reading efficiency. This is achieved by differentiating the reading efficiency in (5.1) with respect to the frame length  $L$  and equate the result to zero:

$$\frac{\partial \eta_{TA}}{\partial L} = 0 \quad (5.2)$$

According to (3.1),  $E$ ,  $S$ , and  $C$  are a function of  $L$ . Taking into account that  $t_e$ ,  $t_s$ ,  $t_c$  are constants for a given system specification, we get:

$$\frac{(t_e E + t_s S + t_c C) t_s \frac{\partial}{\partial L}(S) - t_s S \frac{\partial}{\partial L}(t_e E + t_s S + t_c C)}{(t_e E + t_s S + t_c C)^2} = 0 \quad (5.3)$$

After multiplying both sides by the denominator and dividing by  $t_s$  (non-zero constant), the equation can be simplified to:

$$(t_e E + t_c C) \frac{\partial}{\partial L}(S) + t_s S \frac{\partial}{\partial L}(S) = S \frac{\partial}{\partial L}(t_e E + t_c C) + t_s S \frac{\partial}{\partial L} S \quad (5.4)$$

After subtracting the term which is multiplied by  $t_s$ , the equation finally results in:

$$\{t_e E + t_c C\} \frac{\partial}{\partial L}(S) = S \frac{\partial}{\partial L} \{t_e E + t_c C\} \quad (5.5)$$

Then, substituting the values of  $E$ ,  $S$ , and  $C$  from (3.1) leads to:

$$\begin{aligned} & \left\{ t_e L \underbrace{\left(1 - \frac{1}{L}\right)^n}_{E} + t_c \underbrace{\left(L - \left(1 - \frac{1}{L}\right)^{n-1} (L - n - 1)\right)}_C \right\} \\ & \times \underbrace{\frac{\partial}{\partial L} n \underbrace{\left(1 - \frac{1}{L}\right)^{n-1}}_S}_{S} \\ & = n \underbrace{\left(1 - \frac{1}{L}\right)^{n-1}}_S \\ & \times \frac{\partial}{\partial L} \left\{ t_e L \underbrace{\left(1 - \frac{1}{L}\right)^n}_{E} + t_c \underbrace{\left(L - \left(1 - \frac{1}{L}\right)^{n-1} (L - n - 1)\right)}_C \right\} \end{aligned} \quad (5.6)$$

By simplifying the result, the final exact equation for the proposed Time-Aware

frame length is given by the implicit equation:

$$\left(1 - \frac{n}{L_{TA}}\right) = (1 - C_t) \left(1 - \frac{1}{L_{TA}}\right)^n, \quad (5.7)$$

where  $n$  is the number of tags, and  $C_t$  is the slot duration constant defined as  $C_t = \frac{t_e}{t_c}$  with  $0 < C_t \leq 1$ , as  $t_e \leq t_c$  in practical applications. (5.7) shows the exact relation between the proposed Time-Aware frame length  $L_{TA}$  and the number of tags  $n$ , which takes into consideration the time difference in the slot durations.

Unfortunately, (5.7) is an implicit equation. We will now derive an approximate, but explicit equation. (5.7) can be also expressed as:

$$\left(1 - \frac{1}{\beta}\right) = (1 - C_t) \left(1 - \frac{1}{\beta n}\right)^n, \quad (5.8)$$

where  $\beta = \frac{L_{TA}}{n}$ . As we are focusing on systems with many tags we can use the approximation

$$\lim_{n \rightarrow \infty} \left(1 - \frac{1}{\beta n}\right)^n = e^{-\frac{1}{\beta}}, \quad (5.9)$$

which simplifies (5.7) to:

$$\left(1 - \frac{1}{\beta}\right) = (1 - C_t) e^{-\frac{1}{\beta}}. \quad (5.10)$$

Analysis of (5.7) indicate that the relevant values for  $\beta = \frac{L_{TA}}{n}$  are in the region close to one. Hence, we can develop a Taylor series for  $e^{-\frac{1}{\beta}}$  around one which leads to:

$$e^{-\frac{1}{\beta}} \simeq 1 - \frac{1}{\beta} + \frac{1}{2\beta^2} \quad (5.11)$$

After substituting (5.10) and additional simplifications we get:

$$\beta^2 C_t - \beta C_t + 0.5(C_t - 1) = 0 \quad (5.12)$$

By solving (5.12), and rejecting the negative solution we finally obtain:

$$L_{TA} = \frac{n}{2} \left(1 + \sqrt{\frac{2}{C_t} - 1}\right) \quad (5.13)$$

The proposed equation gives a linear relation wrt. the number of tags  $n$ , and includes the slot duration constant  $C_t$ , which can be easily varied as a function

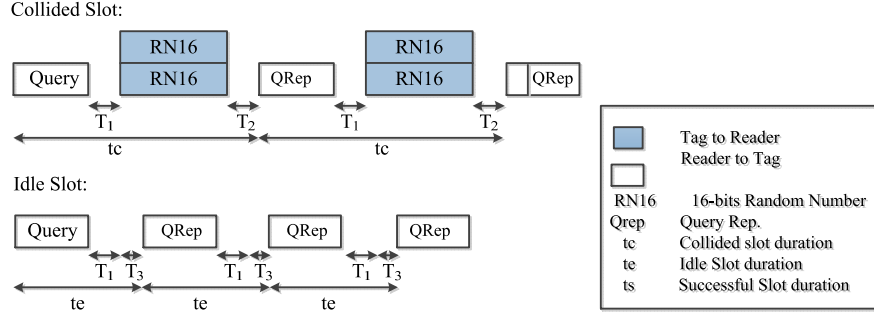


Figure 5.3: Slot durations during tag inventory rounds for the ISO 18000-6C standard

of the transmission rate and the working standard.

### 5.1.2 Slot Duration Constant Calculation For The ISO 18000-6c Protocol

In this section, we will discuss in details how we calculate the slot duration constant  $C_t$  from the physical layer parameters. Figure 5.3 shows the timings of collided and empty slots. Each slot contains different sequences of reader to tag commands and tag replies. Based on the EPCglobal C1 G2 standard [3], the slot duration constant is

$$C_t = \frac{t_e}{t_c}, \quad (5.14)$$

where the empty slot duration  $t_e$  is given by:

$$t_e = T_{QRep} + T_1 + T_3. \quad (5.15)$$

Here,  $T_{QRep}$  is the query repeat command time:

$$T_{QRep} = T_{FS} + T_{command}, \quad (5.16)$$

with,  $T_{FS} = 3.5 \cdot T_{ari}$ ,  $T_{command} = 6 \cdot T_{ari}$ , and  $T_{ari} = \frac{DR}{2.75} T_{pri}$ . By substituting in (5.16) we get

$$T_{QRep} = 3.5 \cdot DR \cdot T_{pri}, \quad (5.17)$$

where  $T_{ari}$  is reader symbol duration,  $T_{pri} = \frac{1}{BLF}$ ,  $BLF$  is the tag backscatter

Table 5.1: Available slots duration constants  $C_t$  of the EPCglobal C1 G2 standards

Divide Ratio: $DR$	Modulation: $M$	Pilot Length: $n_p$	$C_t$
8	1	0	0.47
		12	0.41
	2	4	0.35
		16	0.28
	4	4	0.23
		16	0.18
	8	4	0.14
		16	0.1
	1	0	0.7
		12	0.65
64/3	2	4	0.57
		16	0.5
	4	4	0.43
		16	0.35
	8	4	0.3
		16	0.22

link frequency and  $DR$  is the so-called divide ratio constant that can take the two values  $DR = 8$  or  $\frac{64}{3}$ . Finally,  $M$  equals to 1, 2, 4, or 8, which represents the modulation types FM0, Miller 2, 4, or 8, respectively.  $T_1$  is the time from the reader transmission to the tag response, which can be expressed as:

$$T_1 = \max \{DR \cdot T_{pri}, 10 \cdot T_{pri}\} \quad (5.18)$$

Next,  $T_3$  is the time that the reader waits after  $T_1$  before issuing another command. As it has no constraints, it can be assumed to be zero. After substituting (5.17) and (5.18) in (5.15),  $t_e$  can be expressed as:

$$t_e = T_{pri} \cdot (3.5 \cdot DR + \max \{DR, 10\}). \quad (5.19)$$

Next, the collided slot duration  $t_c$  is given by:

$$t_c = T_{QRep} + T_1 + T_2 + T_{RN16}, \quad (5.20)$$

where  $T_2$  is the reader response time starting from the end of the tag response,  $T_2 = 6 \cdot T_{pri}$ , and  $T_{RN16}$  is the duration of 16 bits temporary data, 6 bits preamble,  $n_p$  pilot tones, i.e.  $T_{RN16} = (22 + n_p) \cdot T_{pri}$ . Therefore,  $t_c$  can be expressed as:

$$t_c = T_{pri} \cdot (3.5 \cdot DR + \max\{DR, 10\} + 6 + 22 \cdot M + n_p \cdot M). \quad (5.21)$$

From equations (5.19) and (5.21), the final expression of  $C_t$  is:

$$C_t = \frac{3.5 \cdot DR + \max\{DR, 10\}}{3.5 \cdot DR + \max\{DR, 10\} + 6 + 22 \cdot M + n_p \cdot M}. \quad (5.22)$$

Table 5.1 shows the values of the slots durations constant of the EPCglobal C1 G2 standards. According to table 5.1, the slot duration constant  $C_t$  varies from 0.1 to 0.7, and this affects the optimum frame length directly. According to figure 5.2, the slot duration constant  $C_t = 0.18$ , which verify the theoretical results in table 5.1.

### 5.1.3 Closed Form Solution VS. Numerical Solution

Figure 5.4a shows the behavior of the proposed frame length formula in (5.13) compared to the numerical solution in [35] for the complete range the slot duration constant  $C_t$  for  $0 < C_t \leq 1$ . In the simulation, we used a fixed number of  $n = 100$  tags. According to figure 5.4, the proposed equation approaches the numerical solution proposed at [35] in the full range of  $C_t$  with a very small bias comes from the Taylor series approximation in (5.11). According to the EPCglobal C1 G2 standard [3] the frame length is allowed to take only quantized values (power of 2). Figure 5.4b shows that the proposed frame length fully match the numerical solution in the full range of  $C_t$ .

Figure 5.5 shows a the maximum reading efficiency using the proposed frame length formula in (5.13) and the numerical solution of the frame length proposed in [35]. According to figure 5.5, the proposed formula gives identical results with the numerical solution. However, unlike the complex table look-up presented in [35], our approach only is based on a linear equation, which is a function of the number of tags  $n$ .

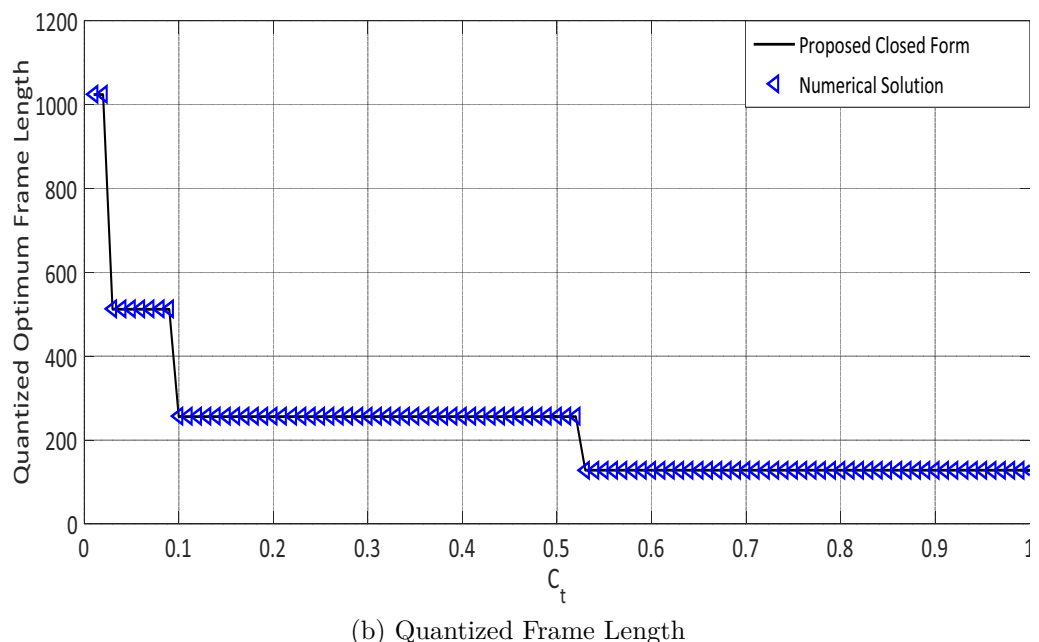
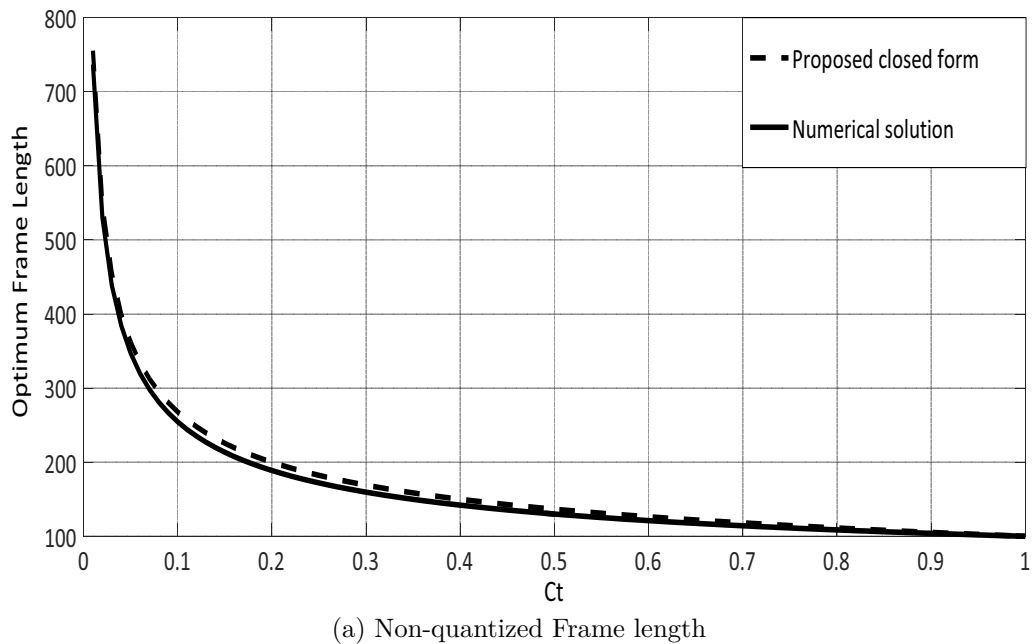


Figure 5.4: Optimum frame length  $L_{TA}$  as a function of the slot duration constant  $C_t$  ( $n = 100$  tags). The conventional case with identical slot durations corresponds to  $C_t = 1$ .

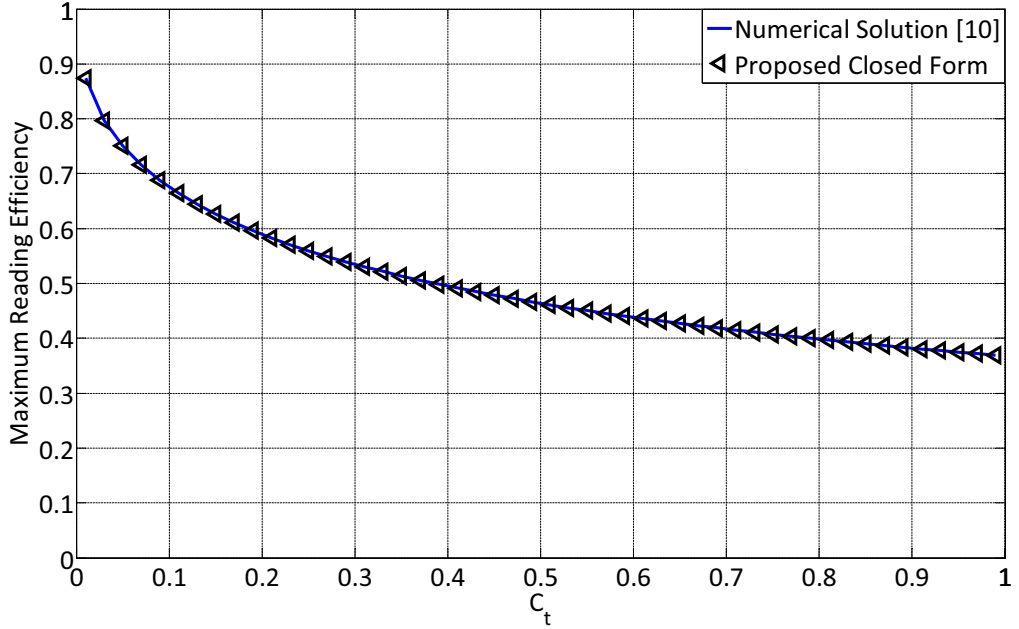


Figure 5.5: Maximum reading efficiency

### 5.1.4 Mean Reduction in Reading Time

Figure 5.6 shows simulation results for the reading time reduction of the proposed optimal Time-Aware frame length  $L_{TA}$  wrt. the classical optimal frame length  $L = n$  as a function of the slot duration constant  $C_t$ . These simulations assume a perfect knowledge of the number of tags  $n$ . According to the figure,  $C_t = 0$  means that the idle slot duration time  $t_e$  is quite small wrt. the collided slot duration time  $t_c$ . In this case, the proposed Time-Aware frame length can reduce the average reading time by up to 12% compared to the conventional optimization criterion. With  $C_t = 1$ , which means that the slot durations are of identical length, we obtain the efficiency of the classical optimization, i.e.  $L = n$ .

In practice, the number of tags in the interrogation region is unknown. Hence, the anti-collision algorithms in real RFID systems consist of two stages: The first stage estimates the number of tags in the interrogation area  $\hat{n}$ . The second stage calculates the optimal frame length  $L_{opt}$  based on  $\hat{n}$  for maximizing the reading efficiency. Figure 5.7 shows the mean reduction of the reading time using the proposed Time-Aware frame length for the proposed ML number of tags estimation and some well-known tag estimation algorithms using the value

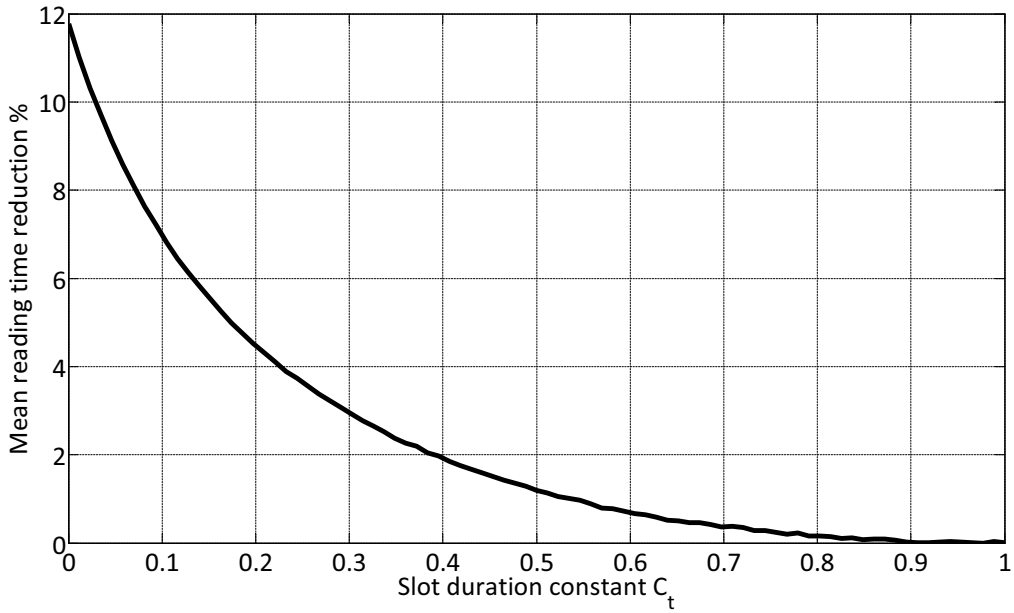


Figure 5.6: Percentages of saving time using the proposed TAFSA for an ideally known number of tags (1000 iterations for each step)

of the slot duration constant  $C_t = 0.2$ . The main issue of these simulations is to show the practical effect on the reading time by working with the proposed frame length using different tag estimation algorithms. Each curve presents the mean reduction of the reading time between the proposed frame length and the conventional frame length  $L = n$  using the same estimation algorithm. When a simple tag estimation technique is used like Lower bound [14] or Schoute [13], we can reduce the reading time in the order of 10 to 12 %, and we gain around 9 % for better estimation algorithms like MFML [36] and Biased Chebyshev [37], and finally we gain 6 % using the proposed ML estimation algorithm. According to figure 5.7, in case of better estimation algorithms, the mean reading time reduction approaches the curves assuming perfect knowledge of the number of tags, because it decreases the number of FSA iterations to identify the total number of tags in the reading area. However, using non-accurate number of tags estimation algorithms, FSA needs more iterations, with more FSA frame length adaptations, which gives more importance for the proposed formula compared to the classical frame length adaptations.

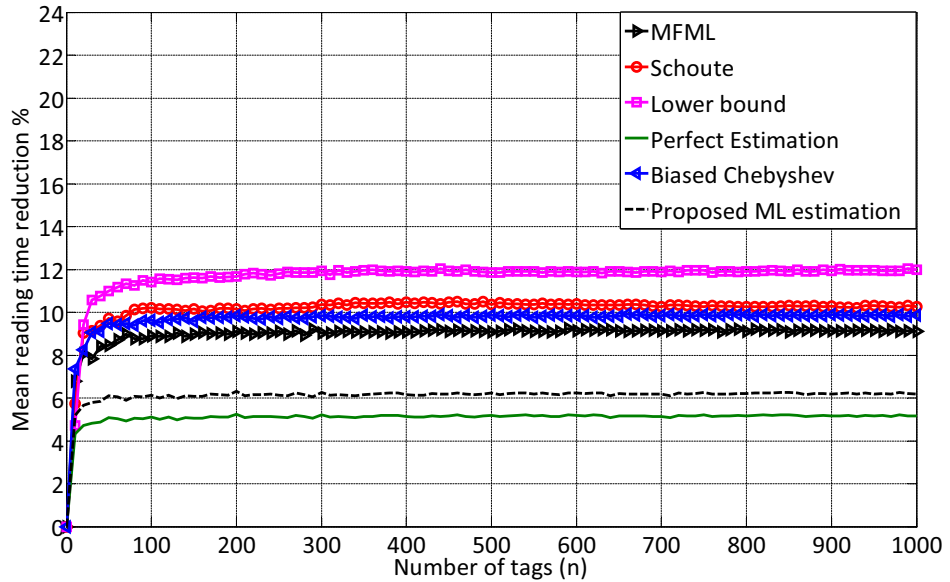


Figure 5.7: Percentages of saving time using the proposed TAFSA compared to the conventional frame length  $L = n$  for different anti-collision algorithms using  $C_t = 0.2$

## 5.2 Time and Collision Recovery Aware System

Recently, modern RFID readers are able to decode one of the collided tags. this phenomena called “Collision Recovery capability”. According to the literature we can divide the previous research for the optimization of the frame length into three different groups:

- The first group considered only the average collision recovery probability for the frame length optimizations, such as [17]. The authors proposed a closed form equation for the optimum frame length maximizing the reading throughput per frame.
- The second group considered only the different slot durations, such as [35, 38] and as shown in the first proposal at the previous section. However, no closed form solution for the optimum frame length was derived. They calculate the optimum frame length numerically.
- The third group considered the different slot durations and the collision

recovery probability, such as [33, 39, 40]. Both [33, 39] gave numerical solutions for the optimum frame length versus the collision recovery probability and the number of tags. The main problems of their numerical solutions occur when taking into account the multiple degrees of freedom: the solutions require a complex multidimensional look-up table that has to consider all possible degrees of freedom. [40] uses curve fitting to find a closed form solution for the optimum frame length at a specific collision recovery probability and timing. However, this solution can not be generalized for all values of slot's timing and collision recovery probabilities.

In this section, we will derive a closed form solution for the optimum frame length by optimizing the reading throughput per frame that does not require any look-up table [33, 39]. In addition, we take into consideration the average collision recovery probability and the different slot durations. Moreover, we will clarify how we calculate the collision recovery probability based on the physical layer.

### 5.2.1 Closed Form Solution For Time and Collision Recovery Aware System

Now, we will derive the proposed optimal time and collision recovery aware frame size  $L_{TCA}$  that takes into consideration the different slot durations and the collision recovery probability. Thus, we firstly will introduce a new reading efficiency called Time and Collision Recovery Aware reading efficiency  $\eta_{TCA}$ . The main properties for this efficiency are the consideration of the different slot durations and the average collision recovery probability.

In this efficiency, we add the average collision recovery probability  $\alpha$  to the time aware efficiency in (5.1). Therefore the time and collision recovery probability aware efficiency can then be written as:

$$\eta_{TCA} = \frac{t_s \cdot S_c}{t_e \cdot E_c + t_s \cdot S_c + t_c \cdot C_c}. \quad (5.23)$$

where  $E_c$ ,  $S_c$  and  $C_c$  are respectively the number of empty, successful, an collided slots after adding the effect of the collision recovery probability  $\alpha$ . Their

relation is given by:

$$E_c = E, S_c = S + \alpha \cdot C, C_c = (1 - \alpha) \cdot C. \quad (5.24)$$

The goal is to find the optimum frame length  $L_{TCA}$  which maximizes the proposed reading efficiency in 5.23. This is achieved by differentiating the reading efficiency  $\eta_{TCA}$  of (5.23) with respect to the frame length  $L$  and equate the result to zero.

Clearly, the frame length  $L$  is an integer value. Therefore, differentiating the equation is not fully correct. However, we will later show that the resulting error is negligible. According to (5.24),  $E_c$ ,  $S_c$ , and  $C_c$  are a function of  $L$ . However,  $t_e$ ,  $t_s$ ,  $t_c$  are constants for a given system configuration. Thus, the equation can be simplified to:

$$\frac{(t_e E_c + t_s S_c + t_c C_c) t_s \frac{d}{dL}(S_c) - t_s S_c \frac{d}{dL}(t_e E_c + t_s S_c + t_c C_c)}{(t_e E_c + t_s S_c + t_c C_c)^2} = 0. \quad (5.25)$$

After multiplying both sides by the denominator and dividing by  $t_s$  (non-zero constant), and subtracting the term, which is multiplied by  $t_s$ , the equation results in:

$$(t_e E_c + t_c C_c) \frac{d}{dL}(S_c) = S_c \frac{d}{dL} (t_e E_c + t_c C_c). \quad (5.26)$$

Then, the substitution by the values of  $E_c$ ,  $S_c$ , and  $C_c$  from (5.24) leads to the final exact equation for the proposed time and collision recovery probability aware frame length:

$$(1 - \alpha) \cdot (1 - \frac{n}{L_{TCA}}) + \alpha \cdot C_t \cdot \left(1 - \frac{1}{L_{TCA}}\right) + (C_t - 1) \cdot (1 - \alpha) \cdot \left(1 - \frac{1}{L_{TCA}}\right)^n = 0, \quad (5.27)$$

where  $n$  is the number of tags, and  $C_t$  is the slot duration constant defined as  $C_t = \frac{t_e}{t_c}$ . (5.27) shows the exact relation between the proposed collision recovery and time-aware optimum frame length  $L_{CTA}$  and the number of tags

$n$ . This equation takes into consideration the collision recovery probability and the different slot durations. However, this solution depends on a recursive equation. For reaching an explicit equation, (5.27) can be expressed as:

$$(1 - \alpha) \cdot (1 - \frac{1}{\beta}) + \alpha \cdot C_t \cdot \left(1 - \frac{1}{\beta n}\right) + (C_t - 1) \cdot (1 - \alpha) \cdot \left(1 - \frac{1}{\beta n}\right)^n = 0, \quad (5.28)$$

where  $\beta = \frac{L_{TCA}}{n}$ . As we are focusing on systems with a large number of tags  $n$ , we can use the approximation

$$\lim_{n \rightarrow \infty} \left(1 - \frac{1}{\beta n}\right)^n = e^{-\frac{1}{\beta}}, \quad (5.29)$$

which simplifies (5.28) to:

$$(1 - \alpha) \cdot \left(1 - \frac{1}{\beta}\right) + \alpha \cdot C_t \cdot \left(1 - \frac{1}{\beta n}\right) + (1 - \alpha) \cdot (C_t - 1) e^{-\frac{1}{\beta}} = 0. \quad (5.30)$$

The analysis of (5.27) indicates that the relevant values for  $\beta = \frac{L_{TCA}}{n}$  are in the region close to one [33]. Hence, we can develop a Taylor series for  $e^{-\frac{1}{\beta}}$  around one which leads to:

$$e^{-\frac{1}{\beta}} \simeq 1 - \frac{1}{\beta} + \frac{1}{2\beta^2}. \quad (5.31)$$

After substituting (5.30) and some additional simplifications, we get:

$$\beta^2 C_t - \beta C_t \left(1 + \frac{\alpha}{n}\right) - 0.5 (1 - \alpha) \cdot (1 - C_t) = 0. \quad (5.32)$$

As  $\frac{\alpha}{n} \ll 1$ , (5.32) can be expressed as:

$$\beta^2 C_t - \beta C_t - 0.5 (1 - \alpha) \cdot (1 - C_t) = 0. \quad (5.33)$$

By solving (5.33) and rejecting the negative solution we finally reach to the

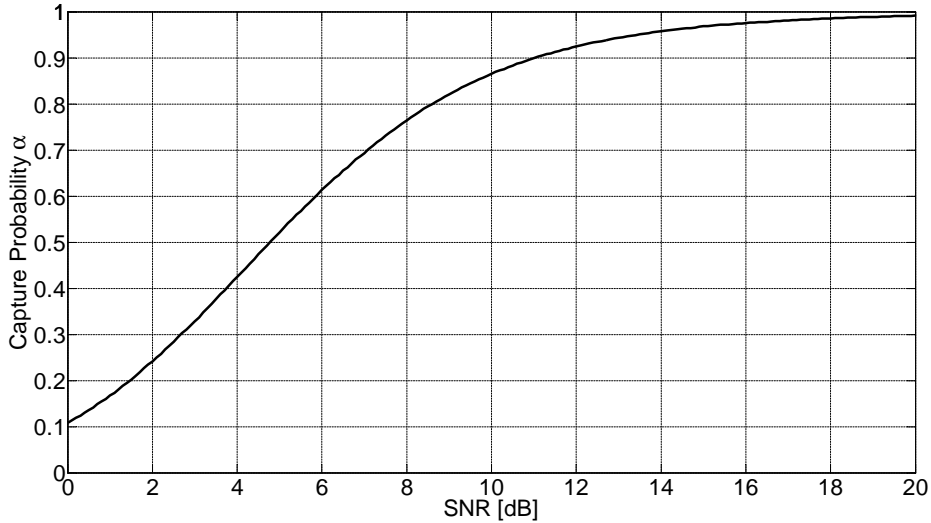


Figure 5.8: Average collision recovery probability versus the signal to noise ratio

final solution:

$$L_{TCA} = \frac{n}{2} \left( (1 - \alpha) + \sqrt{(1 - \alpha)^2 + \frac{2}{C_t} (1 - \alpha) \cdot (1 - C_t)} \right). \quad (5.34)$$

As the optimization of (5.1) is a convex optimization problem, and there exists only one non-negative solution of (5.33), (5.34) leads to the global optimum. According to the literature, [39] is the only work who used the same performance metric  $\eta_{TCA}$  to get the optimum frame length. However, in this work the authors did not propose any closed form solution and they have to rely on Multi-dimensional look-up tables.

### 5.2.2 Average Collision Recovery Probability Calculation

In this part, we will discuss in details how can we calculate the average collision recovery probability from the physical layer. The average collision recovery probability varies in the range of  $0 \leq \alpha \leq 1$ . Its value depends on the Signal to Noise Ratio (SNR). In this work, we measure the SNR for each slot. Then, we calculate the average SNR per frame. In [29], the authors proposed a method to recover the strongest tag reply based the physical layer properties. They have

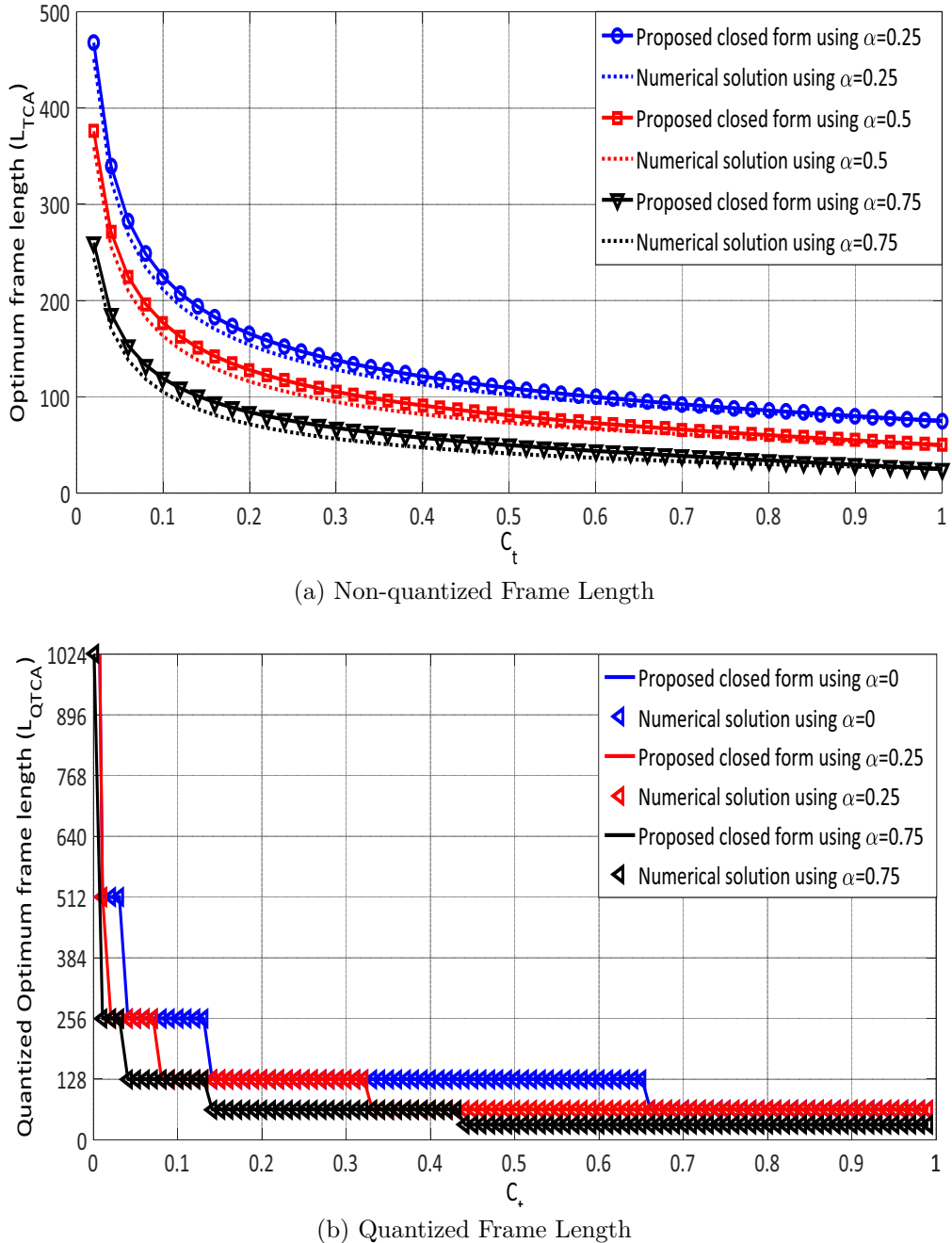


Figure 5.9: Optimum frame length  $L_{TCAs}$  as a function of the slot duration constant  $C_t$  ( $n = 100$  tags) for the capture probabilities  $\alpha = 0.25, 0.5, 0.75$ .

proposed a Bit Error Rate (BER) curve versus the SNR. We want to calculate the average collision recovery probability for a complete collided RN16 packet, which includes 16 random successive bits. The BER is mapped to Packet Error Rate (PER) by simulation as the channel is not Binary Symmetric Channel (BSC). According to [27], The average collision recovery probability can be expressed as:  $\alpha = (1 - PER)$ . Figure 5.8 presents the values of the average collision recovery probabilities versus the average signal to noise ratio per frame. In this work, we calculate the average collision recovery probability from the corresponding average SNR at the current frame.

### 5.2.3 Closed Form Solution VS. Numerical Solution

Now we will compare the proposed closed form equation in (5.34) with the numerical results in [39]. Figure 5.9a shows both algorithms for the full range of the slot duration constant  $C_t$ . Assuming a fixed number of  $n = 100$  tags, figure 5.9a indicates that the proposed closed form approaches the numerical solution for different  $\alpha$  in the full range of  $C_t$ . Due to the proposed approximations, there are slight differences between the proposed closed form and the numerical solution, where the numerical is the exact solution. According to the EPCglobal C1 G2 standard [3] the frame length is allowed to take only quantized values (power of 2). Figure 5.9b shows that the proposed frame length fully match the numerical solution in the full range of  $C_t$ .

### 5.2.4 Mean Reduction in Reading Time

Figure 5.10 shows simulation results for the reading time reduction of the proposed optimal TCRA frame length  $L_{TCRA}$  wrt. the classical optimal frame length  $L = n$  for  $C_t = 0.2$  and different values of the collision recovery probability  $\alpha$ . These simulations assume a perfect knowledge of the number of tags  $n$ . According to figure 5.10, the timing gain increases when the value of  $\alpha$  increases, which gives more advantage to the proposed solution compared to the conventional one.

Figure 5.11 shows the mean reduction of the reading time using the proposed TCRA frame length compared to the conventional frame length  $L = n$  taking into consideration the effect of the number of tags estimation algorithms. Ac-

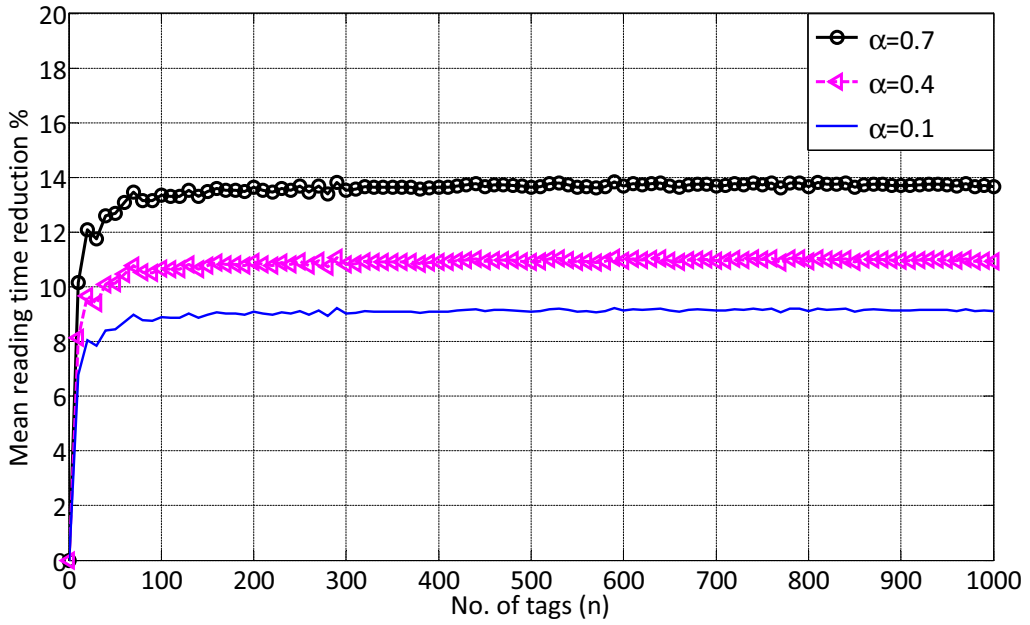


Figure 5.10: Percentages of saving time using the proposed TCRA compared to the conventional frame length  $L = n$  for perfect number of tags estimation using  $C_t = 0.2$  and different values of  $\alpha$

cording to figure 5.11, in case of better estimation algorithms, the mean reading time reduction approaches the curves assuming perfect knowledge of the number of tags. As a result, the newly proposed closed form algorithm provides additional improvements wrt. the classical optimization algorithm when the tag estimation provides inaccurate results.

### 5.3 Multiple Collision Recovery Aware System

In the previous section, we have considered systems with equal collision recovery probability coefficients regardless the number of collided tags per slot. For example, the probability to resolve two collided tags is equal to the probability to resolve three or four collided tags per slot.

In this section, we propose a new reading efficiency metric called Multiple Collision Recovery Coefficients Reading Efficiency  $\eta_{MCRC}$ , which includes a unique collision resolving coefficient for each number of collided tags. Hence, we propose a novel closed form solution for the optimum FSA frame length which

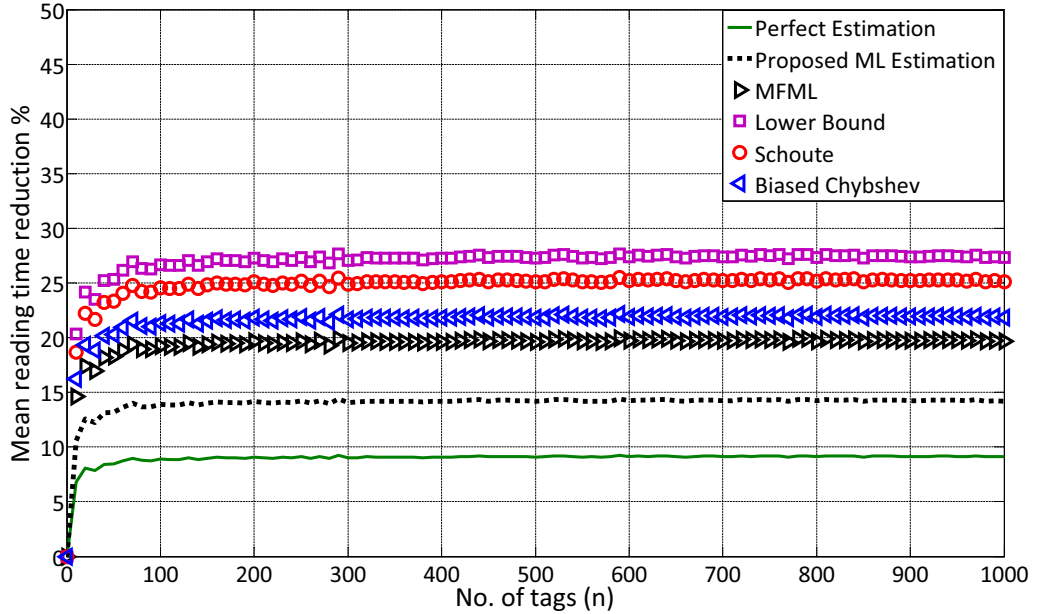


Figure 5.11: Percentages of saving time using the proposed TCRA compared to the conventional frame length  $L = n$  for different anti-collision algorithms using  $C_t = 0.2$  and  $\alpha = 0.1$

maximize the proposed efficiency metric. Then, we calculate these coefficients based on a simple RFID reader model to show how the proposed system could be applied on real-life applications.

### 5.3.1 Closed Form Solution For Multiple Collision Recovery Aware System

we will present a new FSA efficiency metric called Multiple Collision Recovery Coefficients Reading Efficiency  $\eta_{MCRC}$ . Afterwards, a closed form solution for the new optimum frame length  $L_{MCRC}$  under multiple collision recovery coefficients environment will be presented.

The main contribution in this efficiency is that it contains a unique collision recovery coefficient  $\alpha_i$  for each probability of collision  $P_{col.}(i)$ . These new coefficients indicate the ability of the reader to recover one tag from  $i$  collided tags. The proposed reading efficiency  $\eta_{MCRC}$  is expressed as:

$$\eta_{MCRC} = P(1) + \sum_{i=2}^n \alpha_i P_{col.}(i). \quad (5.35)$$

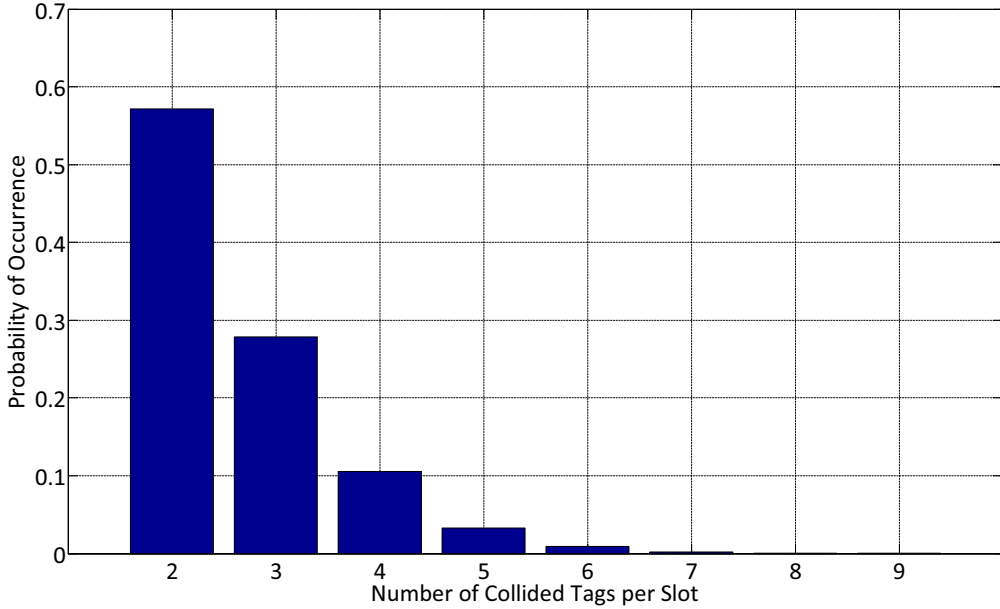


Figure 5.12: Distribution of collision probability for a collided slot in FSA, under condition of  $\frac{n}{2} \leq L \leq 2n$

Figure 5.12 presents the distribution of the average collision probability in a frame of length  $0.5 \cdot n \leq L \leq 2 \cdot n$  uniformly, which is the practical range of the frame length in RFID systems [33]. According to figure 5.12, the probability that the collided slot comes from two, three, or four collided tags is equal to  $P_{col.}(2) + P_{col.}(3) + P_{col.}(4) \simeq 96\%$ , and for the remaining tag collisions  $\sum_{i=5}^n P_{col.}(i) \simeq 4\%$ . Moreover, the values of the collision recovery coefficients  $\alpha_i$ ,  $i > 4$  are practically very small.

Therefore, the proposed  $\eta_{MCRC}$  for the practical RFID environment can be expressed as shown:

$$\eta_{MCRC} = P(1) + \alpha_2 P_{col.}(2) + \alpha_3 P_{col.}(3) + \alpha_4 P_{col.}(4), \quad (5.36)$$

where  $\alpha_2$ ,  $\alpha_3$ , and  $\alpha_4$  are respectively the second, third, and fourth collision recovery coefficients.

The next step is to derive a closed form solution for the new optimum frame length  $L_{MCRC}$  under multiple collision recovery coefficients environment.  $L_{MCRC}$  can be optimized by finding the value of  $L$  which maximizes  $\eta_{MCRC}$ . According to [2], if  $L \gg 1$ , and  $n \gg i$ , we can assume a Poisson distribution:

$$P(i) \simeq \frac{1}{i!} \cdot \beta^{-i} \cdot e^{-\frac{1}{\beta}}, \quad (5.37)$$

where  $\beta = \frac{L}{n}$ . After substituting by (5.37) in (5.36) we get:

$$\eta_{MCRC} = e^{-\frac{1}{\beta}} \cdot \left( \beta^{-1} + \frac{\alpha_2}{2} \beta^{-2} + \frac{\alpha_3}{6} \beta^{-3} + \frac{\alpha_4}{24} \beta^{-4} \right). \quad (5.38)$$

Now we have to find the value of  $\beta$  which maximizes  $\eta_{MCRC}$ . This is achieved by differentiating the reading efficiency in (5.38) with respect to  $\beta$  and equate the result to zero. After differentiating, the equation can be simplified as:

$$-e^{-\frac{1}{\beta}} \cdot \left( \beta^{-2} + \beta^{-3}(\alpha_2 - 1) + \frac{\beta^{-4}}{2}(\alpha_3 - \alpha_2) + \frac{\beta^{-5}}{6}(\alpha_4 - \alpha_3) - \frac{\beta^{-6} \cdot \alpha_4}{24} \right) = 0. \quad (5.39)$$

After multiplying the equation by  $-e^{\frac{1}{\beta}} \cdot \beta^6$ , the equation finally results in:

$$\underbrace{1}_a \beta^4 + \underbrace{(\alpha_2 - 1)}_b \beta^3 + \underbrace{\frac{(\alpha_3 - \alpha_2)}{2}}_c \beta^2 + \underbrace{\frac{(\alpha_4 - \alpha_3)}{6}}_d \beta - \underbrace{\frac{\alpha_4}{24}}_e = 0. \quad (5.40)$$

Equation (5.40) has four roots [41]:

$$\begin{aligned} \beta_{1,2} &= -\frac{b}{4a} - S \pm 0.5 \sqrt{\underbrace{-4S^2 - 2P + \frac{q}{S}}_X} \\ \beta_{3,4} &= -\frac{b}{4a} + S \pm 0.5 \sqrt{\underbrace{-4S^2 - 2P - \frac{q}{S}}_Y}, \end{aligned} \quad (5.41)$$

$$\text{where } P = \frac{8ac - 3b^2}{8a^2}, \quad q = \frac{b^3 - 4abc + 8a^2d}{8a^3}$$

$$\text{and, } S = 0.5 \sqrt{-\frac{2}{3}P + \frac{1}{3a} \left( Q + \frac{\Delta_0}{Q} \right)}, \quad Q = \sqrt[3]{\frac{\Delta_1 + \sqrt{\Delta_1^2 - 4\Delta_0^3}}{2}}.$$

$$\text{with, } \Delta_0 = c^2 - 3bd + 12ae, \quad \Delta_1 = 2c^3 - 9bcd + 27ad^2 - 72ace$$

According to practical ranges for the collision recovery coefficients,  $\alpha_i$ ,  $0 \leq \alpha_i \leq 1$ , and  $\alpha_2 \geq \alpha_3 \geq \alpha_4$ . Therefore, we can proof that the signs of the polynomial coefficients are constant and not changing in all ranges of  $\alpha_i$  and can be as follows:  $a = +$ ,  $b = -$ ,  $c = -$ ,  $d = -$ , and  $e = -$ .

According to Descartes' rules of sign [28], there is only one valid real positive solution for the equation. Now, we will identify which solution is the valid one. There are two possibilities for the solutions:

1. One positive real solution and the remaining three solutions are negative. In this case, all solutions are real and we need just to identify what is the root which has the largest values from the four solutions. According to (5.41), the value of the square roots  $\sqrt{X}$  and  $\sqrt{Y}$  are positive real, because we do not have complex solutions. This means,  $\beta_1 > \beta_2$  and also  $\beta_3 > \beta_4$ . So, the solution will be either  $\beta_1$  or  $\beta_3$ . Moreover, the value of  $S$  should be also positive real, and  $q$  has always negative real value. so  $\beta_3 > \beta_1$  which means in this case that our solution is  $\beta_3$ .
2. Two complex solutions, one real positive solution, and one negative solution. In this case, we have either  $\beta_{1,2}$  or  $\beta_{3,4}$  real solutions.  $S$  should be positive real number, and the complex value comes only from the square roots  $\sqrt{X}$  and  $\sqrt{Y}$ . Moreover,  $q$  has always a negative real value. Therefore, in (5.41) the value of  $X < Y$ . So  $\beta_{1,2}$  must be the complex roots, and as  $\beta_3 > \beta_4$ ,  $\beta_4$  is the negative root and  $\beta_3$  is the positive real root.

Based on the above discussion, the proposed closed form optimum frame length  $L_{MCRC}$  under the multiple collision recovery coefficients environment is:

$$L_{MCRC} = \left( -\frac{b}{4a} + S + 0.5\sqrt{-4S^2 - 2P - \frac{q}{S}} \right) \cdot n \quad (5.42)$$

According to (5.42), the proposed equation gives a linear relation wrt. the number of tags  $n$ , and includes the effect of different collision recovery coefficients. In case that the RFID reader has no collision resolving capability, i.e.  $\alpha_2 = \alpha_3 = \alpha_4 = 0$ , the proposed formula gives  $L_{MCRC} = n$ , which is identical to the frame length in the conventional case. When the RFID reader has a full and equal collision resolving capability for the two, three, and four collided tags per slot, i.e.  $\alpha_2 = \alpha_3 = \alpha_4 = 1$ , the proposed formula gives  $L_{MCRC} = 0.452 \cdot n$ , which matches the results in [19].

### 5.3.2 Collision Recovery Coefficients Calculations

Now the calculation of the the collision recovery coefficients  $\alpha_2$ ,  $\alpha_3$  and  $\alpha_4$  will be clarified, which are the main optimization variables in our proposal. The values

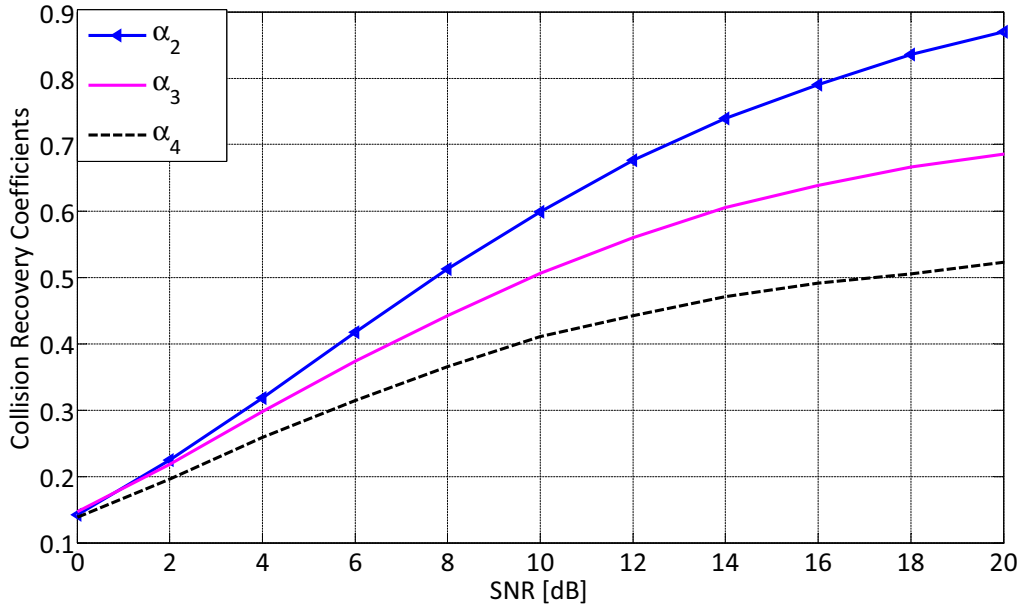


Figure 5.13: Collision recovery coefficients versus SNR using the strongest tag reply receiver. (example)

of these coefficients are strongly depend on the receiver type. Calculations of the collision recovery coefficients are done based on a RFID reader model that utilizes the capture effect. The reader resolves the collision based on the strongest tag reply. Therefore, the collision can be resolved with a certain probability, if the strongest tag reply is stronger than the summation of the other collided tags at the same slot.

The main advantage of this reader is that it does not need any channel state information (CSI) to recover the strongest tag. According to EPCglobal C1G2 standard [3], collisions in RFID systems occur only within the 16 bits packet called *RN16*. If any single bit error occurs in this packet, the total packed has to be considered lost. Therefore, the meaning of the collision recovery probability coefficients  $\alpha_i$  is the probability that the RFID reader can identify a complete *RN16* packet from  $i$  collided tags. Therefore, the collision recovery coefficient can be expressed as  $\alpha_i = (1 - PER_i)$ , where  $PER_i$  is the Packet Error Rate for  $i$  collided tags. In this work, we measure the SNR for each slot, then we calculate the average SNR per frame as  $E\left\{\frac{|h|^2 \cdot x^2}{\sigma^2}\right\}$ , where  $\sigma$  is the standard deviation of the Additive White Gaussian Noise (AWGN) per slot,

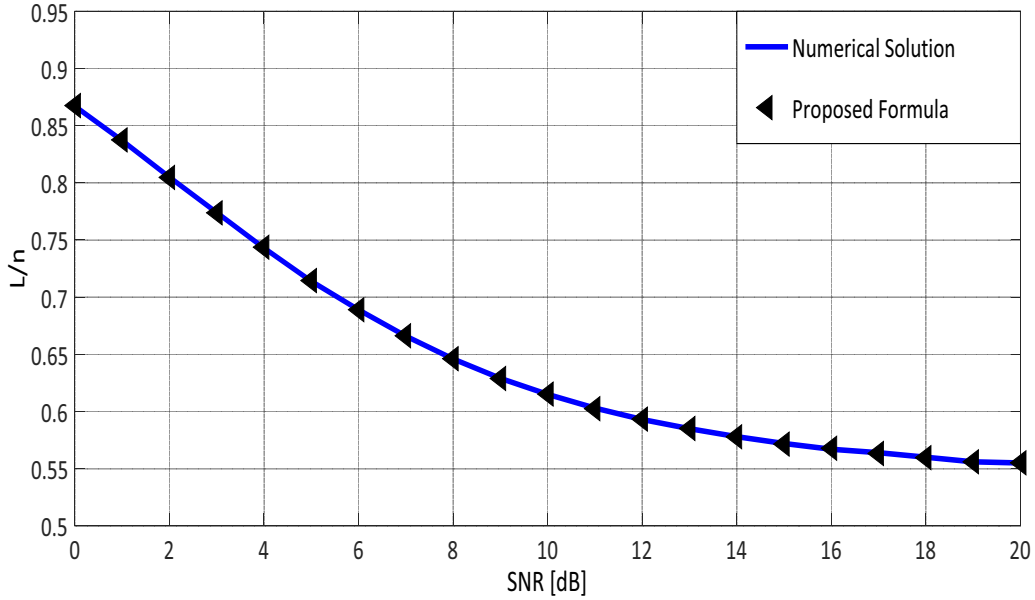


Figure 5.14: Frame length comparison between the proposed formula and the numerical solution versus the SNR using the strongest tag reply receiver.

and we used normalized signal power, i.e.  $E\{x^2\} = 1$ . Based on [29], we assumed that the equivalent channel coefficients  $h$  follow Rayleigh fading. The channel coefficients are independent zero mean circularly symmetric complex Gaussian random variables with normalized energy  $E\{|h|^2\} = 1$ , and all tags are statistically identical, which means all of them experience the same average path loss. Therefore, the average SNR per frame is  $E\left\{\frac{1}{\sigma^2}\right\}$ .

Figure 5.13 shows the values of the collision recovery coefficients versus the average SNR per frame using the strongest tag reply receiver. In these simulations, we used a sampling frequency of  $f_s = 8$  MHz, and tags use FM0 as an encoding scheme. Finally, to clarify the worst case effect of the collision recovery coefficients, we used the highest symbol rate 640 kHz

### 5.3.3 Closed Form Solution VS. Numerical Solution

For each RFID reader, each SNR leads to corresponding values for the collision recovery coefficients  $\alpha_2$ ,  $\alpha_3$  and  $\alpha_4$ . Figure 5.14 shows a comparison frame length comparison between the proposed formula in (5.34) and the numerical solution which maximizes the reading efficiency in (5.38) versus the SNR. Both

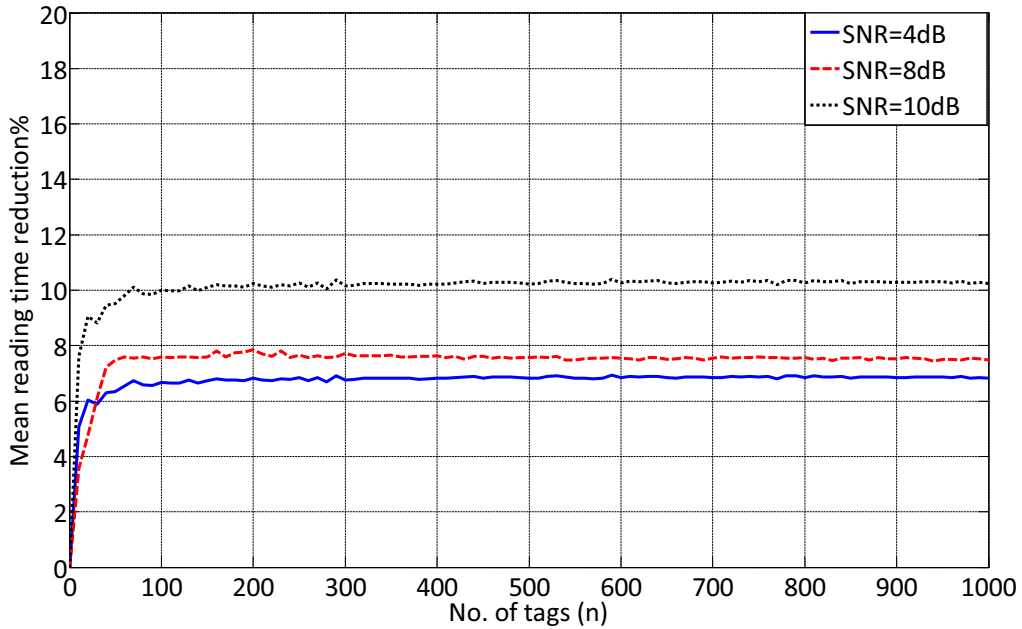


Figure 5.15: Percentages of saving time using the proposed MCR compared to the conventional frame length  $L = n$  for perfect number of tags estimation using  $C_t = 0.2$  and different  $SNR$  values

simulations used the same receiver model, which is the strongest tag reply receiver. According to figure 5.14, the proposed formula gives identical results compared to the numerical solution at the complete SNR range.

### 5.3.4 Mean Reduction in Reading Time

According to practical measurements, the typical range of the SNR for successful slots is 4 to 10 dB. Therefore, we calculated the total average number of slots needed to identify a complete bunch of tags using the strongest tag reply receiver. FSA with initial frame length  $L_{ini} = 16$  is used as an anti-collision algorithm. Figure 5.15 shows a comparison between the Percentages of saving time using the proposed MCR compared to the conventional frame length  $L = n$  for perfect number of tags estimation using  $C_t = 0.2$  and different  $SNR$  values. According to figure 5.15, when the value of the  $SNR$  increases, the collision recovery probability increases. Hence, the mean reduction in reading time also increases.

Figure 5.16 shows the Percentages of saving time using the proposed MCRA

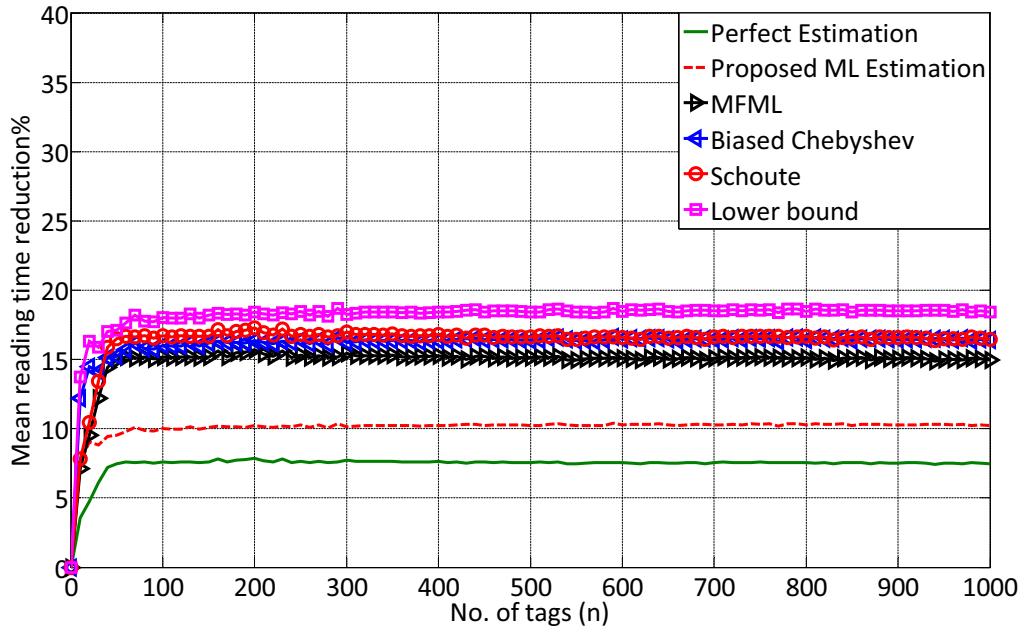


Figure 5.16: Percentages of saving time using the proposed MCRA compared to the conventional frame length  $L = n$  using different anti-collision algorithms with  $C_t = 0.2$  and  $SNR = 4$  dB

compared to the conventional frame length  $L = n$  using different anti-collision algorithms with  $C_t = 0.2$  and  $SNR = 4$  dB. As mentioned before, in case of better estimation algorithms, the mean reading time reduction approaches the curves assuming perfect knowledge of the number of tags.

## 5.4 Time And Multiple Collision Recovery System

In this section we present a new FSA reading efficiency metric called Time Aware Multiple Collision Recovery Coefficients Reading Efficiency  $\eta_{TAMCRC}$ . The main contribution in this new efficiency is: It contains a unique collision recovery coefficient  $\alpha_i$  for each probability of collision  $P(i)$ . These new coefficients indicate the ability of the reader to recover one tag from  $i$  collided tags, where this ability varies based on the number of collided tags. Moreover, it takes into consideration the different slot durations.

### 5.4.1 Closed Form Solution For Time Multiple Collision Recovery Aware System

According to figure 5.12, the probability that a collision results from two or three collided tags is approx. 85%. Moreover, the values of the collision recovery coefficient  $\alpha_i$  when  $i \geq 4$  (i.e. 4 or more collided tags) will be small. Therefore, we will only consider up to three collided tags. We will now normalize the slot duration  $t_k$  of successful and collided tags to unity. We furthermore take the assumption that empty slots are shorter than successful slots (i.e.  $t_0 \leq t_k$ ), which is the case for practical readers. Then, the proposed reading efficiency  $\eta_{TAMCRC}$  can be expressed as:

$$\eta_{TAMCRC} = \frac{P(1) + \alpha_2 P_{col.}(2) + \alpha_3 P_{col.}(3)}{1 + P(0) \cdot (C_t - 1)}, \quad (5.43)$$

where  $C_t = \frac{t_0}{t_k}$  represents the slots duration constant, and  $\alpha_2, \alpha_3$  are respectively the second, third collision recovery coefficients.

The next step is to derive a closed form for the new optimum frame length  $L_{TAMCRC}$  which maximizes  $\eta_{TAMCRC}$ . After substituting by (5.37) in (5.43) we obtain:

$$\eta_{TAMCRC} = \frac{e^{-\frac{1}{\beta}} \cdot (\beta^{-1} + \frac{\alpha_2}{2}\beta^{-2} + \frac{\alpha_3}{6}\beta^{-3})}{1 + e^{-\frac{1}{\beta}} \cdot (C_t - 1)} \quad (5.44)$$

where,  $\beta = \frac{L}{n}$ .

Now we have to find the value of  $\beta$  which maximizes  $\eta_{TAMCRC}$ . This is achieved by differentiating the reading efficiency in (5.44) with respect to  $\beta$  and equate the result to zero:

$$\frac{\partial \eta_{TAMCRC}}{\partial \beta} = 0 \quad (5.45)$$

After differentiating and simplifications, the final equation is a fourth order polynomial:

$$a \cdot \beta^4 + b \cdot \beta^3 + c \cdot \beta^2 + d \cdot \beta + e = 0, \quad (5.46)$$

where:  $a = \underbrace{-C_t}_{(-)}$

$$\begin{aligned}
b &= \underbrace{C_t \cdot (1 - \alpha_2) - 1}_{(-)} \\
c &= \underbrace{2 - C_t - \alpha_2}_{(+)} + \underbrace{\frac{C_t}{2}(\alpha_2 - \alpha_3)}_{(+)} \\
d &= \underbrace{\frac{1}{2}(\alpha_2 - \alpha_3) + \frac{1}{2}\alpha_2 \cdot (1 - C_t)}_{(+)} + \underbrace{\frac{1}{6}C_t \cdot \alpha_3}_{(+)} \\
e &= \underbrace{\frac{1}{6}\alpha_3 \cdot (2 - C_t)}_{(+)}
\end{aligned}$$

As  $0 \leq \alpha_i \leq 1$ ,  $0 < C_t \leq 1$ , and  $\alpha_2 \geq \alpha_3$ , equation (5.46) has four roots [41]:

$$\begin{aligned}
\beta_{1,2} &= -\frac{b}{4a} - S \pm 0.5 \sqrt{\underbrace{-4S^2 - 2P + \frac{q}{S}}_X} \\
\beta_{3,4} &= -\frac{b}{4a} + S \pm 0.5 \sqrt{\underbrace{-4S^2 - 2P - \frac{q}{S}}_Y},
\end{aligned} \tag{5.47}$$

$$\text{with } P = \frac{8ac - 3b^2}{8a^2}, \quad q = \frac{b^3 - 4abc + 8a^2d}{8a^3}$$

$$\text{and } S = 0.5 \sqrt{-\frac{2}{3}P + \frac{1}{3a} \left( Q + \frac{\Delta_0}{Q} \right)}, \quad Q = \sqrt[3]{\frac{\Delta_1 + \sqrt{\Delta_1^2 - 4\Delta_0^3}}{2}}$$

$$\text{with } \Delta_0 = c^2 - 3bd + 12ae, \quad \Delta_1 = 2c^3 - 9bcd + 27ad^2 - 72ace$$

According to the practical ranges of the collision recovery coefficients  $\alpha_i$  and  $C_t$ , we can prove that the signs of the polynomial coefficients are constants and do not change in all ranges of  $\alpha_i$  and  $C_t$ . Thus their signs will be:

$$a = (-), \quad b = (-), \quad c = (+), \quad d = (+), \quad \text{and } e = (+).$$

Using Descartes' rules of sign [28] we can count the number of real positive solutions of the polynomial.

Let us assume that the polynomial in (5.46) is  $P(\beta)$ , and let  $\nu$  be the number of variations in the sign of the coefficients  $a, b, c, d, e$ , i.e.  $\nu = 1$ , and let  $n_p$  be the number of real positive solutions. According to Descartes' rules of sign [28] we get:

- $n_p \leq \nu$ , which means that  $n_p = 0$  or 1.

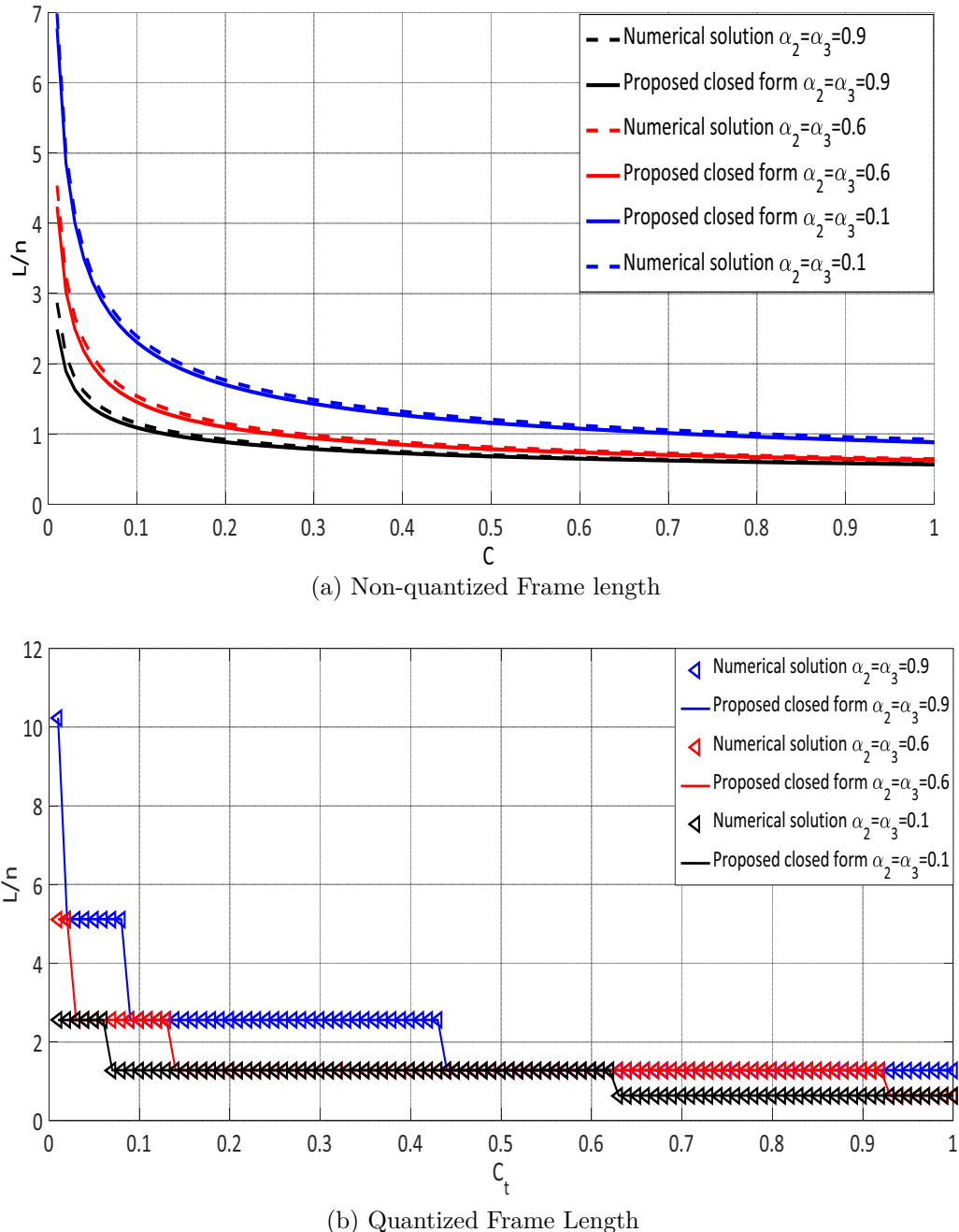


Figure 5.17: Frame length comparison between the proposed formula and the numerical solution versus the SNR using the strongest tag reply receiver.

- $\nu - n_p$  is an even integer. Therefore  $n_p = 1$ .

Consequently, there is only one valid real positive solution, one valid real negative solution, and two complex solutions for our equation. Our target is to identify which solution from the four solutions is the valid one. We have either  $\beta_{1,2}$  or  $\beta_{3,4}$  real solutions, so  $S$  should be a positive real number, and the complex values come only from the square roots  $\sqrt{X}$  and  $\sqrt{Y}$ . According to the coefficient signs:  $q$  must be always positive real value. Therefore, in (5.47) the value of  $X > Y$ . So  $\beta_{3,4}$  have to be the complex roots, with  $\beta_1 > \beta_2$ . Therefore,  $\beta_2$  is the negative root and  $\beta_1$  is the positive real root. Based on the above discussions, the proposed closed form optimum frame length  $L_{TAMCRC}$  under time and multiple collision recovery coefficients environment leads to:

$$L_{TAMCRC} = \left( -\frac{b}{4a} - S + 0.5\sqrt{-4S^2 - 2P + \frac{q}{S}} \right) \cdot n \quad (5.48)$$

The proposed equation gives a linear relation wrt. the number of tags  $n$ , and includes the effect of different collision recovery coefficients and the slot duration constant. The values of these coefficients are set based on the RFID reader type as shown in [1]. The value of  $C_t$  can be calculated based on the transmission rate as shown in [42]. Based on (5.48), if the RFID reader has no collision resolving capability ( $\alpha_2 = \alpha_3 = 0$ ) and equal slots durations are used ( $C_t = 1$ ), we get  $L_{TAMCRC} = n$ . This is identical to the optimum frame length in the conventional case.

#### 5.4.2 Closed Form Solution VS. Numerical Solution

In this section, we will discuss the accuracy of the proposed closed form compared to the numerical solution. Figure 5.17a shows a comparison frame length comparison between the proposed formula in (5.48) and the numerical solution which maximizes the reading efficiency in (5.43) versus full range of the slot duration constant  $C_t$  for different values of collision recovery coefficients  $\alpha_i$ . Both simulations used the same receiver model, which is the strongest tag reply receiver. According to figure 5.17, the proposed formula approaches the numerical solution at the full range of the complete range of  $C_t$ . As mentioned before, the EPCglobal C1 G2 standard [3] allows us only to take quantized frame lengths (power of 2). Figure 5.17b shows that the proposed frame length fully match

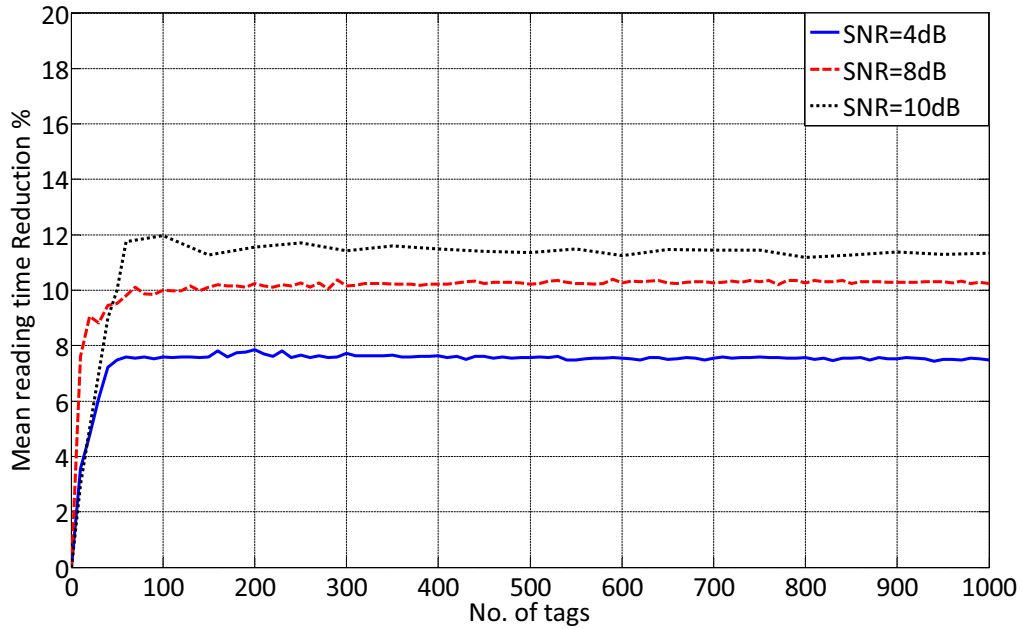


Figure 5.18: Percentages of saving time using the proposed TMCRA compared to the conventional frame length  $L = n$  for perfect number of tags estimation using  $C_t = 0.2$

the numerical solution in the full range of  $C_t$ .

### 5.4.3 Mean Reduction in Reading Time

Figure 5.18 presents the Percentages of saving time using the proposed TMCRA compared to the conventional frame length  $L = n$  for perfect number of tags estimation. The simulation results are based on the slot duration constant  $C_t = 0.2$ , as it is considered as a practical value used in the EPCglobal class 1 gen 2 standards [3] and different values of  $SNR$ . According to figure 5.18, when the value of the  $SNR$  increases, the collision recovery probability increases. Hence, the mean reduction in reading time also increases.

Figure 5.19 shows the Percentages of saving time using the proposed TM-CRA compared to the conventional frame length  $L = n$  using different anti-collision algorithms with  $C_t = 0.2$  and  $SNR = 8$  dB. As mentioned before, in case of better estimation algorithms, the mean reading time reduction approaches the curves assuming perfect knowledge of the number of tags.

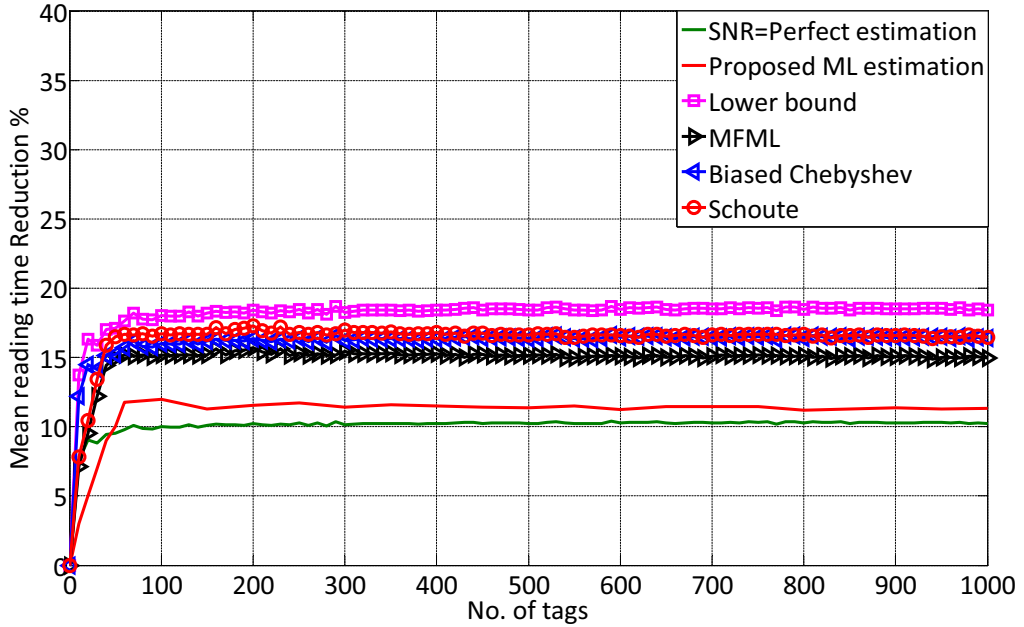


Figure 5.19: Percentages of saving time using the proposed TMCRA compared to the conventional frame length  $L = n$  using different anti-collision algorithms with  $C_t = 0.2$  and  $SNR = 8$  dB

## 5.5 Summary Results

The most important performance metric in RFID systems is the average total reading time for a bunch of tags. According to Dynamic Frame Slotted ALOHA (DFSA) [13], The total reading process for a bunch of tags is divided into successive variable length frame lengths cycles. To optimize each reading cycle, we optimize the FSA frame length as a function of the remaining unidentified number of tags in the reading area. Thus, we should have a precise number of tags estimation algorithm to find the right optimum frame length.

In this section, we will summarize the performance of the proposed systems in a total reading time comparison between the proposed frame lengths and the conventional DFSA, which assumes that  $L_{opt} = n$  and the theoretical limit of the EPC global C1 G2 standard [3], which gives the minimum identification time for UHF RFID system, with total number of slots needed ( $N_{total}$ ) to identify  $n$  number of tags is  $N_{total} = n$ .

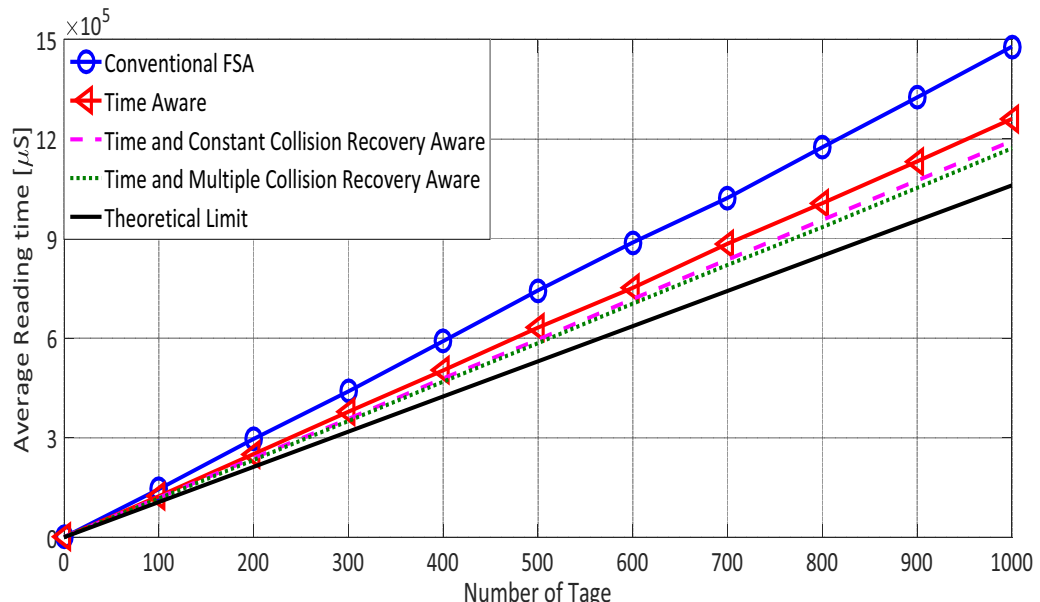
The following simulation results assume the following parameters: Slots duration constant  $C_t = 0.2$ , with  $te = 60 \mu s$ ,  $tc = 360 \mu s$ , and  $ts = 1060 \mu s$ ,

which are practical values from real measurements using a Universal Software Defined Radio Peripheral (USRP B210) [31]. Average Signal to Noise Ration  $SNR = 10$  dB, with strongest tag reply receiver which leads to the following collision recovery coefficients,  $\alpha_2 = 0.6$ ,  $\alpha_3 = 0.5$ ,  $\alpha_4 = 0.4$ .

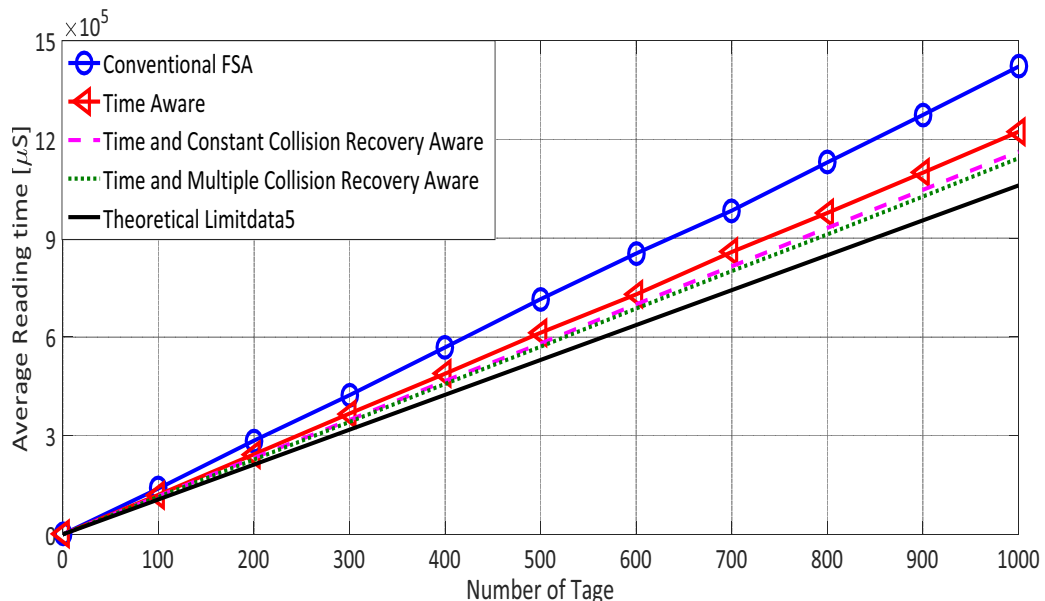
Simulation results is divided into two parts:

- Figure 5.20a presents a simulation results for the average reading time using conventional ML number of tags estimation [25], which neglect the collision recovery capability of the PHY layer. According to figure 5.20a, the Time Aware frame length gives 15 % saving in the average total reading time compared to the conventional FSA. The Time and Constant Collision Recovery Aware frame length results 5 % more than the Time Aware frame length average saving in the average total reading time compared to the conventional due to the new information about the collision recovery coefficient. In the Time and Constant Collision Recovery Aware we have assumed that the average collision recovery probability  $\alpha = \alpha_2$ . In case of the Time and Multiple Collision Recovery frame length, we have 22 % average saving in the reading time. This is due to considering the different values of the collision recovery coefficients.
- Figure 5.20b shows the average reading time using the proposed Collision Recovery Aware ML number of tags estimation, which considers the collision recovery capability of the PHY layer. According to figure 5.20b, the average total reading time using the Collision Recovery Aware number of tags estimation for the all proposed frame lengths and the conventional FSA are reduces with  $\simeq 5\%$  compared to the case of using the conventional ML number of tags estimation [25].

According to figure 5.20, we still have  $\approx 10\%$  lag of performance between the the proposed systems and the theoretical limit of the EPC global C1 G2 standard [3]. The main reason of this lagging performance is that all the allowed optimization was only in the reader side. To follow the EPC global C1 G2 standard [3], the tags could not be modified. Thus in the next chapter, we will propose backwards compatible improvement of the EPCglobal Class 1 Gen 2 standard. The system is compatible with the EPCglobal class 1 gen 2 standards, i.e. the proposed tags could be jointly operated with conventional tags



(a) Using conventional ML number of tags estimation



(b) Using collision recovery aware ML number of tags estimation

Figure 5.20: Comparison between the average reading time of the proposed systems, conventional FSA and the theoretical limit

and identified by conventional readers without affecting the performance. Additionally, conventional tags can also be operated together with the proposed tags and can be identified by the proposed reader.



# Chapter 6

## Compatible Improvements of UHF Standard

In well-known UHF RFID standards, e.g. EPCglobal class 1 gen 2 standards [3] allows only for a single tag acknowledgment, even if the physical layer is able to identify multiple collided tags. This results in an overall reduced performance. Recent researches have focused on this problem e.g. [2] used the post-preamble proposed in [1] with a Multi Input Multi Output (MIMO) receiver to resolve collisions. The authors assumed that all the recovered tags can be acknowledged in parallel. However, due to this post-preamble, this technique is not compatible with the EPCglobal class 1 gen 2 standards [3]. Therefore, their proposal would require a new RFID standard. Furthermore, acknowledging more than one tag in parallel would cause a new problem called “tag collision” due to the simultaneous reception of multiple Acknowledgment commands at the tag side. Moreover, this parallel acknowledgment will also cause Electronic Product Code (EPC) collisions at the reader side. The EPC packet is much longer than the RN16 packet, so it needs an advanced collision recovery algorithm, which will decrease the system performance.

For overcoming this drawbacks, we propose in this part a system that has the capability to acknowledge multiple tags within a single slot, resulting in a significantly increased performance. Our proposal offers the benefit that it is backwards compatible with existing EPCglobal C1 G2 tags and readers. Hence, our improved tags can be read by conventional readers without affecting the performance. Furthermore, existing tags can be read simultaneously with our



Figure 6.1: Conventional tag response

improved tags by optimized readers.

This chapter is organized as follows: Section 1 presents a brief discussion about the conventional reading process using the EPCglobal C1 G2 standards. In section 2, we describe the proposed new system including the modifications of the tags and the reader. The performance of the proposed system will be analyzed in section 3. Finally, section 4 contains the practical measurements and the simulation results.

## 6.1 EPCglobal C1 G2 Reading Process

In this section, we will describe briefly the conventional reading algorithm of the EPCglobal C1 G2 standards. At the beginning, the reader powers the tags in the reading area with a continuous wave (CW). At this time, the powered tags are in the Ready state waiting for the frame size information from the reader. Then, the reader broadcasts the frame size and notifies all tags of the beginning of a new frame with a Query command. As soon as the tags receive this command, each tag selects a slot from the frame by setting its slot counter, and enters the Arbitrate state. When the tag slot counter is equal to zero, the tag enters the Reply state and backscatters its 16 bits random number (RN16) as a temporary ID in addition to a 18 bits pilot and preamble used for synchronization as shown in figure 6.1.

According to Frame Slotted ALOHA, each slot has three possibilities: 1. No tag reply: The reader considers this slot as an empty slot and transmits a Query-Rep command asking the tags to decrement their slot counters. 2. Only one tag responds (successful slot): The reader transmits an Acknowledge command including the received RN16. Here the acknowledged tag enters the Acknowledged state and replies with its EPC code. 3. Multiple tags reply (collided Slot): Here we have two possibilities: Systems that have no collision recovery capability as shown in figure 6.2 (a): In such systems, the reader fails

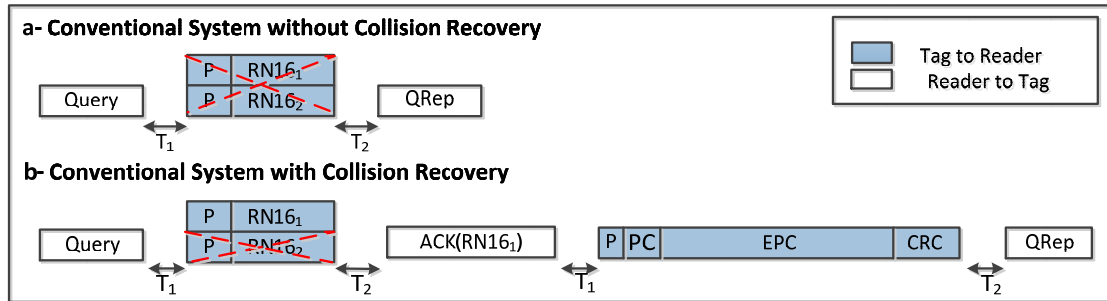


Figure 6.2: Two tags collided slot according to EPCglobal class 1 gen 2 standards

to identify any RN16, so it queries the next slot by sending another Query-Rep command. As soon as the collided tags receive the Query-Rep command, they enter the Arbitrate state waiting for the next frame. The maximum reading efficiency in such systems is 36%, if the working frame length is equal to the tag population size.

On the other hand, systems that have collision recovery capability as shown in figure 6.2 (b): These systems have the ability to identify at least one RN16 from the responding tags. Then, the reader broadcasts an Acknowledge command including one of the identified RN16s. The tag which has the same RN16 replies its EPC code and mutes itself until the end of the reading process. However, the remaining tags forget their RN16s and enter the Arbitrate state waiting for the next frame. The main disadvantage of such systems is that the reader can only acknowledge one tag from the collided tags in a slot, even if it has the capability to identify all the responding RN16s. For overcoming this drawback, we propose a backwards compatible extension.

## 6.2 Proposed System Description

In this section, the detailed descriptions of the proposed tags and readers will be presented. Afterwards, we will show the performance of the proposed system compared to conventional approaches.

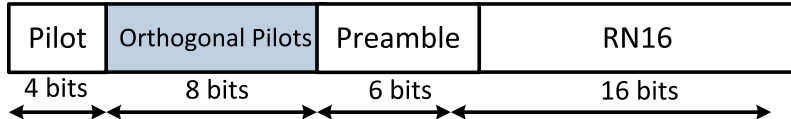


Figure 6.3: Tag response of the proposed tags including the new pilot sequences

### 6.2.1 Proposed Tag

The proposed tag has the ability to act like conventional UHF EPCglobal class 1 gen 2 tags, which is the default mode. However, it loads extra properties when it is in the Ready state and receives a new command called Switch command from the proposed reader. The following part presents the main modifications in the proposed tag:

According to the EPCglobal class 1 gen 2 standards [3], conventional tags backscatter two possible preambles with the RN16 packet, either the short version (6 bits preamble) or the long version 18 bits (12 bits zeros as a pilot + 6 bits of the short version). For the proposed tag, we use only the long version, but with a new structure. The new structure is as shown in figure 6.3 (4 bits zeros used for synchronization and 8 bits orthogonal pilots used for channel estimation). Table 6.1 shows an example of the orthogonal pilots, which are similar to the orthogonal post-preamble used in [1]. The innovation here is in dividing the 12 pilot bits of the long version of the conventional tag response to 4 zero bits and 8 orthogonal pilot bits. The 8 orthogonal pilot bits have to be orthogonal to the other pilot bits and also orthogonal to the conventional pattern  $P_1$  (8 zero bits). This property gives our proposal the advantage to have the conventional long version tag reply as a valid tag response in the new system. This is in contrast to the proposal by [1], where the conventional tags are not compatible with their system.

In case of a resolved collision of multiple RN16s, we can apply our proposed pseudo parallel reading process. A tag receiving its valid RN16 replies with its EPC and goes to the Acknowledged state. In contrast, a tag receiving an invalid RN16 (e.g. valid for another tag) goes to a new state called Wait state. In this new state the tag memorizes its RN16 until one of the two possibilities: a) Receiving an Acknowledgment command containing its RN16. In this case the tag replies with its EPC and goes to the Acknowledged state. b) Receiving

Table 6.1: Set of 8 orthogonal sequences [1]

Sequence	Orthogonal Pilots
$P_1$	1 -1 1 -1 1 -1 1 -1 1 -1 1 -1 1 -1 1 -1
$P_{18}$	1 -1 1 -1 1 -1 1 1 -1 1 -1 1 -1 1 -1 1 -1
$P_{69}$	1 -1 1 1 -1 1 -1 1 -1 1 -1 -1 1 -1 1 -1
$P_{86}$	1 -1 1 1 -1 1 -1 -1 1 -1 1 1 -1 1 1 -1 -1
$P_{171}$	1 1 -1 1 -1 -1 1 -1 1 1 -1 1 -1 1 -1 1 -1
$P_{188}$	1 1 -1 1 -1 -1 1 1 -1 -1 1 -1 1 1 -1 1 -1
$P_{239}$	1 1 -1 -1 1 1 -1 1 -1 -1 1 1 -1 -1 1 1 -1
$P_{256}$	1 1 -1 -1 1 1 -1 -1 1 1 -1 -1 1 1 -1 -1

Table 6.2: Proposed switch command

	Command
Number of bits	16
Description	1110001001100000

a command different from the Acknowledged command. In this case the tag goes to the Arbitrate state waiting for a new command.

When the proposed tag is in the Acknowledged state and receives a Query, Query-Adjust, or Acknowledgment command with a different RN16, it goes to the Ready state where it mutes itself until the end of the inventory process.

Figure 6.4 presents a state diagram with the required modifications of the tag state diagram given in [3] on page 47 figure 6.19.

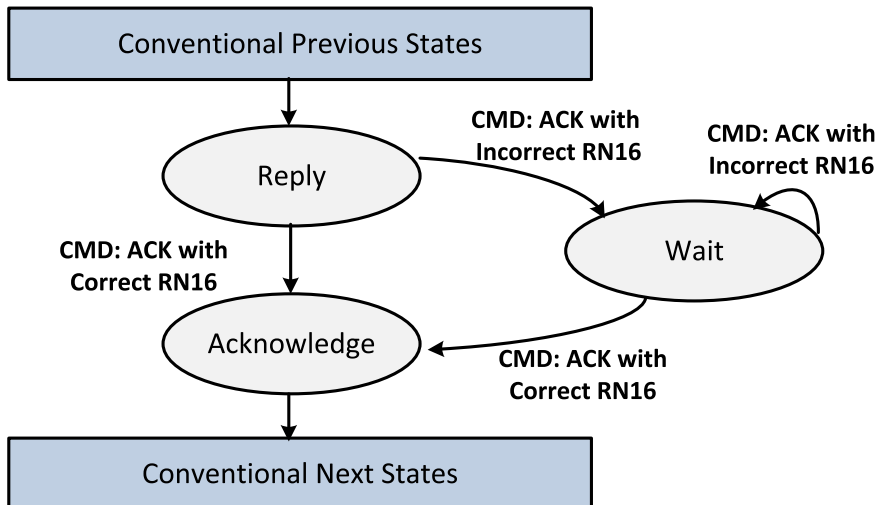


Figure 6.4: Modified part of tags state diagram

### 6.2.2 Proposed Reader

The proposed reader applies the normal FSA based on the conventional UHF EPCglobal class 1 gen 2 standard, which means that it is able to operate normally with conventional tags. It starts its reading process with a new command called Switch command to check if there are new tags in the reading area. It checks the tags replies. If there is any orthogonal pilot from table 6.1, it switches to the new mode. If it receives only conventional tag replies, it works in the conventional mode.

The following part presents the main modifications of the proposed reader:

The Switch command should exist in the proposed reader. The main purpose of this command is to switch the new tags from the conventional mode to the new mode. It should be transmitted before the Query command. The conventional tags will consider this Switch command as an unknown command, but the proposed tags will recognize that they are working in the new system. Table 6.2 presents an example for the Switch command code, which is a16 bits command from the future use part of EPCglobal class 1 gen 2 standards (*cf.* table 6.18 of [3]).

As discussed before, there are many problems in acknowledging more than one tag per slot in parallel, like the tag collisions, and the EPC collision at the reader side. On the other hand, the new system should benefit from the

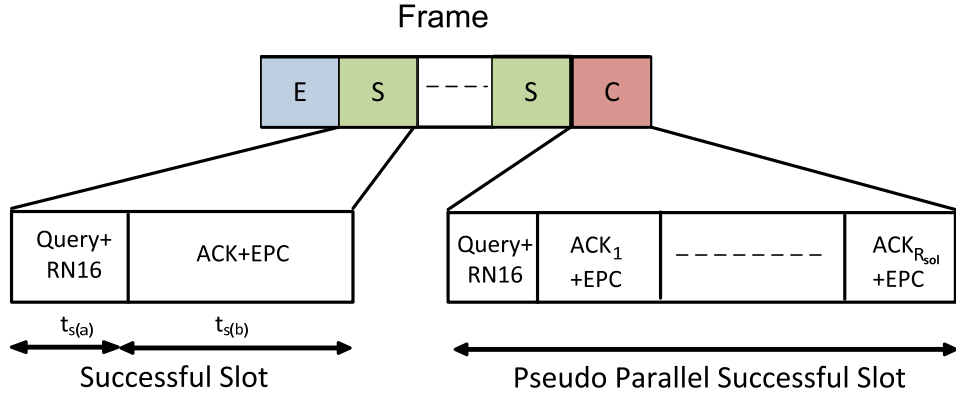


Figure 6.5: Example of the proposed pseudo parallel successful slot with parallel Query command and RN16 followed by successive Acknowledgment commands and EPCs

collision resolving capabilities of the modern readers. Therefore, the proposed reader has the capability of converting this collided slot into a pseudo parallel successful slot.

The reader starts each slot with a Query-Rep command asking for the RN16 of each tag. Then each tag backscatters its RN16 including one random orthogonal pilot from table 6.1 if it is one of the proposed tags or the conventional pilot ( $P_1$  from table 6.1) if it is a conventional tag. In case of a collided slot, the reader does the following steps:

- Use the orthogonal pilots to do channel estimation for the collided tags. Afterwards, use the channel information to recover the collided RN16s using a MIMO receiver, e.g. the receiver proposed in [2].
- Count the number of recovered tags replies in the “Reply Counter”.
- Recognize if one of these replies is a conventional pilot or not by checking if one of the collided pilots is the conventional one,  $P_1$  in table 6.1. If yes, this is a conventional tag.

Using these information, the reader checks first if one of the replied tags is a conventional tag. In this case the reader only acknowledges this tag and waits for its EPC, ignoring the remaining new tags. If all collided tags are new tags, the reader starts acknowledging them successively ordering them from the weakest to the strongest reply. The Reply Counter counts down with each received EPC from a tag and then sends the successive Acknowledgment

Table 6.3: Example for unique pilot collision scenarios for up to eight colliding tags per slot [2]

Number of received tags $R$	Probability of unique scenario $P_{s_1}$
1	$P_{s_1} = 1$
2 1+1	$P_{s_1} = 0.875$
3 1+1+1	$P_{s_1} = 0.656$
4 1+1+1+1	$P_{s_1} = 0.41$
5 1+1+1+1+1	$P_{s_1} = 0.205$
6 1+1+1+1+1+1	$P_{s_1} = 0.077$
7 1+1+1+1+1+1+1	$P_{s_1} = 0.019$
8 1+1+1+1+1+1+1+1	$P_{s_1} = 0.002$

command until the Reply Counter reaches to zero. Figure 6.5 shows an example for the pseudo parallel successful slot.

### 6.3 Performance Analysis

Based on the new system, we propose a new reading efficiency formula considering the advantages of the new system:

$$\eta_{new} = \sum_{R=1}^M P(R) \cdot \left( \sum_{l=1}^R P_{S_l}(R) \cdot R_{sol} \cdot \beta \right), \quad (6.1)$$

where  $P(R)$  is the probability that exactly  $R$  tag are active in one slot. It can be presented as:

$$P(R) = \binom{n}{i} \left( \frac{1}{L} \right)^i \left( 1 - \frac{1}{L} \right)^{n-i} \quad (6.2)$$

$M$  presents the maximum number of tags that can be resolved. For the proposed case,  $M$  is the number of orthogonal codes, i.e.  $M = 8$ , and  $R_{sol}$  is the number of recovered tags.

Since the colliding tags have randomly distributed pilots, several collision scenarios are possible as shown in [2].  $P_{S_l}(R)$  represents the probability that scenario  $S_l$  happens. It can be calculated from the binomial distribution as explained in [2]. For the proposed case, we consider only the unique scenarios  $(1 + 1 + \dots + 1)$ , i.e. if more than one tag has the same pilot, the reader will not be able to resolve this collision. Therefore, we have limited number of scenarios. Table 6.3 shows all values of the unique scenarios  $P_{S_l}(R)$ .

According to figure 6.5, the conventional successful slot  $t_s$  is divided in to two parts: The first part presents the time of the Query-Rep command and the RN16 tag reply  $t_{s(a)}$ , the second part is the time of the Acknowledgment command and the EPC tag reply  $t_{s(b)}$ . Thus, the successful slot time is:

$$t_s = t_{s(a)} + t_{s(b)}, \quad (6.3)$$

where  $t_{s(a)}$  and  $t_{s(b)}$  can be expressed as:

$$\begin{aligned} t_{s(a)} &= T_{qRep} + T_1 + T_2 + T_{RN16} \\ t_{s(b)} &= T_{ACK} + T_1 + T_2 + T_{EPC} \end{aligned} \quad (6.4)$$

Table 6.4 shows numerical values from the EPCglobal class 1 gen 2 standards [3] as a function of the link pulse-repetition interval  $T_{pri}$ . According to these values, the time of the Query-Rep command and receiving the RN16s presents 30% of the conventional successful slot duration. The time of the Acknowledgment command and the EPC tag reply represent 70% of the conventional successful slot duration.

For comparability, the proposed reader does not acknowledge more than one tag in parallel. However, we propose a pseudo parallel successful slots. The reader sends a Query command in parallel to all the tags, then receives the RN16s in parallel. Next, the reader sends Acknowledgment commands successively to the resolved tags. Therefore, the duration of the proposed pseudo parallel slot is:

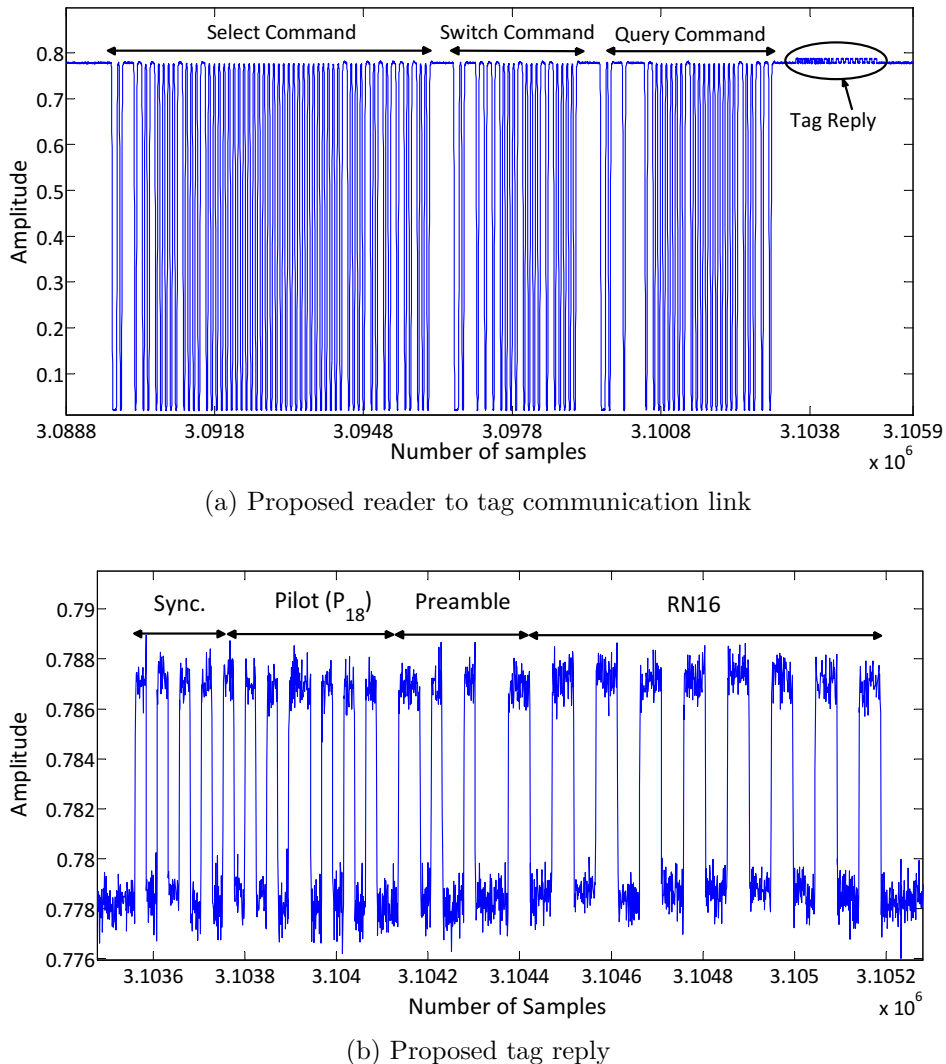


Figure 6.6: Communication link measurement

Table 6.4: System Parameters of EPCglobal class 1 gen 2 standards [3]

Parameters	Values
$T_{Q-Rep}$	$78 T_{pri}$
$T_1$	$10 T_{pri}$
$T_2$	$20 T_{pri}$
$T_{RN16}$	$34 T_{pri}$
$T_{ACK}$	$236 T_{pri}$
$T_{EPC}$	$102 T_{pri}$

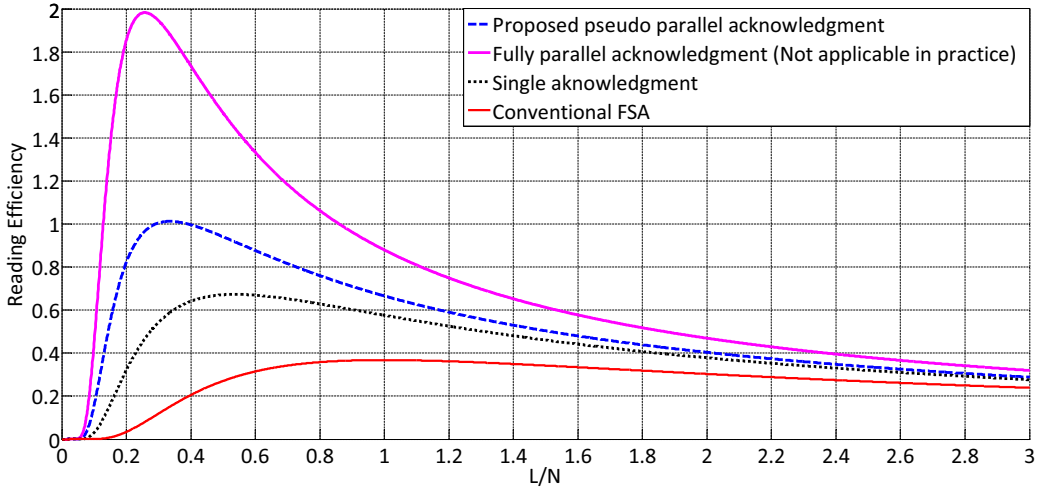


Figure 6.7: Reading efficiency for the conventional FSA and different acknowledgement scenarios using 8-orthogonal pilots

$$t_{pseudo} = t_{s(a)} + R_{sol} \cdot t_{s(b)}, \quad (6.5)$$

where  $R_{sol}$  is the number of recovered tags. These tags are acknowledged successively. Therefore, the proposed efficiency should include a factor representing the effect of the pseudo parallel spreading in time. This factor is called the pseudo parallel factor  $\beta$ . According to the numerical values in table 6.4, it can be expressed as:

$$\beta = \left( \frac{1}{0.3 + 0.7 \cdot R_{sol}} \right) \quad (6.6)$$

## 6.4 Measurement And Simulation Results

We have implemented our proposed tag modifications on the Wireless Identification Sensing Platform (WISP 5.0) [43], and the proposed reader on the Universal Software Radio Peripheral (USRP B210) [31]. A real example of the communication link between the proposed reader and the proposed tags is monitored using the USRP. Figure 6.6a shows a real measurement of the reader to tag communication link. According to figure 6.6a, the link starts with a normal Select command to set some conventional tag parameters. Then the reader broadcasts a Switch command asking the proposed tags to switch to the new

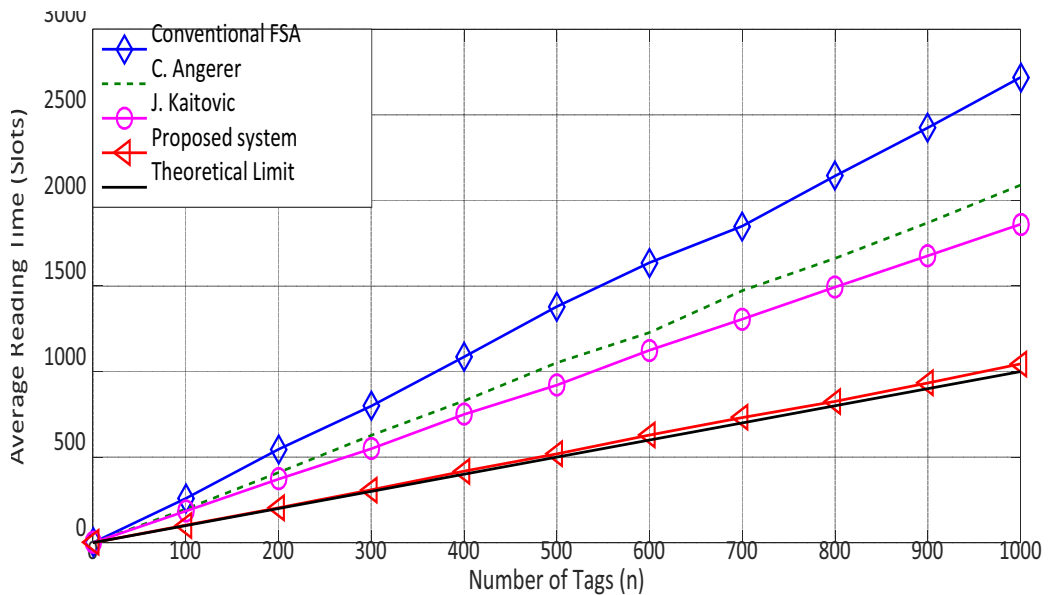


Figure 6.8: Comparison between the average reading time for different systems

mode. The conventional tags will not understand this command, so they simply ignore it. Afterwards, the reader sends a Query command asking the tags to reply with their RN16. Figure 6.6b presents a focused figure of the tag reply of figure 6.6a. As shown in figure 6.6b, the proposed tag reply starts with 4 bits zeros used for synchronization followed by 8 bits (one of the orthogonal pilots in table 6.1). In this example the tag replied with  $P_{18}$ . It is followed by a 6 bits preamble. Finally, the tag backscatters its RN16. The system is tested in a mixed network between the conventional and the proposed tags. The RN16 of the conventional and proposed tags were identified successfully.

The performance analysis is achieved through Monte Carlo simulations. Figure 6.7 shows a comparison between the reading efficiency of the conventional FSA and different acknowledgment scenarios use the 8 orthogonal pilot sequences. The first scenario is the system proposed by [2]. This system assumes fully parallel acknowledgment for all recovered tags. However, this system is not compatible with the EPCglobal class 1 gen 2 standard and can not be applied in practice. The second scenario assumes that it can acknowledge a single tag and neglect the other replies. This system does not benefit from the strong collision recovery capability of the reader. The third one is the proposed pseudo

successful slot. This system compromises between the single tag acknowledgment and the fully parallel acknowledgment with a maximum efficiency almost 100%.

Figure 6.8 shows the average reading time of the proposed system compared to the conventional FSA and other recent EPCglobal class 1 gen 2 compatible systems using collision recovery techniques. According to figure 6.8, the average reading time of our proposed system is decreased compared to the conventional FSA by 60%. In [29] the authors proposed a collision recovery system that is able to recover up to two collided tags. However, in our simulations we have assumed that the authors are able to recover all collided tags. According to this assumption, the average reading time of our proposal is 50% lower than the reading time of [29]. Moreover, the average reading time of our proposed system is 35% lower than average reading time of the system proposed by [44] using single acknowledgment. Finally, The proposed system approaches the theoretical limit of the EPC global C1 G2 standards [3]. This gain is only reachable using the modified compatible tags. However, the proposed maximum performance using the conventional tags was presented in the results of chapter 5.



# **Chapter 7**

## **Conclusion And Future Work**

### **7.1 Conclusion**

### **7.2 Future Work**



# **List of Abbreviations**

FSA	Framed Slotted ALOHA
RFID	Radio Frequency Identification



# Bibliography

- [1] J. Kaitovic, M. Simko, R. Langwieser, and M. Rupp, “Channel estimation in tag collision scenarios,” in *RFID (RFID), 2012 IEEE International Conference on*, pp. 74–80, April 2012.
- [2] J. Kaitovic, R. Langwieser, and M. Rupp, “A smart collision recovery receiver for rfids,” *EURASIP Journal on Embedded Systems*, vol. 2013, no. 1, 2013.
- [3] “EPC radio-frequency protocols class-1 generation-2 UHF RFID protocol for communications at 860 MHz 960 MHz version 1.1.0 2006.”
- [4] A. Zanella, “Estimating collision set size in framed slotted aloha wireless networks and rfid systems,” *Communications Letters, IEEE*, vol. 16, pp. 300–303, March 2012.
- [5] F. Vernon, “Applications of the microwave homodyne,” *Journal of Transactions of the IRE Professional Group on Antennas and Propagation*, vol. vol. 4, pp. 110–116., 1952.
- [6] D. Harris, “Radio transmission system with modulatable passive responder,” *US. Patent*, 2927321, 1960.
- [7] W. Charles, “Portable radio frequency emitting identifier,” *US. Patent* 4384288, 1973.
- [8] R. Hush and C. Wood, “Analysis of tree algorithms for rfid arbitration,” in *In IEEE International Symposium on Information Theory*, p. 107, IEEE, 1998.

- [9] A. E. M.Jacomet and U. Gehrig, “Contactless identification device with anticollision algorithm,” in *in: IEEE Computer Society, Conference on Circuits, Systems, Computers and Communications*, 1999.
- [10] A. Leon-Garcia and I. Widjaja, *Communication Networks: Fundamental Concepts and Key Architectures*. McGraw-Hill Press, Boston, 1996.
- [11] J. E. Wieselthier, A. Ephremides, and L. A. Michaels, “An exact analysis and performance evaluation of framed aloha with capture,” *IEEE Transactions on Communications*, vol. 37, pp. 125–137, Feb 1989.
- [12] J. Park, M. Y. Chung, and T.-J. Lee, “Identification of RFID Tags in Framed-Slotted ALOHA with Tag Estimation and Binary Splitting,” in *First International Conference on Communications and Electronics, 2006. ICCE '06.*, pp. 368–372, 2006.
- [13] F. Schoute, “Dynamic Frame Length ALOHA,” *IEEE Transactions on Communications*,, vol. 31, no. 4, pp. 565–568, 1983.
- [14] H. Vogt, “Efficient object identification with passive RFID rags,” in *International Conference on Pervasive Computing, Zürich*,, Aug. 2002.
- [15] L. Zhu and T. Yum, “Optimal framed aloha based anti-collision algorithms for rfid systems,” *IEEE Transactions on Communications*,, vol. 58, pp. 3583–3592, December 2010.
- [16] H. Vogt, “Multiple object identification with passive rfid tags,” in *Systems, Man and Cybernetics, 2002 IEEE International Conference on*, vol. 3, pp. 6 pp. vol.3–, Oct 2002.
- [17] B. Li and J. Wang, “Efficient anti-collision algorithm utilizing the capture effect for iso 18000-6c rfid protocol,” *Communications Letters, IEEE*, vol. 15, pp. 352–354, March 2011.
- [18] X. Yang, H. Wu, Y. Zeng, and F. Gao, “Capture-aware estimation for the number of rfid tags with lower complexity,” *Communications Letters, IEEE*, vol. 17, pp. 1873–1876, October 2013.

- [19] L. C. V. L. D. De Donno, L. Tarricone and M. M. Tentzeris, "Performance enhancement of the rfid epc gen2 protocol by exploiting collision recovery," *Progress In Electromagnetics Research B*, vol. 43, 53-72, 2012.
- [20] D. Lee, K. Kim, and W. Lee, "*Q+-Algorithm: An Enhanced RFID Tag Collision Arbitration Algorithm*", pp. 23–32. Berlin, Heidelberg: Springer Berlin Heidelberg, 2007.
- [21] I. Joe and J. Lee, "A novel anti-collision algorithm with optimal frame size for rfid system," in *Software Engineering Research, Management Applications, 2007. SERA 2007. 5th ACIS International Conference on*, pp. 424–428, Aug 2007.
- [22] M. Daneshmand, C. Wang, and K. Sohraby, "A new slot-count selection algorithm for rfid protocol," in *Communications and Networking in China, 2007. CHINACOM '07. Second International Conference on*, pp. 926–930, Aug 2007.
- [23] J.-R. Cha and J.-H. Kim, "Dynamic framed slotted aloha algorithms using fast tag estimation method for rfid system," in *Consumer Communications and Networking Conference*, vol. 772, 2006.
- [24] B. S. Wang, Q. S. Zhang, D. K. Yang, and J. S. Di, "Transmission control solutions using interval estimation method for epc c1g2 rfid tag identification," in *2007 International Conference on Wireless Communications, Networking and Mobile Computing*, pp. 2105–2108, Sept 2007.
- [25] W.-T. Chen, "An accurate tag estimate method for improving the performance of an rfid anticollision algorithm based on dynamic frame length aloha," *Automation Science and Engineering, IEEE Transactions on*, vol. 6, pp. 9–15, Jan 2009.
- [26] A. Zanella, "Estimating collision set size in framed slotted aloha wireless networks and rfid systems," *Communications Letters, IEEE*, vol. 16, pp. 300–303, March 2012.

- [27] H. Salah, H. Ahmed, J. Robert, and A. Heuberger, “A time and capture probability aware closed form frame slotted aloha frame length optimization,” *Communications Letters, IEEE*, vol. 19, pp. 2009–2012, Nov 2015.
- [28] D. Struik, *A Source Book in Mathematics 1200-1800*. Princeton University Press, 1986.
- [29] C. Angerer, R. Langwieser, and M. Rupp, “Rfid reader receivers for physical layer collision recovery,” *Communications, IEEE Transactions on*, vol. 58, pp. 3526–3537, December 2010.
- [30] E. Vahedi, V. Wong, I. Blake, and R. Ward, “Probabilistic analysis and correction of chen’s tag estimate method,” *Automation Science and Engineering, IEEE Transactions on*, vol. 8, pp. 659–663, July 2011.
- [31] Ettus Research, “USRP B210.” <http://www.ettus.com/product/details/UB210-KIT>, 2015.
- [32] X. Xu, L. Gu, J. Wang, G. Xing, and S.-C. Cheung, “Read more with less: An adaptive approach to energy-efficient rfid systems,” *Selected Areas in Communications, IEEE Journal on*, vol. 29, pp. 1684–1697, September 2011.
- [33] J. Alcaraz, J. Vales-Alonso, E. Egea-Lopez, and J. Garcia-Haro, “A stochastic shortest path model to minimize the reading time in dfsa-based rfid systems,” *IEEE Communications Letters*, vol. 17, pp. 341–344, February 2013.
- [34] G. Khandelwal, A. Yener, K. Lee, and S. Serbetli, “Asap : A mac protocol for dense and time constrained rfid systems,” in *IEEE International Conference on Communications, 2006. ICC ’06.*, vol. 9, pp. 4028–4033, June 2006.
- [35] A. Zanella, “Adaptive batch resolution algorithm with deferred feedback for wireless systems,” *IEEE Transactions on Wireless Communications*, vol. 11, pp. 3528–3539, October 2012.
- [36] J. Vales-Alonso, V. Bueno-Delgado, E. Egea-Lopez, F. Gonzalez-Castano, and J. Alcaraz, “Multiframe maximum-likelihood tag estimation for rfid

- anticollision protocols,” *Industrial Informatics, IEEE Transactions on*, vol. 7, pp. 487–496, Aug 2011.
- [37] J. R. A. H. Hazem A. Ahmed, Hamed Salah, “An efficient rfid tag estimation method using biased chebyshev inequality for dynamic frame slotted aloha,” *Smart Systech*, 2014 (accepted).
- [38] D. Liu, Z. Wang, J. Tan, H. Min, and J. Wang, “Aloha algorithm considering the slot duration difference in rfid system,” in *RFID, 2009 IEEE International Conference on*, pp. 56–63, April 2009.
- [39] H. Wu and Y. Zeng, “Passive rfid tag anticollision algorithm for capture effect,” *IEEE Sensors Journal*, vol. 15, pp. 218–226, Jan 2015.
- [40] A. Mokhtari, mehregan mahdavi, R. E. Atani, and M. Maghsoodi, “Using capture effect in dfsa anti-collision protocol in rfid systems according to iso18000-6c standard,” *Majlesi Journal of Mechatronic Systems*, vol. 1, no. 3, 2012.
- [41] M. Abramowitz and I. A. Stegun, *Solutions of Quartic Equations*. New York: Dover,, 1972.
- [42] C. Wang, M. Daneshmand, K. Sohraby, and B. Li, “Performance analysis of rfid generation-2 protocol,” *Wireless Communications, IEEE Transactions on*, vol. 8, pp. 2592–2601, May 2009.
- [43] Sensor Systems Laboratory. <http://sensor.cs.washington.edu/WISP.html>, 2011.
- [44] M. Nabeel, A. Najam, Y. Duroc, and F. Rasool, “Multi-tone carrier technique for signal recovery from collisions in uhf rfid with multiple acknowledgments in a slot,” in *Emerging Technologies (ICET), 2013 IEEE 9th International Conference on*, pp. 1–5, Dec 2013.